Retrospective Theses and Dissertations

Iowa State University Capstones, Theses and Dissertations

1-1-1972

Determination of Fe, Mn, Zn, Cu, and Mo in soybean plant material by instrumental neutron activation analysis

Larry Dean Brown
Iowa State University

Follow this and additional works at: https://lib.dr.iastate.edu/rtd

Part of the Engineering Commons

Recommended Citation

Determination of Fe, Mn, Zn, Cu, and Mo in soybean plant material

by instrumental neutron activation analysis

by

Larry Dean Brown

A Thesis Submitted to the

Graduate Faculty in Partial Fulfillment of

The Requirements for the Degree of

MASTER OF SCIENCE

Major: Nuclear Engineering

Iowa State University
Ames, Iowa

1972

TABLE OF CONTENTS

I. INTRODUCTION

There are many methods in use to determine the concentration of trace elements in plant tissue. These include, but are not limited to, direct reading emission spectroscopy, atomic absorption spectroscopy, gas chromotography, x-ray fluorescence, and neutron activation analysis (NAA). The purpose of this research was to investigate the use of instrumental NAA, without employing chemical separation, for determining the concentrations of Fe, Mn, Zn, Cu, and Mo in soybean plant tissue.

The NAA method was chosen to investigate one analytical solution of the plant analysis problem facing the agricultural researcher conducting elemental plant culture deficiency studies. The five elements were chosen since they are considered essential for the growth of crops and, in addition, are present in plants in trace amounts, that is, from about 0.5 parts per million (ppm) to an upper limit of about 200 ppm. In addition, these elements occur in deficient amounts in certain soils of the world [10].

Since Mo is concentrated in plants in smaller amounts than the other elements considered, and since researchers have reported [21] that chemical separation is required for its determination, initial theoretical research of this investigation was devoted to predicting whether or not a standard 3 X 3 inch sodium iodide (NaI) detector crystal and a gamma-ray scintillation spectrometry system could be used to detect Mo in the presence of interfering elements. Results of this research indicated that either greater resolution

than that obtained by the NaI detector or a chemical separation would be required for the determination of Mo.

Based on these results, the remainder of the investigation used a state-of-the-art lithium-drifted germanium [Ge(Li)] detector and its associated gamma-ray spectrometry system in the experimental determination of the five elements in a multiple element detection scheme. The irradiations were performed for one hour with 0.6- to 1.3-gram samples of pulverized soybean (and corn) leaf tissue in the Ames Laboratory Research Reactor (ALRR) at Iowa State University (ISU) at a thermal neutron flux of 10^{13} n/cm^2-sec. Quantitative determinations were made with a Ge(Li) detector of 39.8 cc active volume and a Nuclear Data Series 2200 System Analyzer spectrometry system. After an approximate 20-hour decay period, the Mn concentration was determined from the radioactive ^{56}Mn nuclide, and after a 1- to 2-week decay period, the long half-life nuclides of ^{59}Fe and ^{65}Zn were used to quantify Fe and Zn. Cu and Mo were not determined qualitatively or quantitatively due to a combination of low concentration in the plant material and various interferences in the gamma-ray spectra.

A significant portion of this work was concerned with an error analysis of the determinations. Optimum decay and counting times were empirically determined for Fe, Mn, and Zn which minimized the uncertainties of the results.

The major disadvantage of the technique used in this work is that the long decay and counting times which "optimized" the Fe and Zn determinations will increase the length of time and the cost of the analysis.

A major conclusion of this investigation was that Fe, Mn, and Zn can be determined in soybean plant tissues via instrumental NAA at concentration levels and precisions necessary for the study of elemental deficiencies in the culture of soybeans in the United States. This application also can be extended to studies concerning corn and other species containing approximately the same concentrations of constituents as the soybeans.

II. LITERATURE REVIEW

The first activation analysis experiment in the United States, and the first one with charged particles, was conducted by Glenn T. Seaborg and Jack Livingood at Berkeley, California, in 1938. The first experiments involving NAA were conducted in Europe about two years prior to this [54]. Since then, activation analysis has become a prominent method of analytical qualitative and quantitative analysis. Activation analysis enjoyed a phenomenal growth in the 1950s and 1960s when the number of published papers increased from 13 in 1949 to over 700 in 1969 [44].

Initial applications of NAA were limited to the determination of impurities in a "pure" metal matrix, such as done by Morrison and Cosgrove with Si, Ge, and W in 1955, 1956, and 1957 [42, 43, 12]. With improvements in detection capability through the development of the photomultiplier tube in conjunction with the NaI detector crystal and later the Ge(Li) semi-conductor detector crystal, considerable work has been done on complex matrix materials such as rocks and biological materials, including animal, human, and plant tissues.

Since this study pertains to determining trace elements in plant tissues, previous work on plant tissues and similar biological materials will be reviewed.

In 1956, Bowen reported determining Mn in blood and blood serum using chemical separation and double crystal scintillation spectrometry [7]. In 1959, he reported determining Ga and Mo in tomato seeds using solvent extraction with ether and counting with an end window geiger

counter [6]. Also in 1959, he reported the determination of Cu and Zn in tomato seeds and blood using chemical separation [5]. Later in 1959, Fukai and Meinke reported determining trace elements, including Mo, in marine biological ashes using chemical separation and a 3 X 3 inch NaI detector and scintillation spectrometry [22]. In 1961, Bowen and Cawse reported the determination of Na, K, and P in tomato seeds using chemical separation and beta counting [8]. In 1962, Van Zanten and others reported determining Mo in clover using solvent extraction and 3 X 3 inch NaI scintillation spectrometry [60]. In 1965, Nilubol and Kafkafi reported determining Mn in homogeneous soils and plants using chemical separation and beta and gamma counting [46]. In April, 1965, Samsahl and others reported determining 30 trace elements, including Cu, Fe, Mo, and Zn in human liver tissue using ion exchange group separation and a 3 X 3 inch NaI crystal [53]. In October, 1965, Healy and Bate reported determining Mo in hair and wool using chemical separation and a 3 X 3 inch NaI detector [32].

One of the first uses of a purely instrumental, nondestructive method on plant material was reported by Fourcy and others in 1967. They determined Mn, Cu, and K with a 4 X 4 inch NaI detector and scintillation spectrometry with a 400 channel analyzer without prior chemical separation. By using ion exchange resins, they also determined 13 other elements including Cu, Fe, Zn, Na, and K [21]. During the discussion of this paper, Fourcy stated that "radiochemical separation is required" for the determination of Mo in plants by activation analysis. Also in 1967, Dieckert and others reported determining K and Mn in peanuts, peanut flour, and seedling parts using

the instrumental method with a NaI detector and 256 channel analyzer
[16]. The resulting complex gamma-ray spectra were resolved by the
spectrum stripping method described by Covell [13]. In this same
year, Wainerdi and Menon determined Br in pesticides and plant
materials utilizing three instrumental methods. These were an auto-
mated NaI spectrometer, a 2 cubic centimeter Ge(Li) detector with a
3200 channel analyzer, and a gamma-gamma coincidence unit [61].
Also in 1967, Cooper and others reported detecting over 20 elements
including K, Cu, Mn, Fe, and Zn in blood and tumor tissue utilizing a
35 cubic centimeter coaxial Ge(Li) detector and a Compton suppression
spectrometer [11]. In July, 1967, Steinnes reported the instrumental
determination of Br, Mn, P, K, Na, and Zn in Norway Spruce leaves
utilizing a 3 X 3 inch NaI detector and 400 channel analyzer and
P and K using beta counting with a G-M counter [56]. Quantitative
results, based on the areas under the full energy peaks, were
evaluated by Covell's method [13]. In April, 1967, Livingston and
Smith used radiochemical separation to determine Mo in vegetable tissue
and powdered kale using gamma-ray spectrometry with a NaI detector [37].

In March, 1968, Grimanis reported using a fast radiochemical
separation method to determine Cu in pulverized plant leaves. He
then irradiated the precipitate and used a purely instrumental method
to determine the chemical yield of the separated copper. Both
determinations were made with gamma-ray scintillation spectrometry
[26]. In this paper, Grimanis stated that Cu could not be determined
successfully in plant tissues by instrumental nondestructive analysis
because of interference in the gamma-ray spectrum due to Mn, Na, and K.

In July, 1968, Neuburger and Fourcy reported determining Mo and W in

plants using an anion exchange separation technique and gamma-ray

spectrometry [45]. In October, 1968, Haller and others reported the

determination of 15 elements, including Na, K, Mn, Cu, As, Br, P, Fe,

and Zn in various items of foods such as rice, barley, raisins, beans,

peas, apples, and pears by a purely instrumental method using a

20 cubic centimeter coaxial Ge(Li) detector [30]. Also in October,

1968, Rancitelli and others reported determining some 20 elements,

including Na, Mg, Cl, K, Br, Al, Fe, and Zn in human, beef, and fish

tissue. Their work utilized two detector systems: a high resolution,

five-sided coaxial Ge(Li) detector with a 20 cubic centimeter

active volume and a second system consisting of an anticoincidence

shielded, gamma-gamma coincidence multidimensional analyzer with a NaI

crystal [49]. In May, 1968, Souliotis reported determining Cu and Zn

in ground plant leaves utilizing ion exchange separation and a 3 × 3 inch

NaI detector and a 400 channel analyzer [55].

III. THEORY

A. Principles of Activation Analysis

Neutron activation analysis (NAA) is a method of chemical element qualitative and quantitative analysis based on nuclear reactions between free neutrons and the nuclei of individual atoms of the element undergoing analysis. When a target material, such as pulverized plant leaves, is subjected to irradiation by neutrons from a neutron source, some atoms of all the elements in the target undergo nuclear reactions. These atoms then usually become radioactive, and the characterization of their radioactivity is the basis for the qualitative and quantitative analysis [35, 52].

According to the compound nucleus model, the nucleus of the struck atom captures the neutron forming a compound nucleus which is at an elevated state of energy above the ground state of the compound nucleus. This compound nucleus loses energy by emitting either a gamma ray, in the case of a radiative capture reaction, or an elementary particle such as a proton, alpha particle, or another neutron. These reactions are represented symbolically by (n, γ), (n, p), (n, α), and (n, n). If the energy of the striking neutron is sufficiently high, $(n, 2n)$ or $(n, 2p)$ reactions can occur.

Table I indicates the most probable type nuclear reaction as a function of the neutron energy and of the target nucleus mass number, A. The reactions are in decreasing order of frequency or probability; (n, n) refers to an elastic scattering interaction and (n, n') refers to an inelastic scattering reaction [15].

Table I. The most probable nuclear reaction as a function of neutron energy and target nucleus mass

Neutron energy	Nuclear reactions with nuclei having	
	$25 \leq A \leq 80$	$80 \leq A \leq 240$
0-1 keV	(n, n) (n, γ)	(n, γ) (n, n)
1-500 keV	(n, n) (n, γ)	(n, n) (n, γ)
0.5-10 MeV	(n, n) (n, n')	(n, n) (n, n') (n, p) (n, γ)
	(n, p) (n, α)	
10-50 MeV	(n, 2n) (n, n') (n, n)	(n, 2n) (n, n') (n, n)
	(n, p) (n, np) (n, 2p)	(n, p) (n, np) (n, 2p),
	(n, α) ...	(n, α) ...

The activation analysis technique is based on the fact that the product nucleus B resulting from the nuclear reaction A(n, -)B is usually radioactive, because not all the excitation energy of the compound nucleus is lost with the emission of the photon or particle. The majority of these radioactive nuclides decay with gamma ray emission. These gamma rays can be used to identify the product nuclide and to determine the initial amount of target nuclide in the sample which is related to the amount of the target nuclide produced during irradiation, as given by Eq. (1) for the reaction A(n, γ)B.

$$N_2 = \frac{N_1^o \sigma \phi}{\lambda} (1 - e^{-\lambda t_e}) \tag{1}$$

where N_1^o is the initial number of atoms of target nuclide A in the sample,

N_2 is the number of atoms of product nuclide B produced

during irradiation,

σ is the neutron energy-dependent (n, γ) reaction cross

section for nuclide A in cm^2/nucleus,

ϕ is the neutron flux of the specific energy in neutrons/cm^2/

second (n/cm^2-sec),

λ is the decay constant of the radioactive product nuclide

B in seconds^{-1}, and

t_e is the time of exposure to the neutron source (irradiation)

in seconds.

The following relation holds for N_1^o,

$$N_1^o = \frac{mf\varkappa_o}{W} \qquad (2)$$

and Eq. (1) can be written as

$$N_2 = \frac{mf\varkappa_o \sigma\phi(1 - e^{-\lambda t_e})}{W\lambda} \qquad (3)$$

where   m is the mass of the target element,

f is the relative abundance of nuclide A compared to all

other stable nuclides of the same target element,

$\varkappa_o$ is Avagadro's Number, and

W is the atomic weight of the target element.

Since the number of atoms cannot be counted directly, the activity of

the radioactive atoms, N_2, is used for quantitative calculations where

the activity is given by Eq. (4).

$$A_2 = N_2\lambda \qquad (4)$$

The activity is given in disintegrations per second (dps). Then from Eq. (1) and Eq. (2), the following expression is given for the activity of the product nuclides.

$$A_2 = \frac{mf\varkappa_o \sigma \phi}{W} (1 - e^{-\lambda t_e}) \tag{5}$$

After an infinite length of irradiation time, reached in practice in about six or seven half lives of N_2, the saturation level of activity is reached so that

$$A_{2-sat} = \frac{mf\varkappa_o \sigma \phi}{W} \; dps. \tag{6}$$

At the completion of irradiation, the activity decreases in time with the characteristic half life of the product nuclide according to Eq. (7) where t_d is the decay time after removal from neutron irradiation.

$$A_2 = A_{2-sat}(1 - e^{-\lambda t_e})e^{-\lambda t_d} \tag{7}$$

The activity is measured at some time during this decay period by the detection system which records a number of counts in a time interval. The number of disintegrations, D_2, occurring during a certain counting period, t_c, after an irradiation time, t_e, and a decay time, t_d, is found by integrating the decay period of Eq. (7) over the counting time.

$$D_2 = A_{2-sat}(1 - e^{-\lambda t_e}) \int_{t_1}^{t_2} e^{-\lambda \tau} d\tau$$

$$D_2 = \frac{A_{2-sat}(1 - e^{-\lambda t_e})e^{-\lambda t_d}(1 - e^{-\lambda t_c})}{\lambda} \tag{8}$$

where t_c is the time from t_1 to t_2, or the counting time, and t_d is the decay or waiting time from the end of irradiation to the beginning of the counting time.

The actual number of counts obtained by a detector system is not equal to the number of disintegrations occurring because of the detector efficiency factor, ϵ, and of the counting geometry factor, G. The number of counts obtained during a certain counting period is related to the number of disintegrations occurring during this period by Eq. (9).

$$C = \epsilon GD = \frac{\epsilon Gmf\varkappa_o \sigma\phi}{\lambda W}(1 - e^{-\lambda t_e})e^{-\lambda t_d}(1 - e^{-\lambda t_c}) \qquad (9)$$

The mass of the original target, nuclide A, is given by

$$m = \frac{C\lambda W}{\epsilon Gf\varkappa_o \sigma\phi(1 - e^{-\lambda t_e})e^{-\lambda t_d}(1 - e^{-\lambda t_c})} \qquad (10)$$

If one accurately knows all the variables in Eq. (10), the unknown mass can be computed. However, one seldom accurately knows the detector efficiency factor, the geometry factor, the absolute flux of a particular energy, or the energy-dependent reaction cross section. Therefore, this absolute determination method usually is replaced by the comparison method of analysis in which a known amount of the target nuclide is prepared and used as a standard. This standard is irradiated and counted under identical conditions along with a known mass of the sample containing the unknown amount of the element being analyzed. Then the mass ratio of the unknown to the standard element is calculated from the relationship in Eq. (11).

$$\frac{m_u}{m_s} = \frac{A_u}{A_s} \qquad (11)$$

where m_u is the mass of the unknown element,

m_s is the mass of the standard element,

A_u is the activity of the unknown,

A_s is the activity of the standard,

and the subscripts s and u refer to the standard and unknown,

respectively.

In order to correct for differences in decay and counting times, one must use the saturated activities for the activities in Eq. (11). The ratio of saturated activities is given by Eq. (12), resulting from substituting Eq. (6) into Eq. (9) and solving for $A_{2\text{-sat}}$.

$$\frac{A_u}{A_s} = \frac{A_{2\text{-sat}_u}}{A_{2\text{-sat}_s}} = \frac{\dfrac{C_u \lambda}{\varepsilon_u G_u (1 - e^{-\lambda t_e})_u (e^{-\lambda t_d})_u (1 - e^{-\lambda t_c})_u}}{\dfrac{C_s \lambda}{\varepsilon_s G_s (1 - e^{-\lambda t_e})_s (e^{-\lambda t_d})_s (1 - e^{-\lambda t_c})_s}} \qquad (12)$$

For assumed identical conditions of irradiation, detector counting efficiencies, and geometry factors for identical treatments of the unknown and standard in the comparison method, the ratio becomes

$$\frac{A_u}{A_s} = \frac{C_u (e^{-\lambda t_d})_s (1 - e^{-\lambda t_c})_s}{C_s (e^{-\lambda t_d})_u (1 - e^{-\lambda t_c})_u} \qquad (13)$$

For equal counting times of the unknown and standard, the ratio becomes

$$\frac{A_u}{A_s} = \frac{C_u(e^{-\lambda t_d})_s}{C_s(e^{-\lambda t_d})_u} \tag{14}$$

In the case of a radioactive produce nuclide which decays to a radioactive daughter, rather than to a stable daughter as in the case previously outlined, appropriate equations can be derived to express the activity of the radioactive daughter. This form of expression is required if the radiations of the daughter are used to quantify one of the original constituents of the irradiated material.

The activity of the daughter as a function of the irradiation time and subsequent decay time is found by solving the differential equation, Eq. (15), for the production and decay chain of

$$N_1 \xrightarrow{\sigma} N_2 \xrightarrow{\lambda_2} N_3 \xrightarrow{\lambda_3} \text{Stable}.$$
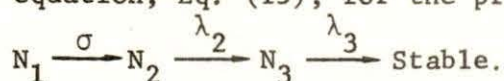
$$\frac{dN_3}{dt_e} = N_2\lambda_2 - N_3\lambda_3 \tag{15}$$

Using Eq. (1) for the value of N_2, one solves Eq. (15) for the number of atoms of N_3 produced during the time of irradiation, t_e, and remaining during the subsequent decay time, t_d, after the end of the irradiation.

$$N_3 = N_1^o\sigma\phi\left[\frac{(1 - e^{-\lambda_3 t_e})}{\lambda_3} + \frac{e^{-\lambda_3 t_e} - e^{-\lambda_2 t_e}}{\lambda_3 - \lambda_2}\right]e^{-\lambda_3 t_d} \tag{16}$$

For the number of N_3 atoms produced by decay of the parent atoms, N_2, during the decay time, t_d, the differential equation is given as Eq. (17).

$$\frac{dN_3}{dt_d} = N_2\lambda_2 - N_3\lambda_3 \quad \text{where} \quad N_2 = \frac{N_1^o\sigma\phi}{\lambda_2}(1 - e^{-\lambda_2 t_e})e^{-\lambda_2 t_d} \tag{17}$$

The solution of Eq. (17) is

$$N_3 = \frac{N_1^o \sigma \phi}{\lambda_3 - \lambda_2} (1 - e^{-\lambda_2 t_e})(e^{-\lambda_2 t_d} - e^{-\lambda_3 t_d}) \tag{18}$$

The activity due to the daughter, N_3, is $A_3 = N_3 \lambda_3$, where N_3 is the sum of Eq. (16) and Eq. (18). If R is the production rate equal to $N_1^o \sigma \phi$, then A_3 is given in Eq. (19).

$$A_3 = R \left[(1 - e^{-\lambda_3 t_e}) + \frac{\lambda_3}{\lambda_3 - \lambda_2} (e^{-\lambda_3 t_e} - e^{-\lambda_2 t_e}) \right] e^{-\lambda_3 t_d}$$

$$+ \frac{R\lambda_3}{\lambda_3 - \lambda_2} (1 - e^{-\lambda_2 t_e})(e^{-\lambda_2 t_d} - e^{-\lambda_3 t_d}) \tag{19}$$

For $t_d = 0$ and $T_e \to \infty$, the saturated activity of A_3 is found to be $R = N_1^o \sigma \phi$, the same as for A_2 in Eq. (6).

The number of disintegrations, D_3, occurring during a counting period, t_c, is found by integrating the decay time of Eq. (19) over the counting period.

$$D_3 = R \left[\frac{\lambda_2(e^{-\lambda_3 t_e} - 1)e^{-\lambda_3 t_d}(1 - e^{-\lambda_3 t_c})}{\lambda_3(\lambda_3 - \lambda_2)} \right.$$

$$\left. + \frac{\lambda_3(1 - e^{-\lambda_2 t_e})e^{-\lambda_2 t_d}(1 - e^{-\lambda_2 t_c})}{\lambda_2(\lambda_3 - \lambda_2)} \right] \tag{20}$$

For the number of counts obtained during the counting period, we have $C = \epsilon GD$, and the saturated activity, $R = N_1^o \sigma \phi$, is given by Eq. (21).

$$R = A_3 = \frac{C\lambda_2 \lambda_3 (\lambda_3 - \lambda_2)}{\epsilon G[\lambda_2^2 (e^{-\lambda_3 t_e} - 1)e^{-\lambda_3 t_d}(1 - e^{-\lambda_3 t_c}) + \lambda_3^2 (1 - e^{-\lambda_2 t_e})e^{-\lambda_2 t_d}(1 - e^{-\lambda_2 t_c})]} \tag{21}$$

With assumed identical detector efficiencies and geometry factors, the ratio of saturation activities for the unknown to the standard is

given by the following expression in the case of the use of these radioactive daughters.

$$\frac{A_u}{A_s} = \frac{C_u[\lambda_2^2(e^{-\lambda_3 t_e} - 1)e^{-\lambda_3 t_d}(1 - e^{-\lambda_3 t_c}) + \lambda_3^2(1 - e^{-\lambda_2 t_e})e^{-\lambda_2 t_d}(1 - e^{-\lambda_2 t_c})]_s}{C_s[\lambda_2^2(e^{-\lambda_3 t_e} - 1)e^{-\lambda_3 t_d}(1 - e^{-\lambda_3 t_c}) + \lambda_3^2(1 - e^{-\lambda_2 t_e})e^{-\lambda_2 t_d}(1 - e^{-\lambda_2 t_c})]_u}$$

(22)

Absolute sensitivity values, or the minimum detectable amounts of a particular element, are difficult to estimate for NAA. This is due to the basic assumptions which must be made for such variables as the irradiation conditions (flux and time of exposure), whether or not chemical separations are performed, the minimum acceptable precision, the efficiency of the detection system-geometry condition, and the decay and counting times [52]. Equation (10) can be solved for the minimum detectable mass by estimating the values for the variables on the right hand side. The number of counts chosen, C, is of primary interest, because this variable has the most influence on the precision (standard deviation) of the determination of this minimum amount. Assuming that the variance of the number of counts equals the number of counts, which is the case for simple counting statistics obeying the Poisson distribution, one would increase the minimum acceptable number of counts in order to reduce the relative error. For example, 100 counts in the full energy peak would result in a standard deviation of $\sqrt{100}$ or a 10% relative error in the area of the peak. Similarly, 1000 minimum counts would result in a standard deviation of 31.62 or 3.16%. The actual number of counts obtained for a given sample depends on the choice of the neutron flux level, the irradiation time, the

decay time before counting, and the counting time. A method for esti-
mating the number of counts in the full energy peak is given later in
this section.

Predicted sensitivities can be quite inaccurate due to unpre-
dictable interferences from other radioactive nuclides, counting-
geometry and detector efficiency factors, and the actual nuclear
parameters such as neutron flux, gamma ray branching ratios, and
reaction cross section. Nevertheless, calculated sensitivities for
various elemental determinations by NAA have been published [3, 27,
35, 40]. These serve as a general guide and usually are based on
chemical separation before counting, fixed neutron flux levels assumed
for the calculation, a minimum detectable decay rate corresponding
to the number of counts obtained during a certain counting time, and
arbitrary maximum irradiation times. In addition, these references
give experimentally determined values approaching the calculated sensi-
tivities.

B.   Gamma-Ray Spectrometry

Gamma-ray spectrometry is based on the types of interactions of
the gamma rays (photons) with the detector crystal materials. The
photons directly ionize matter, creating ion pairs, only about 1/100th
as much as do electrons of the same energy [19]. Therefore, secondary
electrons produced by primary photon interactions create nearly all of
the ion pairs in the crystals. These ion pairs are collected, con-
verted to an electronic pulse, amplified, shaped, and analyzed by a

pulse height analyzer. The resulting pulse height spectrum is used to determine the energy and intensity of the gamma rays.

The photon interactions with matter are of three primary types: photoelectric absorption, Compton (elastic) scattering, and pair production. In Ge, the photoelectric effect is the predominant reaction up to about 0.15 MeV when Compton scattering becomes dominant until about 8 MeV when pair production becomes the major interaction [19].

When a photon interacts with the crystal by these processes, it loses energy to the crystal resulting in the creation of the ion pairs. The resulting pulse height spectrum, which is recorded and displayed by a multichannel pulse height analyzer, is related directly to the energy of the initial photons and their interactions within the crystal.

In the case of the photoelectric effect, all the energy of the photon (except for the electron binding energy) is transferred to an electron in one of the inner shells of the crystal material, knocking the electron free so it can ionize the material. Thus the pulse height spectrum obtains a full-energy pulse corresponding to the full energy of the photon from each recorded photoelectric effect. Up to about 2 MeV, the photoelectric effect is useful in analyzing the photon energy and intensity.

In the case of Compton scattering, some of the energy of the photon is transferred to an electron in the crystal, and the remainder to another photon which is scattered in a new direction. If this photon then escapes from the crystal without further interaction, the total energy deposited in the crystal is less than the full energy

occurring in the case of a photoelectric interaction of the original

photon. The relationship between the energies of the two photons is

given by Eq. (23) taken from page 49 of Ref. [24].

$$E' = \frac{mc^2}{1 - \cos \theta + mc^2/E} \tag{23}$$

where   E is the energy of the incoming photon,

            E' is the energy of the scattered photon,

            mc^2 is the rest mass of an electron (equal to 511 keV), and

            θ is the angle between the original and new directions, or

            the scattering angle.

If the scattered photon undergoes a photoelectric interaction before

leaving the crystal, the sum of the Compton and photoelectric reactions

will result in a full-energy pulse; otherwise, the pulse recorded

will be reduced by E' and will cover all the possible ranges of

energies as the angle θ varies from 0 to 180 degrees. This incomplete

deposit of energy in the crystal results in the "Compton continuum."

This unwanted "noise" in the spectrum interferes with the detection of

photons of energy lower than that creating the continuum. Since the

photoelectric cross section is approximately proportional to Z^5,

where Z is the atomic number of the absorber, and the Compton process

is approximately proportional to Z, the use of a high Z material for

detectors will enhance the photoelectric effect relative to Compton

scattering. The Z numbers for common detector materials are 11 for

Na, 14 for Si, and 32 for Ge.

Pair production occurs when the photon interacts with the electric

field in the vicinity of a nucleus, creating an electron and a positron

pair. The pair deposits energy due to its ionization within the crystal. However, the positron is unstable and will annihilate with an electron, creating two 511 keV photons. If the crystal is large enough, one or even both of these annihilation photons will interact in the crystal by either the Compton or the photoelectric process. Thus, three pulse height peaks can occur from the pair production process: one at the full-energy peak, one at 511 keV less and corresponding to one member escape, and one at 1.02 MeV less and corresponding to two member escape. The single and double escape peaks are useful for analyzing photons with energies greater than 1.02 MeV, which is the threshold energy for the pair production process [19].

Heath [33] has given an expression, Eq. (24), for calculating N_p, the expected number of counts in the full energy peak in scintillation detector gamma-ray spectrometry:

$$N_p = D_2 FT(E)Pa \qquad (24)$$

where D_2F is the number of gamma rays of a given energy emitted from the source during the counting time; D_2 is given by Eq. (8) and F is the fraction of the disintegrations occurring by means of the gamma ray of energy E,

$T(E)$ is the detector efficiency, defined as the fraction of gamma rays emitted from the source which interact with the detector with a loss of a finite amount of energy,

P is the peak-to-total ratio or the ratio of the full energy peak area to the pulse height spectrum total area for a given gamma ray of energy E, and

a is a correction factor for any absorption of gamma rays

due to the use of a beta absorber between the detector

crystal and sample.

The product T(E)P is the probability that a gamma ray of energy E

emitted from the source will result in a pulse in the full energy peak

of the spectrum. Heath has published the calculated values for T(E)

and the experimentally determined values of P for NaI detectors at

various detector to source geometries [33].

C. Error Analysis

The sources of error in NAA must be examined thoroughly and ap-

propriate actions taken so the magnitude of the errors can be mini-

mized. Errors can arise during the following procedures or due to the

following phenomena: sample and standard preparation including

weighing, measuring, and the associated contamination of glassware,

samples, standards, and irradiation containers (vials in which the

materials will remain for counting); neutron thermalization by aqueous

solutions; neutron flux distortion and gradients; material self-

shielding to neutrons; interferences by alternative reactions; and

errors in measuring radioactivity and in timing various events

[23, 48].

Critical sources of error can occur during the preparation of

the samples and standards. As will be shown later, the uncertainty

in the final assay includes the uncertainties in the masses of the

samples and of the standard elements. However, one of the major sources of error in preparing the samples and standards is contamination.

Contamination can be introduced when anything is allowed to come in contact with the materials and irradiation vials prior to irradiation. Therefore, in the analysis for trace metals, cutting and grinding operations should be performed with nonmetallic or noncontaminating utensils, and the irradiation vials should be decontaminated thoroughly. Dust from the atmosphere should not be allowed to settle onto samples or glassware to be used in the analysis. Ashing or drying operations introduce losses if portions of the sample are either absorbed onto the container walls or otherwise lost to the atmosphere. Conversely, contaminants are added to samples and standards from improperly cleaned glassware and irradiation vials and through the use of impure chemical reagents, irradiation vials, and water. The technician's bare hands or contaminated gloves should not be allowed to touch the material since sodium chloride and other contaminants are introduced. The numerous considerations for avoiding contamination are discussed explicitly by Thiers [59]. Contamination on the surface of glassware and irradiation vials can be reduced by a thorough cleaning with strong acid solutions such as aqua regia or 7M nitric acid [51]. Irradiation vials themselves should be analyzed for impurity content. Thiers reports that "high pressure"-produced polyethylene contains several orders of magnitude less metal impurities than any other common container material. Contaminants and impurities cause significant problems if they are the same elements being sought or if they cause substantial interferences in activation or gamma-ray spectrometry.

However, these contaminations are not included in the calculated uncertainty of the standard mass.

Uncertainties in the mass of prepared standards include the uncertainties in the chemical purity of the reagents, weighing, volume measurement, and the atomic weights. The standard mass and its uncertainty are calculated by Eq. (25) which is derived from propagation of errors theory [2, 47].

$$
m_s \pm \sigma_{m_s} = \frac{(MC)\ (WE)\ (PC)\ (VA)}{(VS)\ (WC)} \left[1 \pm \sqrt{\left(\frac{\sigma_{MC}}{MC}\right)^2 + \left(\frac{\sigma_{WE}}{WE}\right)^2} \right.
$$
$$
\left. + \left(\frac{\sigma_{PC}}{PC}\right)^2 + \left(\frac{\sigma_{VA}}{VA}\right)^2 + \left(\frac{\sigma_{VS}}{VS}\right)^2 + \left(\frac{\sigma_{WC}}{WC}\right)^2 \right] \tag{25}
$$

where   MC is the mass of the compound,

WE is the atomic weight of the element,

PC is the purity of the compound,

VA is the volume of aliquot taken for irradiation,

VS is the volume to which the dissolved compound is diluted,

WC is the atomic weight of the compound, and

the error expressions, (e.g., σ_{MC}) are the standard deviations of the specific attributes.

The error in the compound mass is a function of the weighing method. For the "difference" method where the tare weight is subtracted from the gross weight to obtain the net weight, the standard deviation of the difference (also of a sum) is given in Eq. (26) from propagation of errors theory.

$$
\sigma_{(A \pm B)} = \sqrt{\sigma_A^2 + \sigma_B^2} \tag{26}
$$

The other error expressions in Eq. (25) are of two types: volume measurement uncertainties and errors in the precision of the purity of the compound and of the atomic weights. Eckschlager [17] has tabulated approximations for uncertainties in measuring different volumes of solutions. His data are used for the overall absolute uncertainties in the volumes used in this investigation. The errors in the purity and atomic weight values are taken as half the last significant digit of the listed value. Assayed precision data for the purity and atomic weights of the reagents used in this work are tabulated in Appendix A. The elemental atomic weight values and precisions are taken from Ref. [31].

The use of aqueous solutions containing the standard elements introduces an error due to neutron thermalization not achieved in the case of the sample matrix of pulverized plant material. This increases the thermal neutron flux in the standard relative to that in the unknown sample. The result is that Eq. (11) is in error due to too large a value for A_s; that is, the mass of the unknown element is underestimated due to the neutron thermalization in the aqueous solution. Aqueous solutions are desirable in this work, however, in order to reproduce readily the geometry of the unknown sample matrix of pulverized plant tissue. Furthermore, the value of 31 cm^2 for τ, the Fermi Age, results in an average thermalization distance for fission neutrons of about 13.6 cm in light water [24] which is greater than the 5.7 cm length of the aqueous solution in the horizontal irradiation vials in the reactor irradiation tubes. For this reason, and because of an assumption of a presumably larger uncertainty in the flux gradient, explained in the

following paragraph, the effect of thermalization of neutrons in aqueous solutions of the standards is considered negligible.

The presence of adjacent vials in the reactor, containing various samples and standard(s), introduces flux distortion or suppression. However, as pointed out in Ref. [23], the predominant error in the flux effect is the flux gradient of the reactor. This problem was investigated in the ALRR by Romberg [51] as the uncertainty in the flux ratio between locations occupied by the standard and the sample. He determined this uncertainty to be 0.05 where the flux ratio was given as 1.0. Malaby reports that the measured flux gradient in the rabbit tubes of the ALRR varies from 2 to 3% along the longitudinal axis of a rabbit and up to 5% along the radial axis [41]. As pointed out in Ref. [23], one way to reduce the flux gradient error is to rotate the samples and standards during irradiation. This capability was not available in the reactors used in this work, however.

Another source of error in NAA is neutron self-shielding by the matrix materials. This phenomenon occurs when the outer portion of the sample absorbs so many neutrons via nuclear reactions that the center portion receives a lower neutron flux due to a "shielding" effect of the outer atoms. This effect becomes a problem only when there are large neutron cross sections for the elements in the sample or irradiation containers. The relative self-shielding effect between sample and standard can be reduced by preparing standards of the same size, shape, density, and elemental concentration and distribution as that of the unknown sample matrix. Obviously, an exact duplication is impossible, but standards should approximate the samples in terms of the

above features as closely as practicable. Fortunately, research workers [9, 29, 39] have reported that neutron self-shielding is not significant in the analysis of plant material matrixes.

Interferences are caused by alternative reactions to the usually desired (n, γ) reaction for the production of the particular nuclide, $_z X^m$, which is the one measured for determination of the original $_z X^{m-1}$ elemental concentration. These alternative reactions are of five types: (n, p), (n, α), (n, 2n), (n, γ) reactions followed by β^- decay, and (n, γ) reactions followed by β^- decay followed by (n, γ) reactions, all leading to production of the $_z X^m$ nuclide whose activity is measured with no differentiation as to means of production. These reaction chains, including the desired reaction, are illustrated respectively as follows [39]:

$$_z X^{m-1} \ (n, \ \gamma) \ _z X^m \ , \ \text{thermal and low energy neutrons} < 500 \ \text{keV}.$$

$$_{z+1} X^m \ (n, \ p) \ _z X^m \ , \ \text{requires fast neutrons}.$$

$$_{z+2} X^{m+3} \ (n, \ \alpha) \ _z X^m \ , \ \text{requires fast neutrons}.$$

$$_z X^{m+1} \ (n, \ 2n) \ _z X^m \ , \ \text{requires fast neutrons}.$$

$$_{z-1} X^{m-1} \ (n, \ \gamma) \ _{z-1} X^m \xrightarrow{\beta^-} \ _z X^m \ , \ \text{thermal and low energy neutrons}.$$

$$_{z-1} X^{m-2} \ (n, \ \gamma) \ _{z-1} X^{m-1} \xrightarrow{\beta^-} \ _z X^{m-1} \ (n, \ \gamma) \ _z X^m \ , \ \text{thermal and}$$
low energy neutrons.
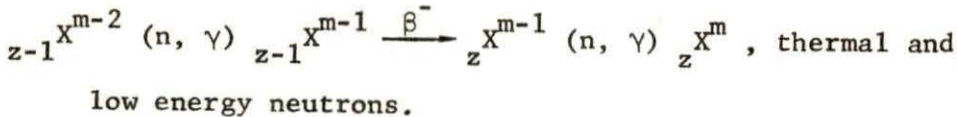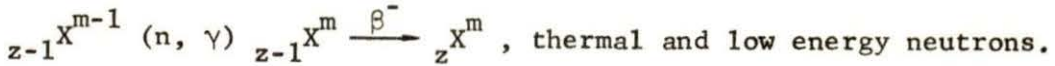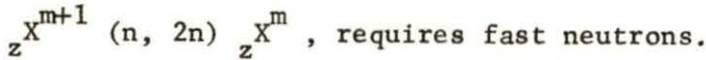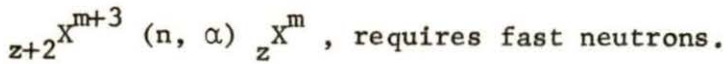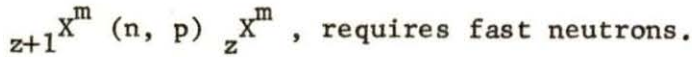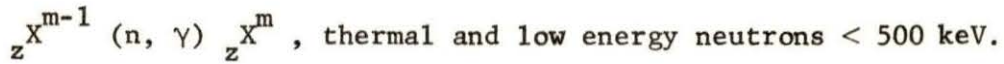
The relative production of the nuclide $_z X^m$ by interfering reactions must be estimated from the reaction cross sections and estimated abundance of the interference-producing nuclides in the unknown sample

matrix in order to evaluate the relative importance of these inter-ferences in the analysis for a particular element.

Uncertainties in radioactivity measurements in this work are characterized as those resulting from measuring the area of the full energy peaks of the gamma-ray pulse height spectra. Errors in peak area determinations are significant in the overall error assessed to the final quantitative determination. Thus any reduction of this uncertainty is of considerable importance. The uncertainty can be reduced by two general means. First, counting statistics can be improved by increasing the counting time and/or by counting at the optimum time to maximize the peak height above the Compton background. Secondly, a method of peak area determination should be used which gives a small variance. In simple counting statistics, assumed to follow a Poisson distribution, the variance of the number of counts is equal to the number of counts, as pointed out earlier. In gamma-ray spectrometry, however, the peak area and standard deviation measure-ments are more complicated because of the methods for measuring the area, which are only approximations [23].

There are numerous methods and computer programs for analyzing gamma-ray spectra and determining the full energy peak areas [28, 65]. These range from relatively simple methods such as digital analysis of the numbers of counts in the peak channels up to the complex methods of Gaussian curve fitting, spectrum stripping and spectrum synthesis by least squares. These methods are applicable to the analysis of complex gamma-ray spectra (when many gamma ray energies are present) and apply to spectra obtained from NaI and Ge(Li) detectors.

The calibrated fraction method of determining the area of the full
energy peak was described by Covell as a simpler method not requiring
a catalog of calibrated pulse height distributions for all the gamma
rays of the mixture in a particular spectrum [13]. Covell also described
the details of a digital method which applied statistical methods of
analysis. Sterlinski modified Covell's method by weighting the counts
in certain channels of the peak in a manner which improved counting
statistics [57, 58]. Baedecker evaluated the above and several other
digital methods of peak area determination [1] and concluded that
Wasson's modification of the total peak area method was the best of the
seven methods investigated in terms of its simplicity and high pre-
cision. All seven methods were applied to Ge(Li) detector-spectrometer
system data in his investigation. Since this work uses the Wasson
method for determining the peak area and variance, a discussion of his
method is included in Appendix B.

A computer program in use at Iowa State University (ISU) is ICPEAX
which evaluates gamma-ray pulse height spectra. This program detects
potential peaks, subtracts background counts, fits a Gaussian
curve to each of these peaks, calculates the areas and standard
deviations of the areas of the peaks, determines the energies of the
peaks from calibration points, and optionally creates a plot
and/or listing of each spectrum. Since this program was used in some
parts of this work, a more detailed discussion of it is included in
Appendix C.

The timing errors resulting from measuring the decay and counting times are insignificant in determining the overall error. Nevertheless, they are included in the error analysis for completeness.

Use of an equation of this form,

$$\sigma_Q^2 = \left(\frac{\partial Q}{\partial X}\right)^2 \sigma_X^2 + \left(\frac{\partial Q}{\partial Y}\right)^2 \sigma_Y^2 ,$$

from propagation of errors theory [2, 47], results in the error in determining the mass of the unknown as given by Eq. (27).

$$m_u \pm \sigma_{m_u} = m_s \frac{C_u}{C_s} \frac{(e^{-\lambda t_d})_s}{(e^{-\lambda t_d})_u} \frac{(1 - e^{-\lambda t_c})_s}{(1 - e^{-\lambda t_c})_u} \frac{\phi_s}{\phi_u}$$

$$\times \left[1 \pm \sqrt{\left(\frac{\sigma_{m_s}}{m_s}\right)^2 + \left(\frac{\sigma_{C_u/C_s}}{C_u/C_s}\right)^2 + \left(\frac{\sigma_{DR}}{DR}\right)^2 + \left(\frac{\sigma_{CR}}{CR}\right)^2 + \left(\frac{\sigma_{\phi R}}{\phi R}\right)^2} \right]$$

(27)

where   DR = Decay Ratio = $\dfrac{(e^{-\lambda t_d})_s}{(e^{-\lambda t_d})_u} = \dfrac{e^{-\lambda t_{d_s}}}{e^{-\lambda t_{d_u}}}$

CR = Counting Ratio = $\dfrac{(1 - e^{-\lambda t_c})_s}{(1 - e^{-\lambda t_c})_u} = \dfrac{(1 - e^{-\lambda t_{c_s}})}{(1 - e^{-\lambda t_{c_u}})}$

ϕR = Flux Ratio = $\dfrac{\phi_s}{\phi_u}$.

This equation is derived from Eq. (11) and Eq. (13) with a flux ratio added so that the estimated flux gradient can be incorporated into the error calculation. From propagation of errors theory,

$$\sigma_{DR}^2 = DR^2 \left[(\sigma_{t_{d_u}} - \sigma_{t_{d_s}})^2 \lambda^2 + (t_{d_u} - t_{d_s})^2 \sigma_\lambda^2 \right]$$

(28)

With the assumption that $\sigma_{t_{d_u}} = \sigma_{t_{d_s}}$, the term $\left(\dfrac{\sigma_{DR}}{DR}\right)^2$ in Eq. (27) becomes

$$[(t_{d_u} - t_{d_s})^2 \sigma_\lambda^2]. \tag{29}$$

Similarly, it can be shown that the term $\left(\dfrac{\sigma_{CR}}{CR}\right)^2$ is equal to

$$\left[\left(\frac{e^{-\lambda t_{c_s}}}{(1 - e^{-\lambda t_{c_s}})}\right)^2 \left(\lambda^2 \sigma_{t_{c_s}}^2 + t_{c_s}^2 \sigma_\lambda^2\right) + \left(\frac{e^{-\lambda t_{c_u}}}{(1 - e^{-\lambda t_{c_u}})}\right)^2 \right.$$

$$\left. \times \left(\lambda^2 \sigma_{t_{c_u}}^2 + t_{c_u}^2 \sigma_\lambda^2\right) - \frac{2\sigma_\lambda^2 t_{c_s} t_{c_u} e^{-\lambda(t_{c_u} + t_{c_s})}}{(1 - e^{-\lambda t_{c_u}})(1 - e^{-\lambda t_{c_s}})}\right] \tag{30}$$

The term $\left(\dfrac{\sigma_{\phi R}}{\phi R}\right)^2$ can be evaluated by estimating the uncertainty in the flux ratio, given by the flux gradient as discussed earlier in this section. The term $\left(\dfrac{\sigma_{ms}}{ms}\right)^2$ is calculated from Eq. (25). Finally, the count ratio term is given by Eq. (31)

$$\left(\frac{\sigma_{C_u/C_s}}{C_u/C_s}\right)^2 = \frac{\sigma_{C_u}^2}{C_u^2} + \frac{\sigma_{C_s}^2}{C_s^2} \tag{31}$$

For the concentration of the unknown element in parts per million (ppm), the microgram mass of the unknown element calculated with Eq. (27) is divided by the mass of the unknown sample in grams.

$$m_u \text{ (in ppm)} = \frac{m_u}{M_{sample}} \tag{32}$$

The error in the concentration is derived from propagation of errors theory and is found to be

$$\sigma_{m_u} \text{ (in ppm)} = \frac{m_u}{M_{sample}} \left[\left(\frac{\sigma_{m_u}}{m_u}\right)^2 + \left(\frac{\sigma_{M_{sample}}}{M_{sample}}\right)^2\right]^{1/2}. \tag{33}$$

IV. EXPERIMENTAL FACILITIES AND EQUIPMENT

The facilities and equipment used included the UTR-10 reactor of the Iowa State University Nuclear Engineering Department, the Ames Laboratory Research Reactor (ALRR), the activation analysis (chemistry) facility and counting equipment in the Nuclear Engineering Laboratory, and counting equipment in Sweeney Hall belonging to the Themis Project of the Defense Department at Iowa State University. These facilities and equipment are discussed as two major topics: irradiation facilities and the gamma-spectrometer system.

Initial irradiation experiments were performed with the UTR-10 reactor, a light water cooled, heterogeneous, tank-type reactor which is moderated with light water and graphite. At maximum power of 10 KW, the neutron flux in the pneumatic rabbit tube is about 7.0×10^{10} n/cm^2-sec. The ALRR was required to obtain the higher flux levels used by previous researchers for the quantitative NAA of trace elements in biological materials. This reactor is a heavy water cooled and moderated, heterogeneous, tank-type reactor with a maximum power rating of about 5 MW which provides various neutron flux levels depending on the particular irradiation facility of the reactor itself [51]. The irradiation facility of the ALRR used in this work was the pneumatic rabbit tube designated as R-4 which has a flux rating of 1.0×10^{13} n/cm^2-sec ($\pm$ 25%) when the reactor is operating at 5 MW [38]. The flux gradient in the rabbit tube was previously discussed in Section III, Theory.

The gamma-ray spectrometer system consisted of an ORTEC coaxial lithium-drifted germanium [Ge(Li)] detector-cyrostat system, a preamplifier, an amplifier, a cathode ray tube oscilloscope, and a Nuclear Data Series 2200 System Analyzer including a 4096 channel Analog to Digital Converter, a Master Control, and a System Memory. The detector crystal was 38.0 mm diameter by 40.0 mm long with a lithium drift depth of 14.6 mm and a diffusion depth of 0.7 mm. The manufacturer's other reported data on the detector were as follows: total active volume = 39.8 cc; measured total resolution = 2.53 keV full width at half maximum using 1.33 MeV photons at 3 μs amplifier time constant; measured peak to Compton ratio = 20.4 to 1.0 peak height to Compton plateau height; and measured efficiency = 6.67% in terms of the area under the full energy peak to that of 3 × 3 inch NaI detector measuring 1.333 MeV photons with a source-to-detector distance of 25 cm. A schematic of the spectrometer and data reduction system is in Fig. 1. A detailed equipment component listing is in Appendix D.

The detector and sample were located in a cubic, 4 inch thick Pb-walled shield or cave lined inside with 0.03 inch thick Cd and then with 0.015 inch thick Cu. The inside dimensions were 32 inches on a side. The Pb prevented most background radiation from reaching the detector while the Cd and Cu reduced the effect of the Pb x-rays produced from the photoelectric absorption of radiation in the Pb shield. The large dimensions of the cave reduced the effect in the crystal due to backscatter of gamms rays by the lead walls [18, 33, 51].

Multichannel Analyzer

Nuclear Data Series 2200 System Analyzer

```
┌──────────────┐
│  H.V. Power  │
│    Supply    │
└──────┬───────┘
       │
       ▼
┌──────────────┐          ┌─────────────────┐   ┌──────────────┐        ┌─────────────────────┐
│   Ge (Li)    │          │   Analog to     │   │  ○ CRT       │        │   Magnetic  Tape    │
│  Detector    │          │    Digital      │   │    Display   │        │ Transport (and Data │
└──────┬───────┘          │   Converter     │   │              │        │   Reduce ) Units    │
       │                  └─────────────────┘   └──────────────┘        └─────────────────────┘
       ▼
┌──────────────┐  ┌───────────┐  ┌──────────┐        ┌──────────────┐   ┌──────────────┐
│    Pre -     │  │           │  │          │        │    Master    │   │  Teletype    │
│  Amplifier   │  │ Amplifier │  │  Memory  │        │   Control    │   │  and Paper   │
└──────────────┘  └───────────┘  └──────────┘        └──────────────┘   │  Tape Punch  │
                                                                         └──────────────┘
                                                                         ┌──────────────┐
                                                                         │    Manual    │
                                                                         │  Processing  │
                                                                         └──────────────┘
```

┌────────────────────┐   ┌──────────────────┐   ┌──────────────────┐
│   Magnetic Tape   │   │   Paper Tape to │   │   IBM 47   │
│ to Card Punch   │◁--│   Magnetic Tape │   │   Paper Tape   │
│ Program PRESTO   │   │   Converter   │   │   to Card Punch │
└────────────────────┘   └──────────────────┘   └──────────────────┘

┌──┐   ┌──────────────────────────────┐
│   IBM 360/65 Computer   │   │   IBM 360/65 Computer.   │
│ ICPEAX plots spectra, labels peak energies,   │   │ MASS computes peak areas,   │
│ and computes peak areas and other peak parameters.   │   │ mass ratios, mass of unknown│
└──┘   │ and performs error analysis.│
                                                            └──────────────────────────────┘

Fig. 1. Schematic of detection, counting, and data handling equipment.
         (Single-dashed lines and parenthesis indicate capabilities not
         used in this work.)

33

V. QUANTITATIVE ANALYSIS

A. Approach to Problem

The problem of performing quantitative analysis of soybean plant material for Fe, Mn, Zn, Cu, and Mo was approached by performing the following tasks:

1) Obtain nuclear, abundance, and other data on all components of the soybean matrix material.

2) From Heath's NaI efficiency data [33], predict the number of counts in the full energy peaks of the primary gamma rays of Mo and of the major interfering gammas. Mo was used for these calculations for reasons discussed later in this section. A computer program was written to perform these calculations using Eq. (24). The results were used to determine if Mo could be detected with the NaI detector in the presence of the interfering gamma rays.

3) Predict the activities of all elements of the matrix for a one gram sample irradiated at a flux of 10^{10} n/cm^2-sec with variable times of irradiation and decay. Program ACTY (Appendix F) was written for this purpose.

4) Conduct an analysis of irradiation safety hazards and obtain approval from the ISU Radiation Safety Committee to irradiate soybean material in the UTR-10 reactor and in the ALRR.

5) Select and obtain the chemical compounds for use in preparing the standards for the five unknown elements, and prepare the bulk standard solutions.

6) Irradiate soybean material and a Mn standard in the UTR-10 reactor at an approximate flux of 6×10^{10} n/cm^2-sec and analyze for Mn with the Ge(Li) detector and Nuclear Data 2200 System Analyzer.

7) After gaining experience with the detection system and familiarity with the soybean gamma-ray spectrum, irradiate replicate samples of soybean and standards in the ALRR at a neutron flux of about 10^{13} n/cm^2-sec and perform quantitative analysis for the five elements.

8) Determine experimentally the "optimum" decay and counting times which result in the least interference and the most precise determination of the unknown elements.

9) Calculate the unknown masses and the associated uncertainties. Program MASS was written to perform these calculations using Eq. (25) through Eq. (33).

10) Check for the presence and effect of the five elements in the irradiation vials and in the water used for preparation of the standards.

A compilation of the nuclear data for the stable isotopes of the five elements is in Table II. Thermal neutron radiative capture reactions were considered to be the predominant reactions occurring in the reactor irradiation facilities. Only those stable nuclides being transmuted directly to a radioactive nuclide of half-life less than one year and giving off gamma rays are listed. Data for the cross sections were taken from Ref. [34], for the possible interferences

Table II. Nuclear and abundance data for radiative capture (n, γ) reactions for Fe, Mn, Zn, Cu, and Mo

Target nuclide	Target nuclide abundance, %	Activation cross section, barns	Product			Possible interference reactions
			Nuclide	Half-life	Major gamma energies, keV, and % occurrence	
^{58}Fe	0.31	0.98	^{59}Fe	45 d	1099.3(56.5)	^{59}Co(n, p)^{59}Fe,
					1291.5(43.5)	^{62}Ni(n, α)^{59}Fe.
^{55}Mn	100.00	13.3	^{56}Mn	2.576 h	846.7(100.0)	^{56}Fe(n, p)^{56}Mn,
					1811.2(29.4)	^{59}Co(n, α)^{56}Mn,
						^{54}Cr(n, γ)^{55}Cr $\xrightarrow{\beta^-}$
						^{55}Mn(n, γ)^{56}Mn.
^{64}Zn	48.89	0.46	^{65}Zn	245 d	1115.5(52.4)	^{63}Cu(n, γ)^{64}Cu $\xrightarrow{\beta^-}$
						^{64}Zn(n, γ)^{65}Zn.
^{68}Zn	18.56	0.1	^{69m}Zn	13.8 h	439.1(100.0)	(n, p) and
^{70}Zn	0.62	0.1	^{71}Zn	2.4 m	511.6(13)	(n, α) reactions
^{70}Zn	0.62	0.01	^{71m}Zn	4.0 h	387.0(100.0)	with Ga and
					488.0(69)	Ge.

Table II. (Continued)

Target nuclide	Target nuclide abundance, %	Activation cross section, barns	Product			
			Nuclide	Half-life	Major gamma energies, keV, and % occurrence	Possible interference reactions
^{63}Cu	69.1	4.5	^{64}Cu	12.8 h	511.0(38) 1345.8(0.48)	$^{64}Zn(n, p)^{64}Cu$, $^{62}Ni(n, \gamma)^{63}Ni \xrightarrow{\beta^-}$ $^{63}Cu(n, \gamma)^{64}Cu.$
^{65}Cu	30.9	1.8	^{66}Cu	5.1 m	1039.2(8.95)	
^{92}Mo	15.86	< 0.006	^{93m}Mo	6.9 h	685.0(97) 1479.0(100.0)	
^{98}Mo	23.75	0.15 ± 0.2[a]	$^{99}Mo/$ ^{99m}Tc	67 h 6.04 h	739.7(13.7) 140.4(81)	$^{102}Ru(n, \alpha)^{99}Mo$, fission of U or Pu.
^{100}Mo	9.62	0.2	$^{101}Mo/$	14.6 m	192.0(25) 506.0(15)	$^{104}Ru(n, \alpha)^{101}Mo$, fission of U or Pu.

[a]Source: [25].

Table II. (Continued)

Target nuclide	Target nuclide abundance, %	Activation cross section, barns	Product Nuclide	Half-life	Major gamma energies, keV, and % occurrence	Possible interference reactions
					590.8(21)	
					1012.4(25)	
					1532.7(11)	
					2089.0(16)	
			^{101}Tc	14.0 m	306.8(88.2)	

from Ref. [35], for the gamma ray energies and per cent emission from Ref. [20], and the remainder were taken from Ref. [36].

According to Koch [35], the interferences indicated in Table II are not significant unless the majority of the matrix atoms are of the element causing the interference. Therefore, these interferences were considered negligible in this work.

An approximate quantitative analysis of soybean plant material, obtained by other laboratory means, was obtained from the ISU Agronomy Department. This analysis, for corn leaves, is in Table III. Analyses of soybean plant tissues are similar to that of the corn leaves [14].

Since Mo was expected to be in smaller quantities than the other four elements being sought, and since Fourcy [21] reported that radio-chemical separation is required for the determination of Mo, computations were performed for the expected number of counts in the full energy peak for Mo and the major interfering elements using Eq. (24) and Heath's data for NaI scintillation spectrometry [33]. Two thermal neutron reactions were considered: ^{98}Mo activated to the ^{99}Mo-^{99m}Tc complex and ^{100}Mo activated to ^{101}Mo. The gamma rays used in the computations were Heath's values of 142 keV from ^{99m}Tc and 1024, 1560, and 2030 keV from ^{101}Mo [33]. Equation (20) was used instead of Eq. (8) for the value of D_2 in the calculation for ^{99m}Tc.

The possible interfering gammas were determined by selecting those tabulated by Heath [33] having energy within $\pm$ 100 keV of the four Mo and Tc gammas. This criterion was based on 10% resolution at 1 MeV. Within this energy region, those gammas of intensity A [33] and known or expected to be in plant tissue were selected for the computations.

Table III. Corn leaf analysis obtained by the Iowa State University
            Agronomy Department from the Ohio Plant Analysis Laboratory
            (circa 1965)

Element	% Dry weight	ppm Dry weight
N	3.0	
K	2.23	
SiO_2	0.53	
Ca	0.51	
P	0.29	
S	0.2-0.3	
Mg	0.27	
Na		179
Fe		113
Mn		80
B		32
Sn		22
Zn		21
Cu		20
Ba		10
Al		< 10
Mo		0.7
Co		0.3

Table IV contains those nuclides selected for the calculations. The data were taken from the same sources as those for Table II except that the energies were taken from Ref. [33] and the cross sections and fraction of decay by the gamma ray in question are from Ref. [36]. The known or expected concentrations in plant tissue were taken from the references as indicated.

The results of representative calculations of the number of counts in the full energy peaks at various times of irradiation and decay for 15 minute counting times are in Table V through Table VIII. From these results, it can be concluded that either more resolution or a chemical separation technique will be required to determine Mo in the presence of these interfering elements.

For this reason, and because nearly all researchers have been using the Ge(Li) detector for multiple element determinations with instrumental NAA, this author chose to use a Ge(Li) detector for the experimental research of this work. The details of the detector system used were discussed in Section IV, Experimental Facilities and Equipment.

Program ACTY (Appendix F) was developed by the author to predict the activities of the individual elements and the total activity of irradiated soybean material. These predicted activities were used to evaluate the radiation safety aspects of the irradiation requests and to predict the proximate peak interferences in the gamma spectrum analysis for the five elements.

The calculations were based on irradiation times limited to one hour to assure low activities, thus allowing early counting. This

Table IV. Nuclides selected for calculation of interference with Mo/Tc gamma rays: NaI spectrometry

Target nuclide	Elemental concentration, ppm, and reference	Target nuclide abundance, %	Activation cross section, barns	Product		
				Nuclide	Half-life	Gamma energy, keV, and % occurrence
^{196}Hg	0.15 [4]	0.146	880.	^{197}Hg	65. h	72(18)
^{130}Ba	10. [14]	0.101	8.8	^{131}Ba	12.0 d	126(28)
^{74}Se	0.18 [4]	0.87	30.0	^{75}Se	120.4 d	134(57)
^{186}W	0.1 [4]	28.4	40.0	^{187}W	24. h	134(9)
^{115}In	0.1 [4]	95.77	154.0	^{116m}In	54. m	137(3)
^{98}Mo	0.7 [14]	23.75	0.15	^{99}Mo	67. h	From ^{99m}Tc
				^{99m}Tc	6.04 h	142(90)
^{113}In	0.1 [4]	4.23	8.	^{114m}In	50.0 d	192(17)

Table IV. (Continued)

Target nuclide	Elemental concentration, ppm, and reference	Target nuclide abundance, %	Activation cross section, barns	Product		
				Nuclide	Half-life	Gamma energy, keV, and % occurrence
^{26}Mg	2700. [14]	11.17	0.027	^{27}Mg	9.5 m	1010(30)
^{100}Mo	0.7 [14]	9.62	0.2	^{101}Mo	14.6 m	1024(25)
^{65}Cu	20. [14]	30.9	2.3	^{66}Cu	5.1 m	1040(9)
^{81}Br	20. [4]	49.48	3.0	^{82}Br	35.3 h	1044(29)
^{64}Ni	10. [4]	1.16	1.15	^{65}Ni	2.56 h	1114(16)
^{81}Br	20. [4]	49.48	3.0	^{82}Br	35.3 h	1475(17)
^{100}Mo	0.7 [14]	9.62	0.2	^{101}Mo	14.6 m	1560(11)
^{139}La	0.1 [4]	99.9	8.9	^{140}La	40.2 h	1597(96)
^{100}Mo	0.7 [14]	9.62	0.2	^{101}Mo	14.6 m	2030(16)
^{115}In	0.1 [4]	95.77	154.0	^{116m}In	54.0 m	2080(20)
^{55}Mn	80. [14]	100.	13.3	^{56}Mn	2.58 h	2120(15)

43

Table V. Calculated number of counts in the full energy peak for ^{99m}Tc and interfering gamma rays from one gram of irradiated plant tissue: NaI spectrometry. (Neutron flux = 6×10^{12} n/cm^2-sec, time of counting = 15 minutes, time of irradiation = 67 hours, source-to-detector distance = 10 cm)

Product nuclide	Energy of gamma ray, keV	Time of decay, hours	Counts in peak, N_p
^{197}Hg	72	67	4667
		134	2284
^{131}Ba	126	67	2415
		134	2055
^{75}Se	134	67	556
		134	548
^{187}W	134	67	6660
		134	962
$\underline{^{99m}\text{Tc}}$	142	67	4.5
		134	0.002
^{114m}In	192	67	163
		134	157

limitation also assured that the polyethylene vials containing aqueous solutions would not rupture due to thermal damage [27]. The polyethylene vials were desirable containers, because they were available and were easy to clean and seal. The predicted activity for irradiation of a one gram sample for one hour at a flux of 10^{13} n/cm^2-sec was about 1.9 mc at the end of the irradiation and 0.12 mc after a decay period of 24 hours.

Table IX indicates the activities of specific nuclides in a one gram sample of a flux of 10^{10} n/cm^2-sec for representative irradiation and decay times, as computed by Program ACTY. These data were

Table VI. Calculated number of counts in the full energy peak for ^{99m}Tc and interfering gamma rays from one gram of irradiated plant tissue: NaI spectrometry. (Neutron flux = 6 × 10^{12} n/cm^2-sec, time of counting = 15 minutes, time of irradiation = 16 hours, source-to-detector distance = 10 cm)

Product nuclide	Energy of gamma ray, keV	Time of decay, hours	Counts in peak, N_p
^{197}Hg	72	0	2930
		8	2690
		24	2265
^{131}Ba	126	0	719
		8	706
		24	679
^{75}Se	134	0	22650
		8	22600
		24	22525
^{187}W	134	0	19936
		8	15824
		24	9969
^{99m}Tc	142	0	1845
		8	737
		24	117
^{114m}In	192	0	41
		8	41
		24	41

used to predict the proximate peak interferences in the gamma spectrum. Two basic irradiation alternatives were considered. The first was a one-hour irradiation at a flux of about 8 × 10^{12} n/cm^2-sec, followed by a 24-hour decay before counting Mn, a 48-hour decay for Cu, a 1-week decay for Mo , and a 2-week decay for Fe and Zn. The second was a short irradiation of about 2 minutes at a flux of 4 × 10^{13} n/cm^2-sec followed by a 30-minute decay (including unloading

Table VII. Calculated number of counts in the full energy peak for ^{99m}Tc and interfering gamma rays from one gram of irradiated plant tissue: NaI spectrometry. (Neutron flux = 6 × 10^{12} n/cm^2-sec, time of counting = 15 minutes, time of decay = 50 hours, source-to-detector distance = 10 cm)

Product nuclide	Energy of gamma ray, keV	Time of irradiation, hours	Counts in peak, N_p
^{197}Hg	72	8	597
		12	1315
^{131}Ba	126	8	322
		12	4809
^{75}Se	134	8	61
		12	100
^{187}W	134	8	2623
		12	3725
$\underline{^{99m}\text{Tc}}$	142	8	1.96
		12	3.82
^{114m}In	192	8	20
		12	30

the rabbit, safety monitoring, and transporting from the ALRR to the Ge(Li) detector, at least 30 minutes average time) and then counting for ^{101}Mo and ^{101}Tc.

For the first alternative, the predicted peak interferences were as follows:

1) ^{56}Mn: none.

2) ^{64}Cu: any positron emitter at the 511.0-keV line; for the 1345.8-keV line, ^{24}Na at 1368.4 keV with an unpredictable amount due to the contaminant nature of Na.

Table VIII. Calculated number of counts in the full energy peak for ^{101}Mo and interfering gamma rays from one gram of irradiated plant tissue: NaI spectrometry. (Neutron flux = 6×10^{12} n/cm^2-sec, time of counting = 15 minutes, source-to-detector distance = 10 cm)

Product nuclide	Energy of gamma ray, keV	Time of irradiation, minutes	Time of decay, minutes	Counts in peak, N_p
^{27}Mg	1010	5	1	397,000
		29.2	29.2	146,300
$\underline{^{101}\text{Mo}}$	1024	5	1	117
		29.2	29.2	109
^{66}Cu	1040	5	1	85,729
		29.2	29.2	3,696
^{82}Br	1044	5	1	4,100
		29.2	29.2	23,600
^{65}Ni	1114	5	1	208
		29.2	29.2	1,015
^{82}Br	1475	29.2	1	10,135
		29.2	14.6	10,090
$\underline{^{101}\text{Mo}}$	1560	29.2	1	124
		29.2	14.6	65
^{140}La	1597	29.2	1	821
		29.2	14.6	818
$\underline{^{101}\text{Mo}}$	2030	29.2	1	143
		29.2	14.6	75
^{116m}In	2080	29.2	1	89,624
		29.2	14.6	75,721
^{56}Mn	2120	29.2	1	4,243,200
		29.2	14.6	3,992,600

Table IX. Predicted activities of specific nuclides in disintegrations per second for variable irradiation and waiting times for a one gram sample of soybean tissue, flux of 10^{10} n/cm²-sec

Product nuclide	Time of irradiation	Half-life	Time of decay						
			0	1 hour	8 hours	24 hours	48 hours	1 week	2 weeks
^{24}Na	1 h	15.0 h	1122	1071	775	370	122	0.478	0.0002
^{42}K	1 h	12.4 h	14466	13679	9250	3783	1037	1.26	0.0001
^{56}Mn	1 h	2.576 h	27483	21000	3194	43.2	0.067	—	—
^{59}Fe	1 h	45.6 d	0.025	0.025	0.025	0.025	0.024	0.024	0.021
^{64}Cu	1 h	12.8 h	313	297	203	85	23	0.035	$4(10)^{-6}$
^{65}Zn	1 h	245 d	0.052	0.052	0.052	0.052	0.051	0.050	0.049
^{82}Br	1 h	35.34 h	NC[a]	NC	NC	NC	22.9	2.18	0.08
^{99}Mo	1 h	66.7 h	0.022	0.022	0.021	0.018	0.014	0.0039	0.0007
^{99m}Tc	1 h	6.04 h	0.0018	0.0035	0.013	0.018	0.015	0.0043	0.0008
^{187}W	1 h	23.9 h	NC	NC	NC	NC	0.26	0.008	0.00006
TOTAL		—	69310	37177	13699	4495	1409	163	115

[a]Not calculated.

Table IX. (Continued)

Product nuclide	Time of irradiation	Half-life	Time of decay			
			0	15 minutes	30 minutes	1 hour
^{24}Na	2 m	15.0 h	38	38	37	36
^{27}Mg	2 m	9.5 m	256	86	29	3
^{42}K	2 m	12.4 h	495	488	482	468
^{56}Mn	2 m	2.576 h	1040	972	909	795
^{59}Fe	2 m	45.6 d	0.0008	0.0008	0.0008	0.0008
^{64}Cu	2 m	12.8 h	10.7	10.6	10.4	10.1
^{65}Zn	2 m	245. d	0.0017	0.0017	0.0017	0.0017
^{69m}Zn	2 m	13.8 h	0.058	0.067	0.074	0.084
^{101}Mo	2 m	14.6 m	0.100	0.051	0.025	0.006
^{101}Tc	2 m	14.0 m	0.005	0.040	0.038	0.017
TOTAL		—	21518	1780	1556	1362

3) ^{99}Mo at 739.7: ^{82}Br at 776.5 keV; relative count rate was predicted as 1 to 3400, Mo to Br.

4) ^{99m}Tc at 140.4: ^{187}W at 134.2 keV; relative count rate was predicted as 4 to 1, Tc to W.

5) ^{59}Fe at 1291.5: ^{82}Br at 1317.1 keV; relative count rate was predicted as 1 to 2.5, Fe to Br.

6) ^{59}Fe at 1099.3: ^{65}Zn at 1115.5 keV; relative count rate was predicted as 1 to 2.3, Fe to Zn.

7) ^{65}Zn at 1115.5: see 6) above.

For the second alternative for Mo, the predicted peak interferences were as follows for counting starting after a 30-minute decay:

1) ^{101}Mo at 192.0: ^{27}Mg at 170.8 keV; relative count rate was predicted as 1 to 40, Mo to Mg.

2) ^{101}Mo at 506.0: ^{69m}Zn at 439.1 keV; relative count rate was predicted as 1 to 15, Mo to Zn.

3) ^{101}Tc at 306.8: ^{42}K at 312.9 keV; relative count rate was predicted as 1 to 3, Tc to K.

Since the short irradiation predictions were not particularly favorable for Mo determinations, and because of the time problems in safety monitoring and transporting the irradiated samples from the ALRR to the Ge(Li) detector, the longer irradiation and decay times and the longer half-lives of ^{99}Mo/^{99m}Tc were used for the initial experimental conditions.

B. Cleaning Polyethylene Irradiation Vials and Glassware

Distilled, demineralized (clean) water used in this work was
obtained from the shield experiment tank inlet stream of the UTR-10
reactor. This water was passed through a resin bed water softener and
distilled with a Barnstead Water Still before being placed into the
shield tank. The water in the shield tank was circulated through a
metal screen filter, a string-fiber filter, and a mixed bed resin de-
mineralizer. The water used in this work and referred to herein as
clean water was obtained from the outlet of the demineralizer. The
measured resistivity of this water during the period of use in this
research varied from 1.0 to 1.27 microhms.

The polyethylene vials in which the samples and standards were
placed for irradiation and counting were 2-1/4 inches long by 21/32 inch
in diameter with a hinged snap lid. They were cleaned prior to and
after filling by a method similar to that described by Romberg [51].
The open vials were stirred in 7M nitric acid for at least five minutes
and then in clean water for another five minutes. They were then air
dried between fresh paper towels to reduce contamination from the
atmosphere. They were dried for at least an hour before standard
solutions were placed into them and for more than twelve hours before
the plant tissue was transferred.

All glassware used in this research was cleaned with aqua regia
or concentrated nitric acid before the initial use, followed with
scrubbing in hot, soapy water (Sparkleen detergent) and a thorough
rinsing with tap water and then clean water. The inside of the pipettes

could not be cleaned with a brush, but they were otherwise cleaned in
the same manner.

C. Preparing Standards and Samples for Irradiation

The five elemental standards were prepared from the following
compounds: Ferric Nitrate = $Fe(NO_3)_3 \cdot 9H_2O$; Manganous Sulfate Mono-
hydrate = $MnSO_4 \cdot H_2O$; Zinc Acetate, Dihydrate = $(CH_3COO)_2Zn \cdot 2H_2O$;
Cupric Sulfate, Anhydrous = $CuSO_4$; and Molybdenum Trioxide = MoO_3.
The compounds were weighed with a Christian Becker Chainomatic Balance,
Model AB-4, Serial Number A15881, and Class S weights manufactured
by Henry Troemner Inc., Philadelphia. The balance and weights were
calibrated [17] by a set of Ainsworth Class M weights, Serial Number
19357, obtained from the Ames Laboratory, AEC, which were calibrated
in 1953 and recalibrated in 1969 (mg weights only). During weighing
operations, the Ferric Nitrate noticeably picked up water from the
atmosphere. The weight and its uncertainty were estimated appropriately.

Weighed amounts of the compound were dissolved in a 1 liter volume
of clean water except for the MoO_3 which included 95 ml of NH_4OH in
the liter of solution. The Mo was further diluted by 50 ml of the
original solution to 1 liter of clean water. All bulk standard solu-
tions were prepared so that 1-ml or 0.5-ml aliquot portions would
contain about the same mass of the unknown element as expected to be
in one gram of the plant material. Table X contains the details of
the standard preparations with the masses and standard deviations
calculated from Eq. (25).

Table X.   Prepared standards

Element	Mass of compound, grams	Volume to which diluted, ml	Concentration ± standard deviation, µg per ml		Aliquot portion irradiated, ml	Mass irradiated, $m_s \pm \sigma_{m_s}$, µg		Standard deviation, %
Fe	0.9027	1000.	123.9	2.11	1.00 ± 0.017	123.91	2.11	1.70
Mn	0.1241	1000.	40.30	0.688	1.00 ± 0.017	40.30	0.688	1.71
Zn	0.1513	1000.	44.97	0.780	0.50 ± 0.01	22.5	0.46	2.03
					1.00 ± 0.017	44.97	0.780	1.74
Cu	0.1398	1000.	55.66	0.954	0.50 ± 0.01	27.8	0.56	2.00
Mo	0.1166	1000., then 50:1000	3.88	0.067	0.50 ± 0.01	1.9	0.04	2.0
					1.00 ± 0.017	3.88	0.067	1.73
Mn (for January irradiations)						128.20	2.19	1.71

Each bulk standard container was shaken thoroughly and about 5 ml poured into a clean 30 ml or 50 ml beaker. The solution was pipetted from this beaker and transferred to a clean polyethylene vial which was held upright in another small beaker. Aliquot portions of all five elemental standard solutions were placed into one vial with one pipette. This pipette was cleaned thoroughly between transfers of different elemental aliquots by passing clean water through it several times and then was dried by suction. A "to-deliver" pipette was used, therefore the amount clinging to the walls of the pipette contributed a negligible error.

The initial irradiation with a multiple-element standard resulted in a precipitate forming in the standard vial. The addition of 0.5 ml concentrated nitric acid in subsequent standards prior to heat sealing and irradiation prevented recurrence of a precipitate.

During the course of the irradiations, it was suspected that the method of cleaning the pipette could be unsatisfactory if it allowed transfer of small amounts of the previous element during subsequent transfers. This possibility was never confirmed positively, but the cleaning procedure was changed to include drawing concentrated nitric acid into the pipette midway in the flushing operations with the clean water and increasing the amount of water flushing after the nitric acid was drained out of the pipette.

A weighing procedure was developed by the author to assure uniform, efficient operations. The tare weight consisted of a clean 30 ml beaker holding a clean polyethylene vial in an upright position. The beaker and vial were removed from the balance pan, the vial removed

from the beaker, and the sample material poured into the vial. Tissues, paper towels, and forceps were used to handle the vial to reduce moisture and other contamination. Care was taken so no extraneous material entered the vial. A funnel prepared from Whatman #2 Qualitative filter paper was used to direct the material into the vial. The outside surfaces of the vial were brushed clean of all material before weighing to reduce errors. The vial of material was placed in the beaker and both were weighed to obtain the gross weight.

After the weighing was completed, the vial lid was snapped shut, an identifying notch was cut into the bottom edge, and the vial was heat sealed by rotating the lid-end in a conical indentation in a hot metal slab.

Care was taken to assure that the volumes of the plant material used were as identical as possible to that of the aqueous standard volumes. The plant material could be tapped down into a minimum volume in the sealed vials, and assurance was made that the volume could visually be made equal to that of the standard volume.

After the vial had cooled, moderate pressure was placed on the sides of the vial with gloved fingers to assure a tight seal had been formed. The seals of the standard vials were checked also. The sealed vials were recleaned with nitric acid and clean water as described above. After the vials had dried, they were placed in plastic bags and taken to the reactor facility for loading into the rabbit.

For irradiations in the UTR-10 reactor, one standard vial and one unknown sample vial were placed adjacent to each other in the rabbit. At the ALRR facility, four vials were loaded into a large,

plastic rabbit for irradiation in facility R-4. These four vials consisted of either two standards and two unknowns or one standard and three unknowns. In the irradiation of the water samples and empty vial, five vials were placed in the large rabbit. The bottoms of the vials were aligned and kept in position with packing material placed in the rabbits. In the ALRR rabbits, the cluster of vials (four or five to a cluster) was left in the plastic bag and was held together with a rubber band. The plastic bag provided a packing between the vials and the inside circumference of the rabbit, thus holding the vials snuggly in position.

D. Irradiations

Three samples of pulverized plant material were obtained from the ISU Agronomy Department [14] to be analyzed for the five elements. The first sample was a mixture composed of portions of several individual soybean plot samples. This bulk sample was mixed thoroughly to approach homogeneity in the sub-sampling. A total of seven sub-samples were taken from this bulk sample and irradiated in January and March, 1972. The January irradiation was in the UTR-10 reactor with one standard and one sample for the determination of Mn only. Three March irradiations were done in the ALRR, each with two standards and two samples for the determination of the five elements. Multiple countings were performed on some of these seven sub-samples for a total of ten replicate determinations of Mn and sixteen of Fe and Zn. There

were no determinations for Cu and Mo for reasons discussed in the fol-
lowing sub-section.

The second and third samples obtained from the Agronomy Department
consisted of pulverized corn and soybean tissue, respectively. Each
bulk sample was mixed thoroughly to approach homogeneity in the sub-
samples withdrawn for irradiation. Three sub-samples of each were
irradiated in April, 1972, in the ALRR along with one standard con-
taining Fe, Mn, and Zn; no attempt was made to determine Cu and Mo.
Due to multiple countings, there were five replicates of soybean and
four replicates of corn for Mn and three replicates of each for Fe
and Zn.

In addition, three samples of water, one empty vial, and one
standard were irradiated in April, 1972, in the ALRR to determine
the approximate concentration of Fe, Mn, and Zn in the water and ir-
radiation vials. The water sources were ordinary tap water from the
Nuclear Engineering Laboratory, distilled and demineralized (clean)
water from the UTR-10 reactor shield experiment tank, and water passed
through an Illinois Water Treatment Company Double Ion Exchanger
belonging to the ISU Radiological Services Group (RSG). Each sample
contained four ml of water, the approximate amount in the standards
used in this research. The UTR-10 shield tank water, which was used
to prepare the bulk standards, was pipetted into the vial with the
pipette previously used in preparing standards and then cleaned by
the method described previously without the use of the concentrated
nitric acid. The tap water and RSG water were not pipetted but were
placed directly into the vials from the tap and the outlet tube of

the ion exchanger, respectively. Results of these irradiations are contained in Section VI.

E. Activity Measurements

Initial activity measurements with the Nuclear Data Series 2200 System Analyzer were taken with the amplifier coarse gain at 20 and the fine gain at 926. The Analog to Digital Converter conversion gain was 1024 and the Digital Zero Shift was not used. The source to detector distance was adjusted so the dead time was 10% or less for all counting. The timer was in the live time mode throughout this work.

The original amplifier setting resulted in a calibration factor of about 3.06 keV per channel at the Mn 846.7 line. At this setting, the 1024 channel memory covered energies from about 100 keV to about 2760 keV. This calibration factor resulted in so few channels per peak that the amplifier coarse gain was changed to 50 and the fine gain to 879. This resulted in a calibration factor of 1.17 keV per channel at the Mn 846.7 line and a memory range from 65 keV to 1170 keV. This range included all the peaks of interest in this work except for the 1291.5 line of ^{59}Fe, and 1811.2 line of ^{56}Mn, the 1345.8 line of ^{64}Cu, and the 1532.7 and 2089.0 lines of ^{101}Mo. These were all of secondary importance, except the ^{64}Cu gamma at 1345.8 keV, so that most of the measurements were taken with these settings. The Digital Zero Shift was set to 512 in order to get the ^{64}Cu gamma within the memory range for Cu analysis.

Manganese was quantitatively determined after a 19- to 28-hour
decay period with the 846.7 keV gamma which had a peak height to
^{42}K Compton plateau height ratio varying from 2.5:1 to 6:1 depending
on the length of decay and counting. After a 1-, 2-, or 3-week decay
period, Fe and Zn were quantitatively determined with the 1099.3 and
1115.5 gammas, as predicted earlier in this section. The peak
height to background ratios for the ^{59}Fe gamma varied from 5:1 to 8:1
depending on the decay and counting times used. For the ^{65}Zn, peak
height to background ratios varied from 14:1 to 20:1. These ratios
for Fe and Zn were obtained with 13- to 14-day decay times and 9-
to 11-hour counting times.

A resolution problem occurred in the case of Zn at the 1115.5 keV
gamma due to a lower intensity interference peak from either the
1121.2 keV gamma of 115-day ^{182}Ta or the 1120.5 keV gamma of 83.9-day
^{46}Sc in the spectra of unknown plant material. The interference did
not occur in the standard spectra. The identification of this inter-
ference was not determined, although the energy calibration suggests
it was ^{46}Sc. Since radiochemical separation was not employed, the
presence of the lower intensity inteference peak with a long half-life
caused problems in determining the Zn peak area. Since Wasson's method
of peak area determination uses only a portion of the channels, toward
the center of a peak, those channels at the edge of the Zn peak containing
primarily pulses from the interference gamma were discarded in deter-
mining the Zn peak area. It is quite likely, however, that the Zn
concentrations reported in this work are too high due to the presence
of the interference pulses in the channels used for the Zn peak areas.

No Mo or Tc peaks appeared above the Compton background of ^{42}K in the unknown plant material spectra. The spectra of the standards, which did not contain K or Na, resulted in a ^{99m}Tc peak at 140.4 keV which had a peak height to Compton background height ratio of about 4.7:1 for a decay time of 5 days and a counting time of 1 hour. There was no peak at the 739.7 line of ^{99}Mo in the standard spectra counted under the same conditions.

Difficulties were encountered with Cu, also, since the positron annihilation gammas were about 1000 times as intense as expected for Cu alone in the amounts believed to be in the soybean matrix. Thus it was evident that there was considerable positron annihilation from sources other than ^{64}Cu. Much of this probably resulted from pair production in the detector crystal from the ^{42}K and ^{24}Na gammas of energies 1524.7 keV, 1368.4 keV, and 2754.1 keV.

The only other gamma radiation which could be used to detect the 12.8-hour ^{64}Cu was at 1345.8 keV with an emission rate of 0.5% of the nuclide's decays. This gamma was observed in the standard spectrum but was not observed in the unknown soybean matrix spectrum due to the Compton edge background from ^{42}K. The short half-life of ^{66}Cu (5.1 minutes) precluded detection of this nuclide after the 19- to 28-hour decay period.

The pulse height spectra for various plant tissue replicates and standards were recorded on teletype paper. Some spectra also were punched onto paper tapes for later use in the ICPEAX program (Appendix C). The data on the teletype print-out were manually processed for input to the MASS Program for the calculations of the masses and

associated uncertainties of the unknowns. The results are in

Section VI. Representative spectra obtained in this investigation are

in Fig. 2 through Fig. 5.
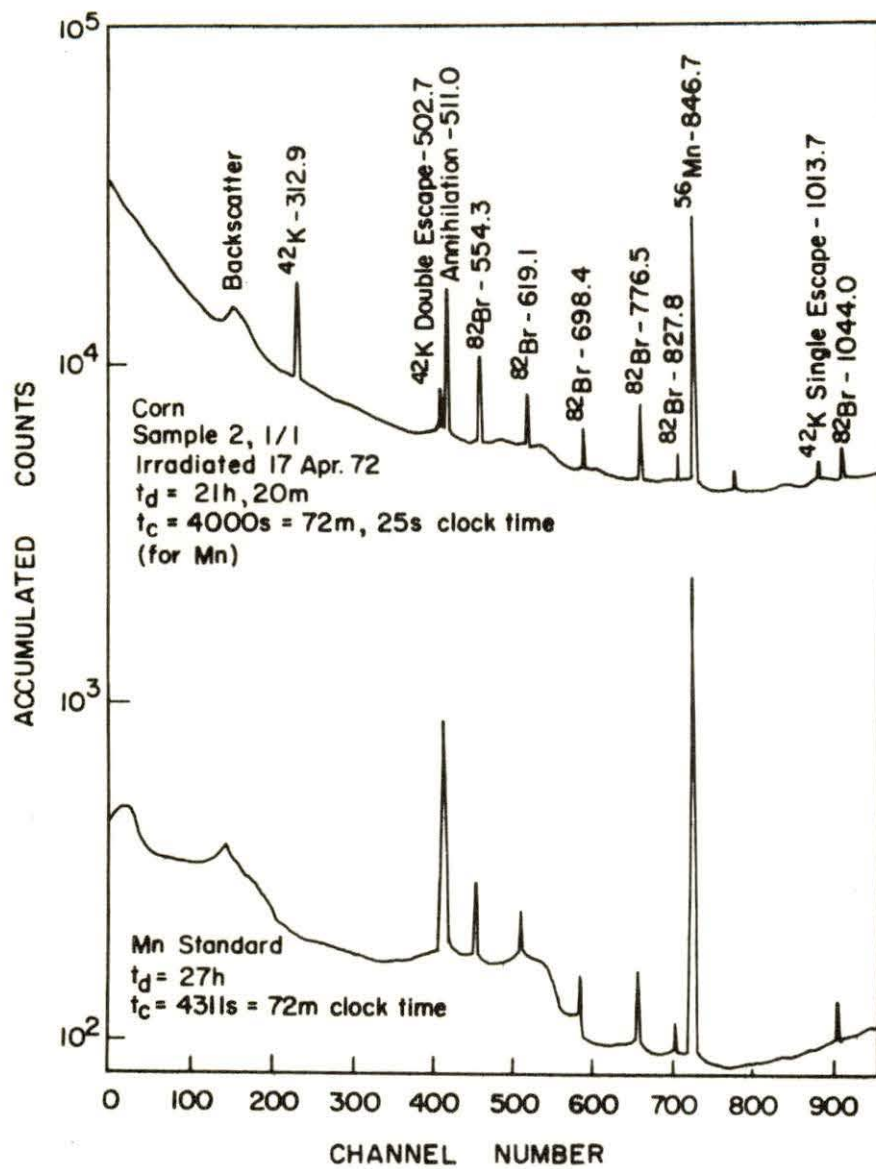
Fig. 2. Spectra for Mn analysis.
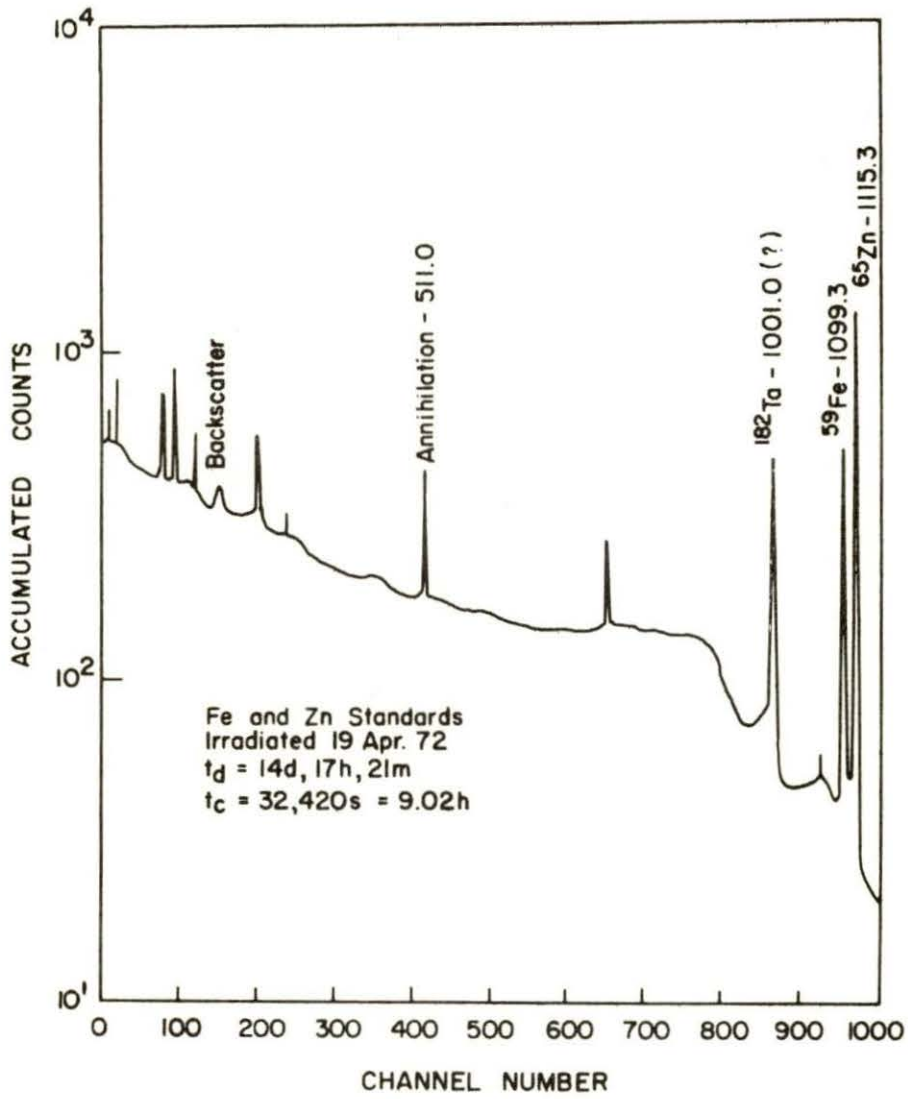
Fig. 3. Spectrum of Fe and Zn standards.
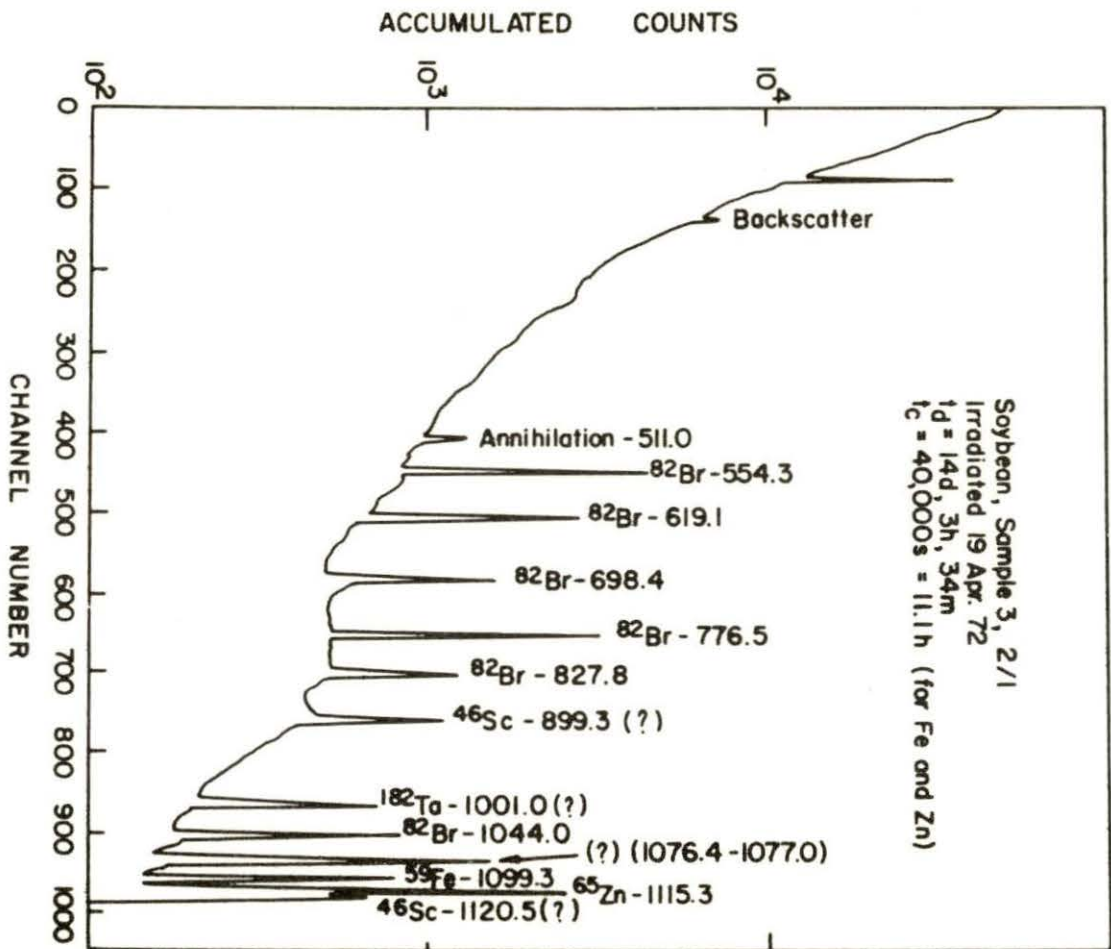
Fig. 4. Spectrum of Fe and Zn unknowns.

The figure shows a plot of ACCUMULATED COUNTS (vertical axis, logarithmic scale from 10^2 to 10^4) versus CHANNEL NUMBER (horizontal axis, from 0 to 1000).

Annotations on the figure:

Soybean, Sample 3, 2/1
Irradiated 19 Apr. 72
t_d = 14d, 3h, 34m
t_c = 40,000s = 11.1h (for Fe and Zn)

Backscatter

Annihilation - 511.0
^{82}Br - 554.3
^{82}Br - 619.1
^{82}Br - 698.4
^{82}Br - 776.5
^{82}Br - 827.8
^{46}Sc - 899.3 (?)
^{182}Ta - 1001.0 (?)
^{82}Br - 1044.0
(?) (1076.4 -1077.0)
^{59}Fe - 1099.3
^{65}Zn - 1115.3
^{46}Sc - 1120.5 (?)

64

Fig. 5. Full-energy peaks of Fe and Zn with interference.

VI. DISCUSSION OF RESULTS

The results of the analyses for the various replicates for Fe,
Mn, and Zn are in Tables XI, XII, and XIII. Included is the un-
certainty (standard deviation) of each individual determination
established from propagation of error theory, Eq. (27). The coeffi-
cient of variation (CV) is defined as 100 σ/μ which is the standard
deviation as percent of the mean value. The unknown mass and its
standard deviation, calculated from Eq. (27), are estimators of the
population parameters μ and σ which are used for the calculation of the
CV values based on the single determinations. At the bottom of the
results for each sample are listed the values of $\bar{x}$ and s (the
sampling mean and sampling standard deviation) and the resulting CV
calculated from a statistical analysis of the sample replicate data
using standard methods [2].

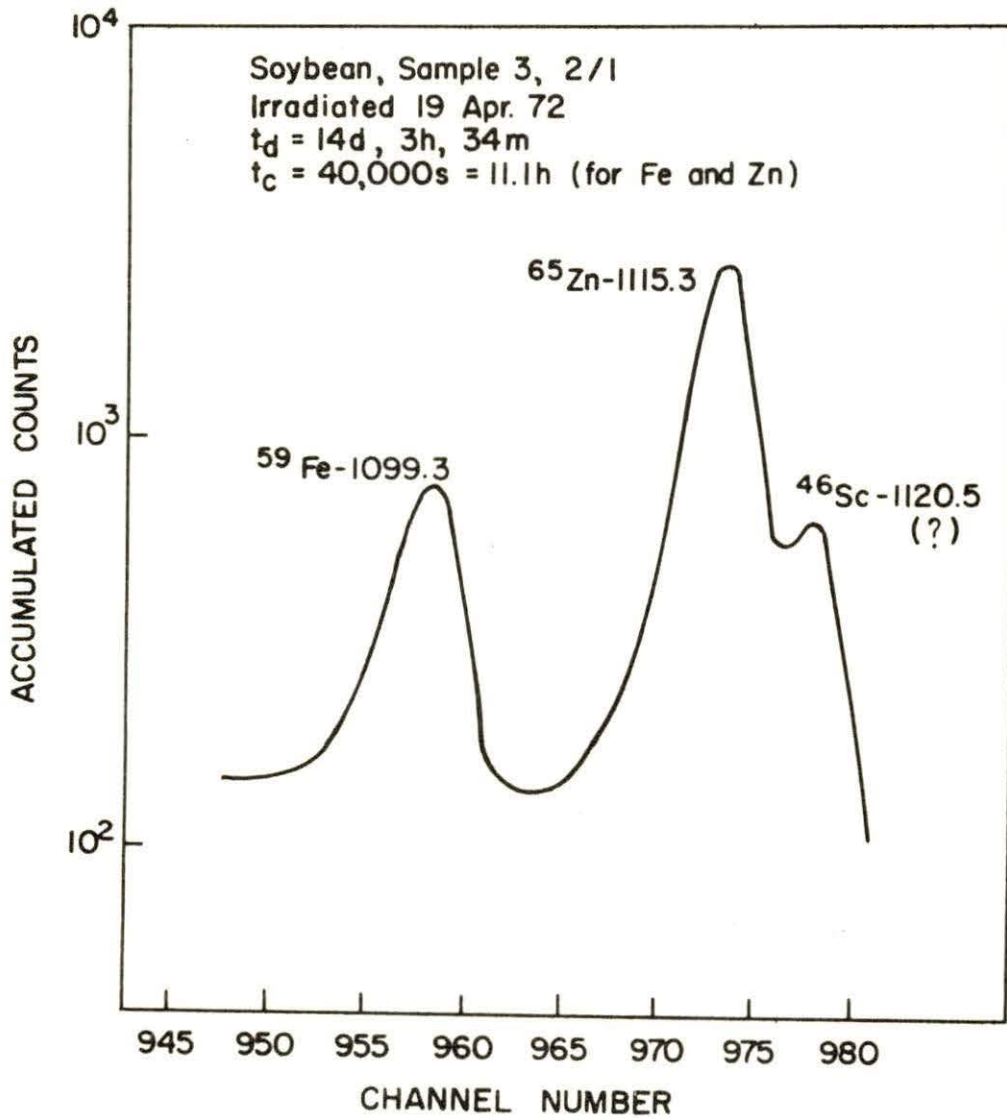The data from these three tables are displayed graphically in
Figs. 6, 7, and 8. The graphs each consist of three parts repre-
senting the three samples. Along the bottom of each graph is indi-
cated for each replicate the time of decay (t_d) elapsed before counting
was started. The counting time is depicted by the circles, squares,
or other symbols at the point of the determined value of the mass of
the unknown element. These graphs show that the smaller uncertainties
occurred for decay times of 13 to 14 days for Fe and Zn and 19 to 21
hours for Mn.

Figures 9, 10, and 11 are graphs of these uncertainties as a func-
tion of decay and counting times for the determinations of the three

Table XI. Analyses of Fe

Sample	Sub-sample/ replicate	t_d, days	Mass ± standard deviation, ppm		CV,[a] %	Assay from atomic absorption, ppm
1	1/1[b]	12	150.0	22.4	14.9	NA[d]
	1/2[b]	19	145.2	16.6	11.4	
	2/1[b]	12	118.7	18.5	15.6	
	2/2[b]	20	116.0	14.6	12.6	
	3/1	7	115.7	22.2	19.2	
	3/2	8	123.3	19.7	16.0	
	3/3	14	118.9	12.6	10.6	
	4/1	7	81.3	21.5	26.4	
	4/2	8	90.3	22.7	25.2	
	4/3	14	112.2	13.0	11.6	
	5/1	4	177.1	91.5	51.6	
	5/2	13	107.4	8.7	8.1	
	5/3	20	94.6	16.9	17.8	
	6/1	4	234.5	91.2	38.9	
	6/2	13	120.1	9.4	7.9	
	6/3	19	109.9	15.3	14.0	

$\bar{x}$ = 125.9, s = 37.2, CV = 29.5%

Sample 1 less replicates 1/1, 1/2, 5/1, 6/1:
$\bar{x}$ = 109.0, s = 13.3, CV = 12.1%

Sample	Sub-sample/ replicate	t_d, days	Mass ± standard deviation, ppm		CV,[a] %	Assay from atomic absorption, ppm
2 (corn)	1/1[c]	13	218.0	15.7	7.2	246[e]
	2/1[c]	13	246.6	17.5	7.1	
	3/1	13	205.7	14.8	7.2	

$\bar{x}$ = 223.4, s = 21.0, CV = 9.4%

[a]Coefficient of variation, % = 100 σ/μ (standard deviation/mean).

[b]Precipitate formed in standard; agitated every 15 minutes during counting.

[c]Precipitate formed in standard, agitated every hour during counting.

[d]None available.

[e]Minnesota Valley Testing Laboratory, New Ulm, Minn.

Table XI.   (Continued)

Sample	Sub-sample/ replicate	t_d, days	Mass ± standard deviation, ppm		CV,[a] %	Assay from atomic absorption, ppm
3	1/1[c]	14	120.3	9.12	7.58	193[e]
	2/1	14	118.3	8.75	7.40	
	3/1	15	106.7	8.15	7.63	

$\bar{x}$ = 115.1, s = 7.32, CV = 6.4%

elements.   It can be noted from these graphs that the "optimum" counting conditions used in this research and resulting in the least uncertainty of the determinations are as follows:

1)   Decay time of 13 days and counting time of 11 hours for
      Fe (CV $\simeq$ 8.0%) and Zn (CV $\simeq$ 5.9%).

2)   Decay time of 19 to 23 hours and counting time of 35 to
      72 minutes for Mn (CV $\simeq$ 5.6%).

Since 11 hours may be considered excessive (too costly) for the additional precision gained, the data show that one can decrease the counting time and still expect to achieve acceptable uncertainties. For Fe, a CV of about 11% was obtained after a 14-day decay and a 5-hour count, and a CV of less than 16% was obtained after a 12-day decay and a 4-hour count.   The same conditions for Zn, which was determined in the same spectrum as was the Fe, resulted in CV values of less than 7%.

The data indicate that a decay period longer than the "optimum" results in a greater uncertainty.   A 20-day decay period for Fe and

Table XII. Analyses of Mn

Sample	Sub-sample/ replicate	t_d, hours	Mass ± standard deviation, ppm		CV,[a] %	Assay from atomic absorption, ppm
1	1/1[b]	34[c]	42.63	2.29	5.37	NA[d]
	1/2[b]	53[c]	41.11	2.20	5.34	
	2/1[b]	25	58.72	5.01	8.53	
	2/2[b]	26	51.19	4.80	9.38	
	3/1	26	39.42	4.83	12.3	
	3/2	27	45.91	5.09	11.1	
	4/1	26	33.11	3.26	9.83	
	5/1	27	40.60	4.12	10.2	
	6/1	21	45.94	2.59	5.64	
	7/1	19	52.36	2.89	5.51	

$\bar{x} = 45.10$, s = 7.42, CV = 16.4%

2 (corn)	1/1[b]	21	126.4	7.02	5.56	164[e]
	2/1[b]	23	135.0	7.62	5.64	
	3/1	20	133.7	7.30	5.46	
	3/2	20	130.5	7.22	5.53	

$\bar{x} = 131.4$, s = 3.84, CV = 2.93%

3	1/1[b]	25	83.58	4.91	5.87	129[e]
	2/1	21	84.53	4.63	5.48	
	2/2	21	82.49	4.58	5.56	
	3/1	23	87.16	4.80	5.51	
	3/2	23	85.05	4.75	5.58	

$\bar{x} = 84.56$, s = 1.75, CV = 2.07%

[a]Coefficient of variation, % = 100 σ/μ (standard deviation/mean).

[b]Precipitate formed in standard; agitated before counting.

[c]Minutes.

[d]None available.

[e]Minnesota Valley Testing Laboratory, New Ulm, Minn.

Table XIII. Analyses of Zn

Sample	Sub-sample/ replicate	t_d, days	Mass $\pm$ standard deviation, ppm		CV,[a] %	Assay from atomic absorption, ppm
1	1/1[b]	12	41.52	2.76	6.66	NA[d]
	1/2[b]	19	41.15	2.54	6.17	
	2/1[b]	12	34.17	2.31	6.77	
	2/2[b]	20	34.63	2.13	6.16	
	3/1	7	32.74	2.70	8.25	
	3/2	8	31.87	2.35	7.38	
	3/3	14	35.63	2.28	6.41	
	4/1	7	35.96	2.76	7.69	
	4/2	8	38.69	2.84	7.35	
	4/3	14	40.43	2.58	6.39	
	5/1	4	38.61	6.68	17.3	
	5/2	13	33.02	1.95	5.89	
	5/3	20	32.19	2.54	7.89	
	6/1	4	31.45	6.29	20.0	
	6/2	13	38.40	2.24	5.85	
	6/3	19	38.69	2.93	7.58	

$\bar{x}$ = 36.20, s = 3.47, CV = 9.57%

Sample	Sub-sample/ replicate	t_d, days	Mass $\pm$ standard deviation, ppm		CV,[a] %	Assay from atomic absorption, ppm
2 (corn)	1/1[c]	13	28.81	1.74	6.05	49[e]
	2/1[c]	13	34.59	2.07	5.98	
	3/1	13	28.67	1.73	6.02	

$\bar{x}$ = 30.69, s = 3.38, CV = 11.0%

Sample	Sub-sample/ replicate	t_d, days	Mass $\pm$ standard deviation, ppm		CV,[a] %	Assay from atomic absorption, ppm
3	1/1[c]	14	32.38	1.91	5.90	46[e]
	2/1	14	30.88	1.81	5.87	
	3/1	15	28.96	1.71	5.89	

$\bar{x}$ = 30.74, s = 1.71, CV = 5.57%

[a]Coefficient of variation, % = 100 σ/μ (standard deviation/mean).

[b]Precipitate formed in standard; agitated every 15 minutes during counting.

[c]Precipitate formed in standard; agitated every hour during counting.

[d]None available.

[e]Minnesota Valley Testing Laboratory, New Ulm, Minn.

Fig. 6. Mass of unknown Fe $\pm$ one standard deviation as a function of decay time and counting time.

Key:

Sub-sample
number

$\quad$ + 1 standard deviation

Mass of unknown

$\quad$ - 1 standard deviation

Counting time:

⊙   11 hours

●   9 hours

⊡   5 hours

△   4 hours

Footnotes:

[a]Mean of replicates for sample 1 $\pm$ 1 standard deviation, excluding replicates 6 and 5 at 4-hour decay and sub-sample 1 at 12- and 19-hour decay.

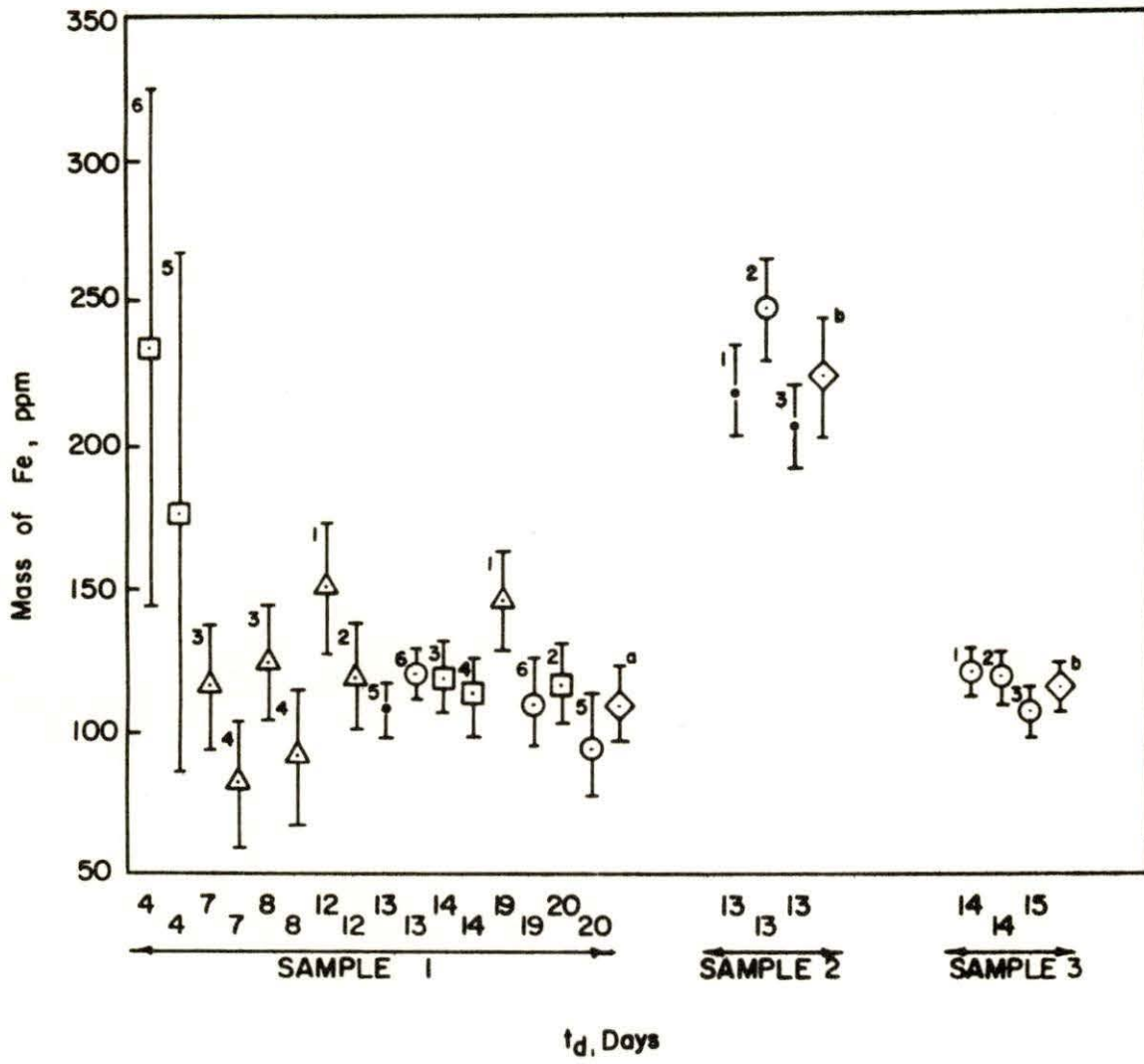[b]Mean of replicates for this sample $\pm$ one standard deviation.

Fig. 7. Mass of unknown Mn ± one standard deviation as a function
of decay time and counting time.

Key:

Sub-sample   + 1 standard deviation
number

                                   Mass of unknown

                                   - 1 standard deviation

Counting time:

⊙   72 minutes

•   57 minutes

▣   35 minutes

△   15 minutes

●   3.67 minutes

Footnote:

[a]Mean of replicates for this sample ± one standard
deviation.
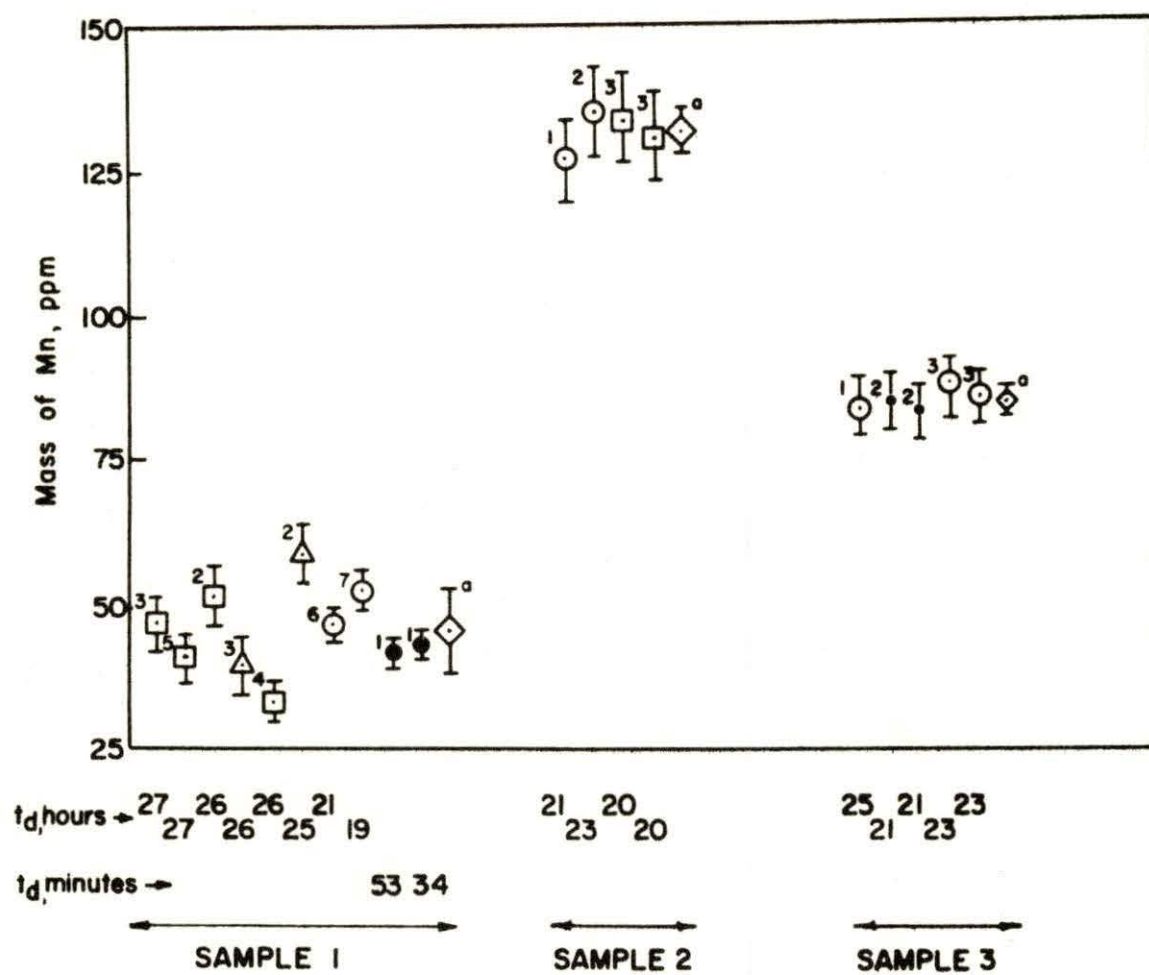
Fig. 8.   Mass of unknown Zn $\pm$ one standard deviation as a function
of decay time and counting time.

Key:

        Sub-sample   + 1 standard deviation
          number

                                          Mass of unknown

                                          - 1 standard deviation

Counting time:

    ⊙   11 hours

    ●   9 hours

    ▣   5 hours

    ▲   4 hours

Footnote:

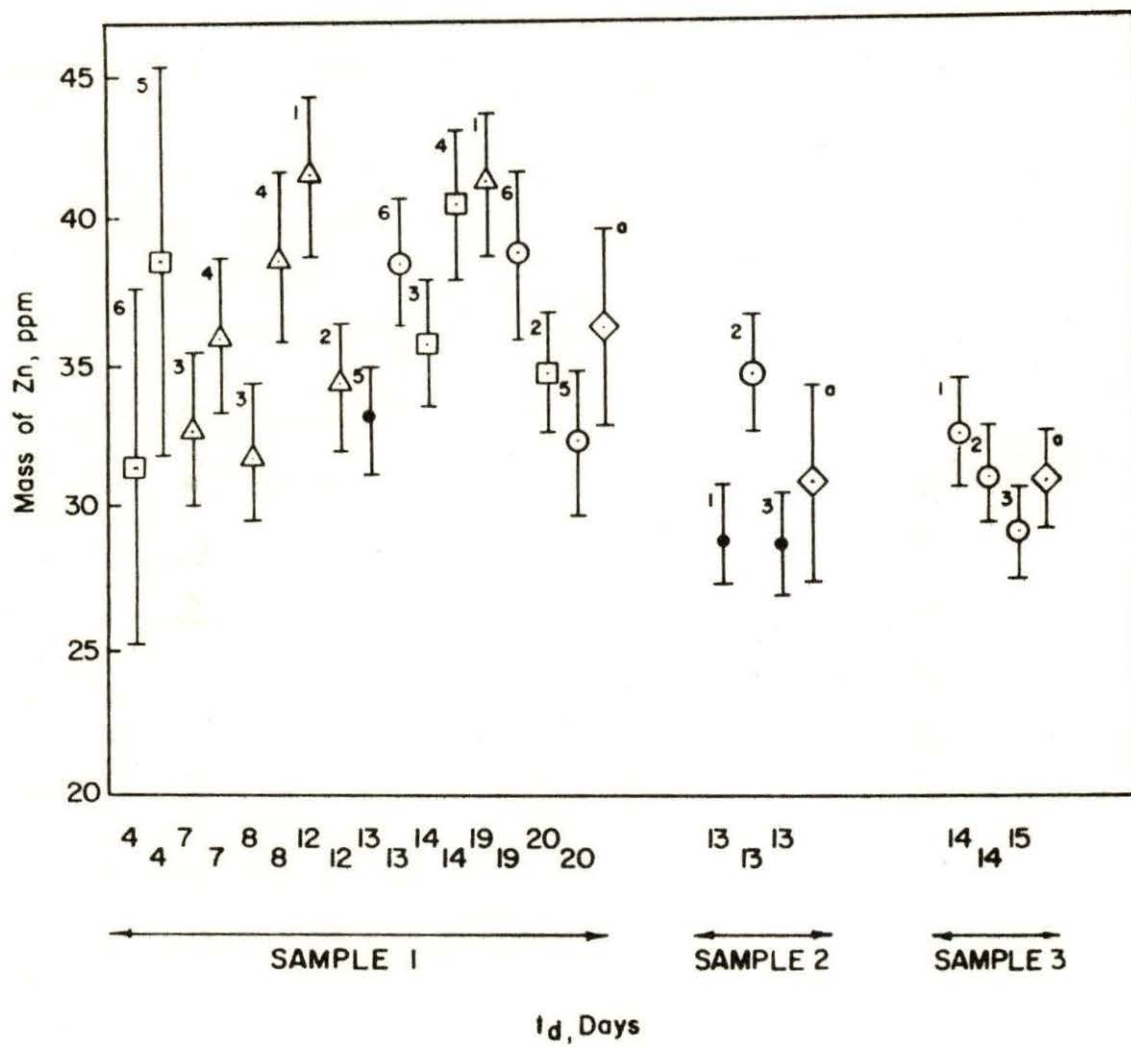   [a] Mean of replicates for this sample $\pm$ one standard
        deviation.

Fig. 9. Coefficient of variation vs time of decay for Fe in sample 1 for various counting times. (Time of irradiation = 1 hour, flux = 10^{13} n/cm^2-sec.)

Counting time:

- ⊙ 11 hours
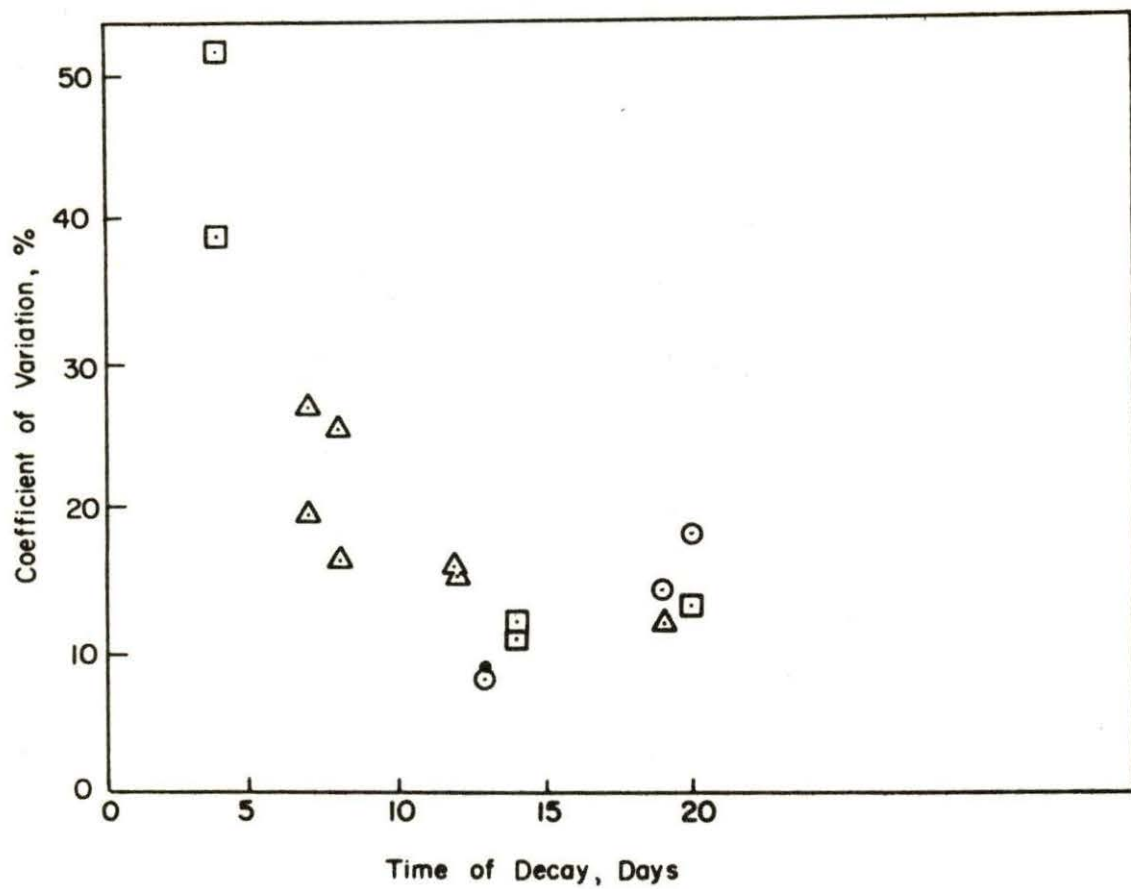- ● 9 hours
- ▣ 5 hours
- ▲ 4 hours

Fig. 10. Coefficient of variation vs time of decay for Mn in samples 1, 2, and 3 for various counting times. (Time of irradiation = 1 hour, flux = 10^{13} n/cm^2-sec.)

Counting time:

⊙ 72 minutes

● 57 minutes

⊡ 35 minutes

△ 15 minutes

● 3.67 minutes

Footnote:

[a]Irradiated in UTR-10 reactor for 15 minutes, flux = 6×10^{10} n/cm^2-sec.
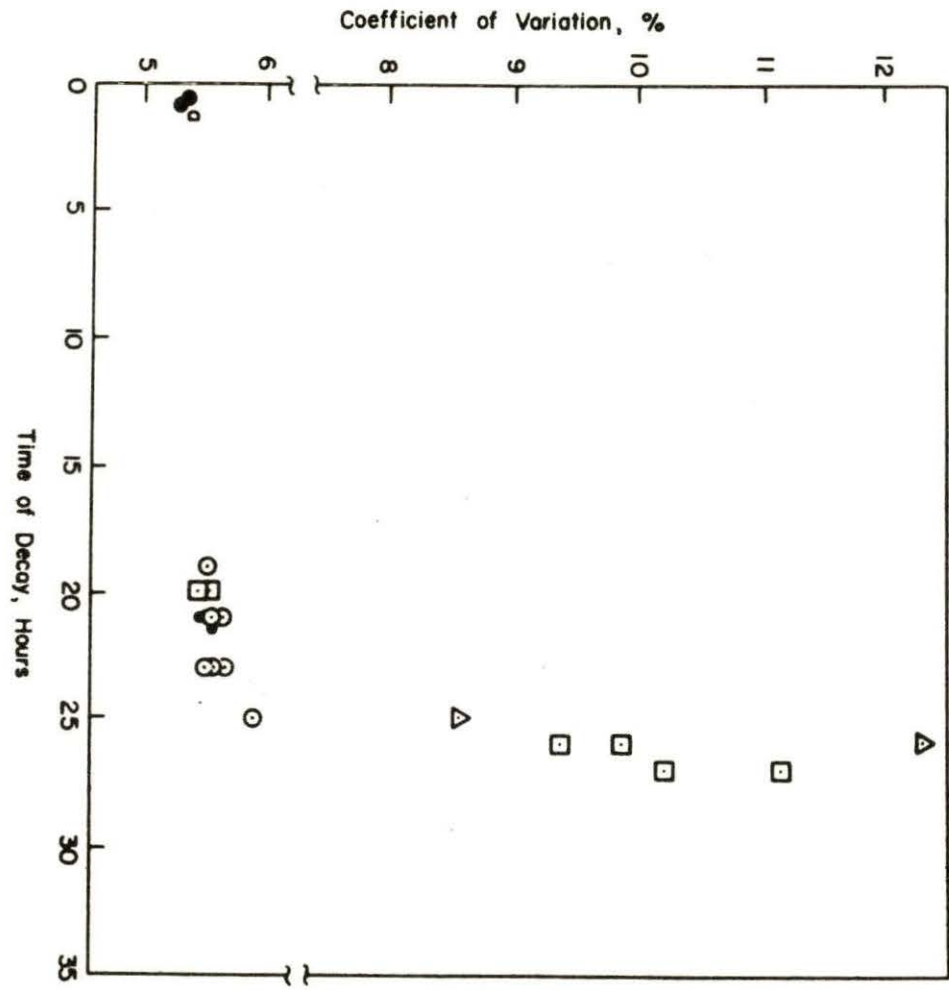
Fig. 11. Coefficient of variation vs time of decay for Zn in sample 1 for various counting times. (Time of irradiation = 1 hour, flux = 10^{13} n/cm^2-sec.)
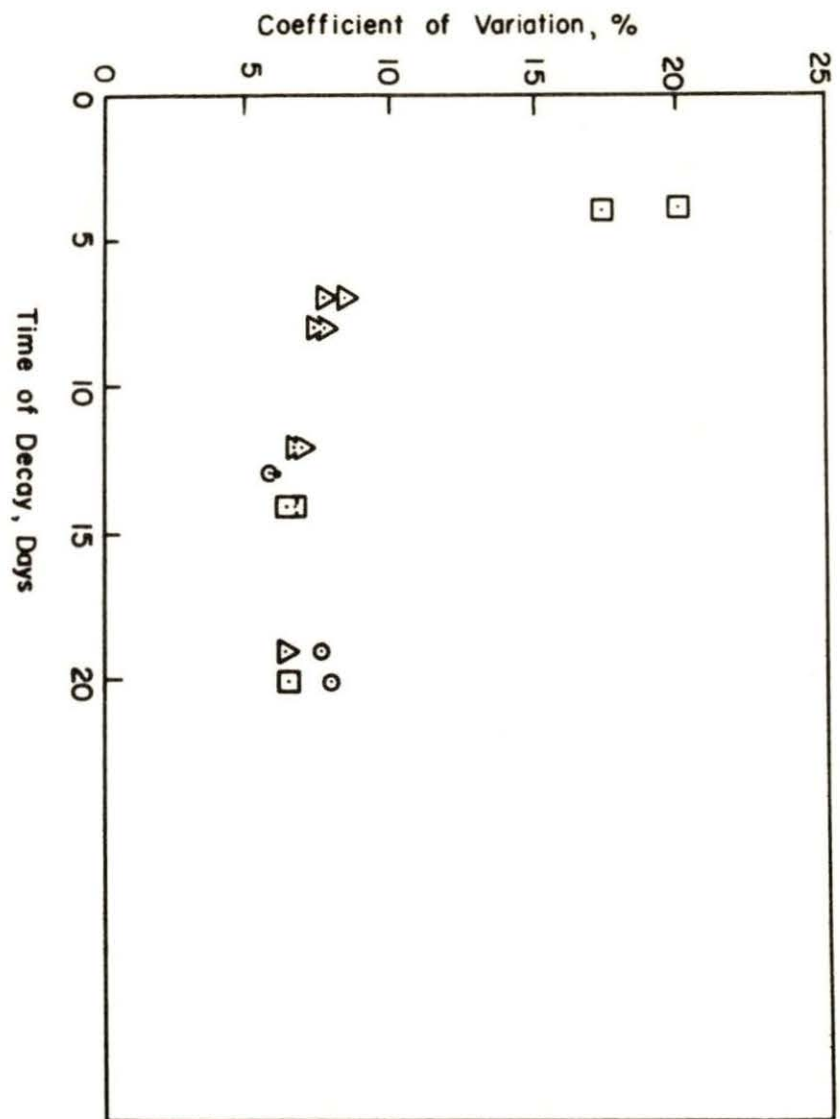
Counting time:

⊙   11 hours

●   9 hours

▣   5 hours

△   4 hours

Zn resulted in an increased CV value, that is, the uncertainty of
the determination increased. This was because the activity of the
Fe and Zn had decreased so that fewer counts were obtained in the
11-hour count at the 20-day decay determination that in a 9-hour count
at the 13-day decay determination. Similarly, for Mn, there were
fewer counts in the 72-minute count at a 25-hour decay time than for
a 57-minute count at a 21-hour decay time. It should be noted that
most of the uncertainty in the Mn determinations after a 25-hour decay
period was due to the shorter counting times of 15 to 35 minutes.
Had the counting times been increased to 72 minutes or longer, the
uncertainty would have been reduced.

Another aspect for consideration is the relative magnitudes of
the contributing uncertainties. These will be illustrated by an
example calculation of the mass of the unknown element and its standard
deviation using Eq. (27) through Eq. (32) and the data for Fe for
replicate 1, sub-sample 1, sample 1. The constants used in the
calculation are as follows:

1) m_s = 123.9 micrograms

2) λ = 0.0000106 minutes^{-1}

3) $\phi_s / \phi_u = \phi R$ = 1.0

4) σ_{m_s} = 2.11 micrograms

5) $\sigma_{t_{d_u}} = \sigma_{t_{d_s}}$ = 0.05 minutes

6) σ_λ = 0.00000005 minutes^{-1}

7) $\sigma_{\phi R}$ = 0.05

8) M_{sample} = 1.1157 grams

9) $\sigma_{M_{sample}}$ = 0.0002828 gram

The activity variables used in the calculations are as follows,

calculated from Wasson's method of peak area determination (Appendix B);

1) C_u = 852.5 counts

2) C_s = 159.0 counts

3) σ_{C_u} = 57.08 counts

4) σ_{C_s} = 19.48 counts

The timing variables used are:

1) t_{d_u} = 12 d, 18 h, 39 m = 18,399 minutes

2) t_{d_s} = 13 d, 3 h, 8 m = 18,908 minutes

3) t_{c_u} = 14,229 seconds

4) t_{c_s} = 3,601 seconds

5) $\sigma_{t_{c_u}}$ = 0.005 × 14,229 = 71.145 seconds

6) $\sigma_{t_{c_s}}$ = 0.005 × 3,601 = 18.005 seconds

The counting times were the live times recorded in seconds by the

Nuclear Data Series 2200 System Analyzer. The uncertainty in

counting times listed in 5) and 6) above is derived from the manu-

facturer's uncertainty value of 0.5% of the elapsed counting time.

From Eq. (27), the mass of the unknown element is calculated as

$$m_u = (123.9)(\frac{852.5}{159.0})\left(\frac{e^{-0.0000106\times18908}}{e^{-0.0000106\times18399}}\right)$$

$$\times \left(\frac{1-e^{-0.0000106\times3601/60}}{1-e^{-0.0000106\times14229/60}}\right) (1.0).$$

m_u = 167.4 micrograms.

From Eq. (29), the decay ratio error term, $\left(\frac{\sigma_{DR}}{DR}\right)^2$, is calculated as

$$(18399 - 18908)^2 (0.00000005)^2 = 6.477 \times 10^{-10} .$$

From Eq. (30), the counting ratio error term, $\left(\frac{\sigma_{CR}}{CR}\right)^2$, is calculated to be equal to 4.99×10^{-5}.

The flux ratio and its uncertainty are assumed to be equal to 1.0 ± 0.05, as discussed in Section III. Therefore, the term

$$\left(\frac{\sigma_{\phi R}}{\phi R}\right)^2 = \frac{0.05^2}{1.0} = 2.5 \times 10^{-3} .$$

From Eq. (31), the area ratio error term, $\left(\frac{\sigma_{C_u/C_s}}{C_u/C_s}\right)^2$, is calculated as

$$\frac{(57.08)^2}{(852.5)^2} + \frac{(19.48)^2}{(159.0)^2} = 1.949 \times 10^{-2} .$$

The final term of the uncertainty calculation is

$$\left(\frac{\sigma_{m_s}}{m_s}\right)^2 = \left(\frac{2.11}{123.9}\right)^2 = 2.91 \times 10^{-4} .$$

The complete uncertainty expression for the mass of the unknown element is then found from Eq. (27) to be

$$\sigma_{m_u} = 167.4 \sqrt{2.91 \times 10^{-4} + 1.949 \times 10^{-2} + 6.477 \times 10^{-10}}$$

$$\overline{4.99 \times 10^{-5} + 2.5 \times 10^{-3}}$$

$$\sigma_{m_u} = 25.0 \text{ micrograms.}$$

This uncertainty in the mass of the unknown is equal to 14.9% of the mass of the unknown. The magnitudes of the uncertainties of the

components of this expression, from the greatest to the least, are

summarized as follows:

1)   Uncertainty in peak area ratio 1.949×10^{-2}

2)   Uncertainty in flux ratio 2.5×10^{-3}

3)   Uncertainty in mass of standard 2.91×10^{-4}

4)   Uncertainty in counting time ratio 4.99×10^{-5}

5)   Uncertainty in decay time ratio 6.477×10^{-10} .

The uncertainty in the peak area ratio of the unknown to the standard

is 14.0% of the area ratio (from $\sqrt{1.949 \times 10^{-2}} \times 100$) which is

greater than the flux ratio uncertainty which was assumed to be 5%.

Equations (32) and (33) are used to calculate the mass of the

unknown element and its standard deviation on a ppm basis. The

calculations are as follows:

$$\text{Mass (in ppm)} = \frac{167.4 \text{ micrograms}}{1.1157 \text{ grams}} = 150.0 \text{ ppm}$$

and

$$\sigma_{\text{Mass}} \text{ (in ppm)} = 150.0 \left[\left(\frac{25.0}{167.4}\right)^2 + \left(\frac{0.0002828}{1.1157}\right)^2 \right]^{1/2}$$

$$= 150.0 \left[(0.149^2 + 0.002534^2) \right]^{1/2}$$

$$\sigma_{\text{Mass}} \text{ (in ppm)} = 22.4 \text{ ppm}.$$

The coefficient of variation (CV) of this determination is 14.9%.

The first term of the standard deviation in ppm is the uncertainty in

the mass of the unknown element which is about 60 times greater than

the second term which is the uncertainty in the mass of the unknown

replicate.

The uncertainty in the mass of the unknown element can be reduced if the area ratio uncertainty is decreased. This can be done by using "optimum" decay and counting times which improve the counting statistics (reduce the standard deviation of the peak areas). For the replicate used in the above example calculation, the unknown had been counted for 4 hours after a 12-day decay period, and the standard had been counted for 1 hour. A different replicate, counted under "optimum" conditions, was replicate 1, sub-sample 1, sample 3. This replicate unknown was counted for 11 hours after a 14-day decay period which resulted in over twice as many counts in the peak as for the replicate in the example calculation. The standard for the second replicate was counted for about 7.9 hours and had nearly 100 times as many counts as the standard which was counted for 1 hour. The resulting area ratio uncertainty for this second replicate was calculated to be $\sqrt{0.29098 \times 10^{-2}}$ $\times\ 100 = 5.41\%$ of the area ratio. This uncertainty is slightly greater than the flux ratio uncertainty of 5%. The overall uncertainty of the ppm assay of this second replicate was calculated to be 7.58%, a decrease from the 14.9% of the first example. This decrease was due almost entirely to the decrease in the area ratio uncertainty due to the improved counting statistics, with a small decrease coming from a decrease of the uncertainty in the mass of the unknown replicate ($\sigma_{M_{sample}}$) from 0.0002828 grams to 0.0001414 grams.

When comparing the single-valued determinations with each other and with the mean and standard deviations computed from a statistical analysis of a number of replicate determinations, one has to make a judgment on which value to accept as the best estimate of the true

concentration of the unknown element. This decision is not unique

to the neutron activation method of quantitative analysis. If various

replicate determinations are available, standard statistical methods

should be used to assist in the analysis. If only one determination

is made for any one sample, this value and its associated uncertainty

are the only data available to the investigator.

From standard statistical treatment of the data obtained for the

three elements in the three samples analyzed in this work, the following

are possible "best estimates" of the elemental concentration in ppm:

1)   Sample 1 (soybeans):

    Fe: 109.0 ± 13.3 ppm, CV = 12.1%

    Mn: 45.1 ± 7.42 ppm, CV = 16.4%

    Zn: 36.2 ± 3.47 ppm, CV = 9.57%

2)   Sample 2 (corn):

    Fe: 223.4 ± 21.0 ppm, CV = 9.40%

    Mn: 131.4 ± 3.84 ppm, CV = 2.93%

    Zn: 30.69 ± 3.38 ppm, CV = 11.0%

3)   Sample 3 (soybeans):

    Fe: 115.1 ± 7.32 ppm, CV = 6.36%

    Mn: 84.56 ± 1.75 ppm, CV = 2.07%

    Zn: 30.74 ± 1.71 ppm, CV = 5.57%.

The above values were obtained from all replications except for

the case of Fe in sample 1 where sub-sample 1 and the 4-hour counts

of sub-samples 5 and 6 were excluded. Plots of these "best estimates"

are on Figs. 6, 7, and 8 at the right edge of each sample's replica-

tions. It is observed that the majority of the single-valued replicate

determinations lie within the range of the "best estimates."
Theoretically, 68.3% of the values should be within plus or minus one
standard deviation of the mean. The number and percent of the determina-
tions for each element in each sample which actually are in this
range are as follows:

1) Sample 1 (soybeans):

    Fe: 8 of 12 for 66.7%

    Mn: 8 of 10 for 80.0%

    Zn: 10 of 16 for 62.5%

2) Sample 2 (corn):

    Fe: 2 of 3 for 66.7%

    Mn: 3 of 4 for 75.0%

    Zn: 2 of 3 for 66.7%

3) Sample 3 (soybeans):

    Fe: 2 of 3 for 66.7%

    Mn: 3 of 5 for 60.0%

    Zn: 2 of 3 for 66.7%.

Taking Fe as an example (Fig. 6 and Table XI), one can make some ad-
ditional observations. Recall that the replicates of sample 1 were dif-
ferent countings of six irradiated sub-samples. First, with the exception
of the results from decay times of 4, 7, and 8 days, the observed concen-
trations in sub-sample 1 of sample 1 were generally differentiable from the
observed concentrations in the other sub-samples of sample 1. This could
have been caused by inhomogeneity of the sample when sub-sample 1 was
taken for irradiation. Furthermore, to a lesser degree the results for
Zn (Fig. 8 and Table XIII) suggest the same observation.

Secondly, the last replicate measured for any Fe sub-sample re-
sulted in a lower concentration than did the previous replicate for
5 of the 6 sub-samples, with sub-sample 4 being the exception. This
would indicate a possible systematic error in that the later countings
consistently gave lower results. However, in the case of Zn for
sample 1 (Fig. 8 and Table XIII) the last replicate was higher for 4
of the 6 sub-samples, a reverse relationship than that for Fe and
leading to a possible conclusion that the later countings gave higher
results. In the Mn determinations of sample 1 (Fig. 7 and Table XII),
2 of the 3 sub-samples which were replicated had lower concentrations
for the later countings. Continuing this analysis for samples 2 and
3, one can examine only the Mn data, because no replicate countings
were taken in these samples for Fe and Zn. For the Mn, lower concentra-
tions occurred in all three of the later countings. Thus, later
countings resulted in lower concentrations of both Fe and Mn in 5 of
6 sub-samples each, but resulted in higher concentrations of Zn in 4
of 6 sub-samples. These results are not conclusive, but they do
indicate there may have been a systematic error occurring which, in
turn, may have been dependent upon the radioactive nuclide involved.
The interesting aspect is that the Fe and Zn measurements were taken
from the same spectra in every case, and any systematic error should
have been in the same direction for these two elements, except for
the fact that different full energy peaks were used.

One can correct the quantitative analyses given by Eq. (27)
for the amount of the unknown element concentrated in the distilled,
demineralized (clean) water and empty polyethylene vial by applying

Eq. (E-11) of Appendix E. The results of this correction are used in Eq. (32) and Eq. (33) for calculation of the corrected concentrations.

The following are estimates of the magnitudes of these elemental concentrations (as contaminants) in micrograms per 4 ml of water (the amount of standard solution used) and per empty vial as determined by instrumental NAA in this work:

1) Fe in water and vial, an estimated value of w for Eq. (E-11):

6- to 7-day decay: 10.35 ± 3.51 µg

12- to 13-day decay: 7.71 ± 1.85 µg

2) Fe in empty vial, an estimated value of V for Eq. (44):

12- to 13-day decay: 3.93 ± 1.97 µg

3) Mn in water and vial, an estimate of w:

6-hour decay: 0.132 ± 0.0074 µg

6-hour decay: 0.11 ± 0.0090 µg

4) Mn in empty vial, an estimate of V:

9-hour decay: 0.0594 ± 0.0038 µg

9-hour decay: 0.0496 ± 0.0044 µg

5) Zn in water and vial, an estimate of w:

6- to 7-day decay: 1.98 ± 0.33 µg

12- to 13-day decay: 2.19 ± 0.19 µg

6) Zn in empty vial, an estimate of V:

12- to 13-day decay: 0.54 ± 1.16 µg.

For the application of these data, the decay times of the above determinations were matched as closely as possible to the decay times of the original determinations in the unknown matrix material being corrected.

Application of Eq. (E-11), Eq. (27), Eq. (32), and Eq. (33) results in the following corrected "best estimates" with the associated uncertainties:

1) Sample 1 (soybeans):

   Fe: 113.0 ± 14.1 ppm, CV = 12.4%

   Mn: 45.2 ± 7.45 ppm, CV = 16.5%

   Zn: 38.9 ± 3.66 ppm, CV = 9.43%

2) Sample 2 (corn):

   Fe: 232.3 ± 21.3 ppm, CV = 9.19%

   Mn: 131.7 ± 3.85 ppm, CV = 2.92%

   Zn: 33.16 ± 3.61 ppm, CV = 10.9%

3) Sample 3 (soybeans):

   Fe: 119.0 ± 7.55 ppm, CV = 6.34%

   Mn: 84.77 ± 1.76 ppm, CV = 2.07%

   Zn: 33.52 ± 1.83 ppm, CV = 5.47%.

These values can be compared to those resulting from the atomic absorption method of analysis as tabulated in Tables XI, XII, and XIII for samples 2 and 3. The corrected values determined in this work are lower than those obtained in other analyses which tends to confirm the belief of researchers in the ISU Agronomy Department that the results of the other analyses are too high [14].

Estimates of the detection limit of instrumental NAA as employed in this work for the analysis of the concentration in a one gram matrix of plant material, such as soybean or corn leaves, for the five elements sought, are as follows:

1) Fe: 10 ppm with a CV of about 34%

2)   Mn: 0.05 ppm with a CV of about 6%

3)   Zn: 0.5 ppm with a CV of about 30%

4)   Cu: > 10 to 30 ppm (not detected)

5)   Mo: > 1 to 5 ppm (not detected).

These estimates are based on empirical determinations of small concentrations of Fe, Mn, and Zn in the water and vials without chemical separation and a maximum acceptable CV of about one third (33.3%) for Fe and Zn and 6% for Mn. These estimates also are based on the "optimum" counting and decay times as determined in this work. The detection limits for Cu and Mo are based on the fact that they could not be detected in a sample containing the usual amount found in soybeans grown in Iowa.

Establishment of these detection limit estimates by extrapolating the results of the water and vial elemental determinations to estimate that expected for plant material should be valid for Fe and Zn since their half-lives are long enough to "out-live" interferences from other constituents in the plant material. However, for Mn, this extrapolation probably is not valid since the Mn is shorter lived than the interfering Na and K Compton background which was not present in the Mn determinations in the water and vials.

These estimates can be compared to the following taken from Guinn [27] for interference-free detection limits for a thermal neutron flux of 10^{13} n/cm^2-sec for a one hour irradiation utilizing 3 X 3 inch NaI spectrometry and a minimum detectable full energy peak count rate of 10 counts per minute for half-lives greater than 1 hour (these data are equivalent to ppm in a one gram sample).

1)   Fe: 10 to 30 μg

2)   Mn: 4 to 9 $(10)^{-6}$ μg

3)   Zn: 1 to 3 $(10)^{-2}$ μg

4)   Cu: 4 to 9 $(10)^{-4}$ μg

5)   Mo: 4 to 9 $(10)^{-3}$ μg.

According to de Mooy [14], analyses for these trace elements for detection of deficiencies in the culture of soybeans in the United States require that the method have the following detection limits and be able to differentiate with certainty between levels of concentration as follows:

1)   Fe: minimum of 30 ppm and differentiate between 30 and 50

2)   Mn: minimum of 15 ppm and differentiate between 15 and 20

3)   Zn: minimum of 12 ppm and differentiate between 12 and 20

4)   Cu: minimum of 4 ppm and differentiate between 4 and 10

5)   Mo: minimum of 0.5 ppm and differentiate between 0.5 and 1.0.

It therefore appears that the instrumental NAA method of this work can satisfy the requirements of determinations of Fe, Mn, and Zn in plant and soil deficiency studies.

The final portion of this section compares the peak areas and concentrations obtained from the Wasson method (Appendix B) to those obtained from the ICPEAX program (Appendix C). The ICPEAX program was used on some replications of the Mn data for the specific purpose of making this comparison. The results are listed in Table XIV and Table XV.

Examination of Table XIV reveals that, for sample 1, the CV of the unknown peak areas obtained from ICPEAX was from 2.2 to 108 times greater

Table XIV. Comparison of Mn peak areas and uncertainties as obtained by the Wasson method and the ICPEAX program

Sample	Sub-sample/ replicate	t_d, hours	t_c, minutes	Wasson method Unknown peak area $\pm\ \sigma_{area}$		CV, %	ICPEAX program Unknown peak area $\pm\ \sigma_{area}$		CV, %
1	1/2	53[a]	14	138,098	421	0.30	115,450	37,960	32.88
	2/2	26	35	3,024	207	6.84	5,785	1,188	20.54
	3/2	27	35	1,901	172	9.04	3,183	644	20.24
2	1/1	21	72	65,022	452	0.69	76,557	6,077	7.94
	2/1	23	72	32,933	396	1.20	39,800	3,171	7.97
	3/1	20	35	42,376	352	0.83	49,550	3,696	7.46
	3/2[b]	20	35	42,376	352	0.83	49,550	3,696	7.46
3	1/1	25	72	19,080	388	2.03	23,048	1,850	8.03
	2/1	21	57	41,044	409	0.99	48,373	3,456	7.14
	3/1	23	72	40,474	457	1.13	47,721	3,418	7.16
	2/2[b]	21	57	41,044	409	0.99	48,373	3,456	7.14
	3/2[b]	23	72	40,474	457	1.13	47,721	3,418	7.16

[a] Minutes.

[b] Different counting time for standard in this replicate compared to the first replicate of this sub-sample.

Table XV. Comparison of Mn concentrations and mass ratios calculated from peak area data obtained by the Wasson method and the ICPEAX program

Sample	Sub-sample/ replicate	t_d, hours	t_c, minutes	Wasson method				ICPEAX program			
				Mass $\pm \sigma_{mass}$, ppm		CV, %	Mass ratio, unknown to standard	Mass $\pm \sigma_{mass}$, ppm		CV, %	Mass ratio, unknown to standard
1	1/2	53[a]	14	41.11	2.20	5.34	0.517	51.6	26.5	51.4	0.649
	2/2	26	35	51.19	4.80	9.38	1.417	89.5	32.0	35.8	2.479
	3/2	27	35	45.91	5.09	11.1	1.120	70.3	25.0	35.6	1.714
2	1/1	21	72	126.4	7.02	5.56	2.215	129.5	16.7	12.9	2.269
	2/1	23	72	135.0	7.62	5.64	2.009	142.0	18.3	12.9	2.113
	3/1	20	35	133.7	7.30	5.46	2.879	134.0	18.3	13.7	2.885
	3/2[b]	20	35	130.5	7.22	5.53	2.810	132.8	18.2	13 7	2.860
3	1/1	25	72	83.58	4.91	5.87	1.932	87.8	11.4	12.9	2.030
	2/1	21	57	84.53	4.63	5.48	2.489	85.4	11.5	13.5	2.513
	3/1	23	72	87.16	4.80	5.51	2.792	88.1	11.9	13.5	2.821
	2/2[b]	21	57	82.49	4.58	5.56	2.428	84.6	11.4	13.5	2.492
	3/2[b]	23	72	85.05	4.75	5.58	2.725	87.3	11.8	13.5	2.797

[a] Minutes.

[b] Different counting time for standard in this replicate compared to the first replicate of this sub-sample.

96

than the CV of the areas obtained from Wasson's method. Table XV
indicates that the CV of the concentration of Mn in the unknown repli-
cates of sample 1 was from 3.2 to 9.6 times greater when calculated
from the ICPEAX data than when calculated from Wasson's method. In
addition, the concentration of Mn was from 1.25 to 1.75 times greater
when calculated from the ICPEAX data compared to calculations from
data obtained from the Wasson method.

The author has no knowledge of the detailed method used in ICPEAX
to compute the uncertainties in the areas of the peaks. For this
reason, comments on the causes for the relatively large differences
in the results for sample 1 obtained from ICPEAX, as compared to those
obtained from the Wasson method, are restricted to considerations of
"optimum" timing. The author suspects, particularly for sub-sample
1/2 which was counted only 14 minutes, that the ICPEAX program
calculated substantial variation in the peak parameters (location,
height, and width) from which the peak areas and, presumably, the
uncertainties were calculated. The area of this peak (115,450 counts)
was about 2.5 times that of most of the other peak areas computed by
ICPEAX, but these other areas all had significantly smaller relative
standard deviations (CV values). In the case of sub-samples 2/2 and
3/2 from sample 1, the ICPEAX values of greater than 20% for the CV of
the peak areas probably were due to the small areas of these peaks
(5785 and 3183 counts, respectively). The CV values for the areas of
these same two peaks obtained by Wasson's method were the greatest of
any obtained by the Wasson method in this comparison, and this was due
to the small number of counts contained therein. It is expected that

an increase in the counting time and a decrease in the length of the decay time, approaching those of the "optimum" conditions established in this work, would have reduced the uncertainties in the peak areas for both methods of data reduction.

The values obtained from ICPEAX for sample 2 and sample 3, which were counted at the "optimum" conditions, all were quite similar to those obtained from Wasson's method. However, the ICPEAX values were consistently larger for all the characteristics of peak areas, mass ratios, concentrations, and uncertainties. The larger peak areas were expected from ICPEAX due to the nature of Wasson's method which does not use all of the peak area. These larger areas were not significant since the standard peaks were also larger. The peak area ratios and the mass ratios of the unknown to standard are the significant comparisons between the two methods, since these ratios directly affect the calculated concentrations of the unknown element as given by Eq. (27).

For samples 2 and 3, the concentrations calculated from peak area data obtained from ICPEAX were all within the range of plus or minus one standard deviation of the concentrations calculated from data obtained from Wasson's method (Table XV). It should be noted that all replications of these two samples were counted at "optimum" conditions for Mn. This contributes to the small CV values obtained by both methods of peak area data reduction for samples 2 and 3.

Since the CV values for the elemental concentrations obtained from Wasson's method were less than half that of the values obtained from ICPEAX, Wasson's method was preferred for the method of data

reduction. Other advantages of the Wasson method were convenience and cost savings. For ICPEAX, the paper tapes must be punched for the entire spectrum and then converted (at $13.50 per hour) to magnetic tape. Then the ICPEAX program must be run with input data concerning energy calibration points for each spectrum. The computer cost for running ICPEAX was about 30¢ per spectrum when 15 spectra were run at one time, the spectra were not listed or plotted, and the number of channels searched were limited to about one-third of each spectrum. Finally, the output of ICPEAX includes the area and standard deviation of each located peak. These data for the peak of interest must be entered into another program, such as a modified MASS, in order to calculate the concentrations and uncertainties of the unknown element from Eq. (27) through Eq. (33), and Eq. (E-11) if corrections are made for contaminating elements in the standard water and vials. On the other hand, program MASS, written by the author, calculates the areas and uncertainties by Wasson's method and then directly uses these areas and uncertainties, along with other input data concerning the experimental conditions, to perform the calculations using Eq. (27) through Eq. (33). The cost of running MASS one time for 44 analyses was 59¢ compared to the ICPEAX run, tape conversion, and modified MASS computer run which cost a total of $14.16 for 13 analyses.

As pointed out in Appendix B, use of Wasson's method in this investigation involved a visual determination of the peak limits from the oscilloscope display in order to compute the background. This method may have been less precise than that used in Baedecker's investigation [1] in which first derivatives were used to determine

peak limits. Additionally, the ICPEAX program has the advantage of providing an objective determination of the background (Appendix C), thus eliminating possible bias on the part of the individual visually selecting the peak limits.

VII. CONCLUSIONS

The following conclusions can be drawn from the results of this investigation:

1. Quantitative instrumental NAA can be employed to determine concentrations of Fe, Mn, and Zn in plant culture deficiency studies with adequate precision for the differentiation between deficient and sufficient concentrations.

2. Cu and Mo cannot be determined qualitatively or quantitatively in irradiated soybean or corn tissue by the instrumental NAA technique of this work when nuclides with long half-lives are used. To the extent of the instrumental technique which was employed in this work and the use of nuclides with long half-lives, this conclusion confirms the statements made by Grimanis [26] in 1968 and Fourcy [21] in 1967 that these elements could not be detected by instrumental NAA in plant tissues.

3. By using empirically determined "optimum" decay and counting times in the analysis for a particular element, one can reduce the uncertainties of the result.

4. On the basis of the concentrations and associated uncertainties determined in water samples and empty polyethylene vials, through the use of the instrumental NAA technique of this work, it is concluded that the estimated detection limits in the analysis of one gram of plant material for various elements are as follows:

    a. Fe: 10 ppm with a coefficient of variation of about 34%.

    b. Zn: 0.5 ppm with a coefficient of variation of about 30%.

    c.   Cu: > 10 to 30 ppm (this element was not detected in

         the irradiated plant samples).

    d.   Mo: > 1 to 5 ppm (this element was not detected in the

         irradiated plant samples).

It is not valid to extrapolate the Mn determinations in the water and vials in order to estimate the detection limit for Mn in plant material. The estimated detection limit for Mn in a relatively interference-free matrix such as tap water or polyethylene vials is 0.05 ppm with a coefficient of variation of about 6% by use of the instrumental NAA technique of this work.

    5.   The Wasson method of peak area determination is preferred to the ICPEAX program for quantifying only a few gamma-ray peaks of a spectrum and when qualitative analysis is not needed. This preference is justified because the Wasson method provides smaller uncertainties of peak area determinations and greater convenience and economy in data handling than does the ICPEAX program.

VIII.   SUGGESTIONS FOR FURTHER WORK

The following suggestions are made for further work:

1.   Since this work did not experimentally investigate the use of
the short half-life nuclides ^{66}Cu, ^{101}Mo or ^{101}Tc for instrumental
quantitative determination of Cu and Mo in plant material, such work
is suggested, especially with state-of-the-art Ge(Li) detector systems.

2.   Since the theoretical analysis by this investigator indicated
that significant interferences in the determination of Mo are expected
from Mg, Cu, Br, La, or Mn (Table VIII), coincidence counting utilizing
the different cascade gammas of ^{101}Mo appears worth investigating.

3.   A Compton suppression spectrometry system was not available
to this investigator. One is being developed by the Ames Laboratory
of the Atomic Energy Commission at Iowa State University which could
be used to investigate the possibility of instrumental determination
of Cu and Mo, as well as other trace elements of interest in plant
material.

IX. BIBLIOGRAPHY

1. P. A. BAEDECKER, Anal. Chem., 43, 3, 405 (1971).

2. P. R. BEVINGTON, Data Reduction and Error Analysis for the Physical Sciences, McGraw-Hill, Inc., New York (1969).

3. H. J. M. BOWEN, in Activation Analysis, Principles and Applications, J. M. A. Lenihan and S. J. Thomson, Ed., pp. 143-148, Academic Press, New York (1965).

4. H. J. M. BOWEN, in Advances in Activation Analysis, J. M. A. Lenihan and S. J. Thomson, Ed., pp. 101-113, Academic Press, New York (1969).

5. H. J. M. BOWEN, International Journal of Applied Radiation and Isotopes, 4, 3/4, 214 (1959).

6. H. J. M. BOWEN, International Journal of Applied Radiation and Isotopes, 5, 3, 227 (1959).

7. H. J. M. BOWEN, J. Nuclear Energy, 3, 18 (1956).

8. H. J. M. BOWEN and P. A. CAWSE, Analyst, 86, 506 (1961).

9. H. J. M. BOWEN and P. A. CAWSE, "The Determination of Inorganic Elements in Biological Tissue by Activation Analysis," AERE-R4309, United Kingdom Atomic Energy Authority, Wantage Research Laboratory, Berkshire (1963).

10. G. B. COOK, in Modern Trends in Activation Analysis, pp. 133-136, Proceedings of 1961 International Conference, A&M College of Texas, College Station, Texas (1961).

11. R. D. COOPER et al., in Nuclear Activation Techniques in the Life Sciences, pp. 65-80, Proceedings of the Symposium, IAEA, Vienna (1967).

12. J. F. COSGROVE and G. H. MORRISON, Anal. Chem., 29, 7, 1017 (1957).

13. D. F. COVELL, Anal. Chem., 31, 11, 1785 (1959).

14. C. J. DE MOOY, Personal Communication (1971 and 1972).

15. D. DE SOETE et al., in Modern Trends in Activation Analysis, J. R. DeVoe, Ed., pp. 699-750, Proceedings of 1968 International Conference, National Bureau of Standards Special Publication 312, Vol. II (1969).

16. J. W. DIECKERT et al., in Isotopes in Plant Nutrition and Physiology, pp. 81-93, Proceedings of the Symposium, IAEA, Vienna (1967).

17. K. ECKSCHLAGER, Errors, Measurement and Results in Chemical Analysis, R. A. Chalmers, Ed., Van Nostrand Reinhold, London (1969).

18. J. S. ELDRIDGE, in Guide to Activation Analysis, W. S. Lyon, Jr., Ed., pp. 80-107, D. Van Nostrand, Princeton, N. J. (1964).

19. H. FIEDLER and O. TENCH, Germanium (Li) Gamma Spectrometer Systems, pp. 2-5, Canberra Industries, Middletown, Conn. (1968).

20. R. H. FILBY et al., "Gamma Ray Energy Tables for Neutron Activation Analysis," WSUNRC-97(2), Washington State University Nuclear Radiation Center, Pullman, Wash. (1970).

21. A. FOURCY et al., in Isotopes in Plant Nutrition and Physiology, pp. 57-68, Proceedings of the Symposium, IAEA, Vienna (1967).

22. R. FUKAI and W. W. MEINKE, Nature, 184, 815 (1959).

23. D. GIBBONS, in Activation Analysis, Principles and Applications, J. M. A. Lenihan and S. J. Thomson, Ed., pp. 85-89, Academic Press, New York (1965).

24. S. GLASSTONE and A. SESONSKE, Nuclear Reactor Engineering, D. Van Nostrand, Princeton, N. J. (1967).

25. M. D. GOLDBERG et al., "Neutron Cross Sections," BNL-325, 2nd ed., Supplement No. 2, Vol. II B, Brookhaven National Laboratory (1966).

26. A. P. GRIMANIS, Talanta, 15, 279 (1968).

27. V. P. GUINN, in Advances in Activation Analysis, J. M. A. Lenihan and S. J. Thomson, Ed., pp. 37-80, Academic Press, New York (1969).

28. V. P. GUINN, Progress in Nuclear Energy, Series IX, Analytical Chemistry, 4, 2, 73 (1965).

29. V. P. GUINN and C. D. WAGNER, Anal. Chem., 32, 3, 317 (1960).

30. W. A. HALLER et al., in Modern Trends in Activation Analysis, J. R. DeVoe, Ed., pp. 177-183, Proceedings of 1968 International Conference, National Bureau of Standards Special Publication 312, Vol. I (1969).

31. Handbook of Chemistry and Physics, R. C. Weast, Ed., The Chemical Rubber Co., Cleveland, Ohio (1969).

32. W. B. HEALY and L. C. BATE, Anal. Chim. Acta, 33, 443 (1965).

33. R. L. HEATH, "Scintillation Spectrometry," IDO-16880-1, 2nd ed., Vol. 1, Idaho Operations Office, Atomic Energy Commission (1964).

34. D. J. HUGHES and R. B. SCHWARTZ, "Neutron Cross Sections," BNL-325, 2nd ed., Brookhaven National Laboratory (1959).

35. R. C. KOCH, Activation Analysis Handbook, Academic Press, New York (1960).

36. C. M. LEDERER et al., Table of Isotopes, 6th ed., John Wiley and Sons, New York (1968).

37. H. D. LIVINGSTON and H. SMITH, Anal. Chem., 39, 4, 538 (1967).

38. W. H. LOOMIS, Personal Communication (March 1972).

39. B. A. LOVERIDGE and A. A. SMALES, in Methods of Biochemical Analysis, Vol. 5, D. Glick, Ed., pp. 225-272, Interscience Publishers, New York (1957).

40. W. S. LYON, JR., in Guide to Activation Analysis, W. S. Lyon, Jr., Ed., pp. 143-171, D. Van Nostrand, Princeton, N. J. (1964).

41. K. L. MALABY, Personal Communication (April 1972).

42. G. H. MORRISON and J. F. COSGROVE, Anal. Chem., 27, 810 (1955).

43. G. H. MORRISON and J. F. COSGROVE, Anal. Chem., 28, 320 (1956).

44. National Bureau of Standards Technical Note 467, Part 1, "Activation Analysis: A Bibliography," G. J. Lutz et al., Ed., U. S. Government Printing Office, Washington, D. C. (1971).

45. M. NEUBURGER and A. FOURCY, Journal of Radioanalytical Chemistry, 1, 289 (1968).

46. A. NILUBOL and U. KAFKAFI, in Isotopes and Radiation in Soil-Plant Nutrition Studies, pp. 63-69, Proceedings of the Symposium, IAEA, Vienna (1965).

47. R. T. OVERMAN and H. M. CLARK, Radioisotope Techniques, p. 108, McGraw-Hill, Inc., New York (1960).

48. R. C. PLUMB and J. E. LEWIS, Nucleonics, 13, 8, 42 (1955).

49. L. A. RANCITELLI et al., in Modern Trends in Activation Analysis, J. R. DeVoe, Ed., pp. 101-109, Proceedings of 1968 International Conference, National Bureau of Standards Special Publication 312, Vol. I (1969).

50. D. M. ROBERTS, Personal Communication (April 1972).

51. W. ROMBERG, Impurities in MgO by Instrumental Neutron Activation Analysis, unpublished M.S. thesis, Iowa State University, Ames, Iowa (1969).

52. H. H. ROSS, in Guide to Activation Analysis, W. S. Lyon, Jr., Ed., pp. 1-13, D. Van Nostrand, Princeton, N. J. (1964).

53. K. SAMSAHL et al., International Journal of Applied Radiation and Isotopes, 16, 273 (1965).

54. G. T. SEABORG, in Modern Trends in Activation Analysis, J. R. DeVoe, Ed., pp. xv-xvii, Proceedings of 1968 International Conference, National Bureau of Standards Special Publication 312, Vol. I (1969).

55. A. G. SOULIOTIS, Analyst, 94, 359 (1969).

56. E. STEINNES, Talanta, 14, 753 (1967).

57. S. STERLINSKI, Anal. Chem., 40, 13, 1995 (1968).

58. S. STERLINSKI, Anal. Chem., 42, 2, 151 (1970).

59. R. E. THIERS, in Methods of Biochemical Analysis, Vol. 5, D. Glick, Ed., pp. 273-335, Interscience Publishers, New York (1957).

60. B. VAN ZANTEN et al., Talanta, 9, 213 (1962).

61. R. E. WAINERDI and M. P. MENON, in Nuclear Activation Techniques in the Life Sciences, pp. 33-50, Proceedings of the Symposium, IAEA, Vienna (1967).

62. H. P. YULE, Anal. Chem., 38, 1, 103 (1966).

63. H. P. YULE, Anal. Chem., 38, 7, 818 (1966).

64. H. P. YULE, Anal. Chem., 40, 10, 1480 (1968).

65. H. P. YULE, in Modern Trends in Activation Analysis, J. R. DeVoe, Ed., pp. 1155-1204, Proceedings of 1968 International Conference, National Bureau of Standards Special Publication 312, Vol. II (1969).

X. ACKNOWLEDGMENTS

The author wishes to express his appreciation to the United States Army for providing the finances and the opportunity with which to attend graduate school. Appreciation is extended to Dr. G. Murphy for his guidance throughout the period of study and for the assistance provided by the Department of Nuclear Engineering.

The author is indebted to his major professor, Dr. R. A. Hendrickson, for invaluable assistance and interest throughout the course of this investigation.

Others deserving recognition are Dr. D. M. Roberts for providing guidance, equipment, and the ICPEAX computer program; Dr. C. J. de Mooy for providing sample specimens and other assistance; Dr. A. F. Voigt and Mr. W. H. Loomis for irradiations in the Ames Laboratory Research Reactor; personnel of the radiological services groups at both the university and the Ames Laboratory Reactor Division; and Mr. K. L. Malaby of the Ames Laboratory Reactor Division for his advice and assistance.

Finally, deep appreciation is extended to the author's wife and children for their understanding and helpfulness during this investigation.

XI. APPENDIX A: SPECIFICATIONS OF REAGENTS USED

1. Ammonium Hydroxide: NH_4OH

   Manufacturer . . . . J. T. Baker

   Grade. . . . . Baker Analyzed Reagent

   Lot Number 36825

   Analysis . . . . . . Material

Material	%
Assay (as NH_3)	29.7
CO_2	0.0002
Cl	0.00001
PO_4	0.00003
Total Sulfur (as SO_4)	0.00005
Cu	0.000005
As	0.0000005
Heavy Metals (as Pb)	0.00001
Fe	0.000005
Ni	0.000005

2. Cupric Sulfate, Anhydrous: $CuSO_4$

   Form . . . . Powder

   Manufacturer . . . . J. T. Baker

   Grade. . . . . Baker Analyzed Reagent

   Lot Number 39782

   Analysis . . . . . . Material

Material	%
Assay ($CuSO_4$)	100.0
Insolubles	0.006
Cl	0.001

Material	%
Fe	0.004
Ammonium Sulfide Metals, other than Fe (as Ni)	0.008

3. Ferric Nitrate: $Fe(NO_3)_3 \cdot 9H_2O$

Form . . . . Crystal

Manufacturer . . . . J. T. Baker

Grade. . . . . Baker Analyzed Reagent

Lot Number 36890

Analysis . . . . . .

Material	%
Assay $(Fe(NO_3)_3 \cdot 9H_2O)$	99.3
Insolubles	0.003
Cl	0.0003
SO_4	0.005
Mn	0.0003

4. Manganous Sulfate Monohydrate: $MnSO_4 \cdot H_2O$

Form . . . . Powder

Manufacturer . . . . J. T. Baker

Grade. . . . . Baker Analyzed Reagent

Lot Number 38772

Analysis . . . . . .

Material	%
Assay $(MnSO_4 \cdot H_2O)$	99.9
Insolubles	0.003
Cl	0.0004
Heavy Metals (as Pb)	0.002

Material	%
Fe	0.001
Ni	0.0005
Zn	0.003

5. Molybdenum Trioxide: MoO_3

Form . . . . Powder

Manufacturer . . . . J. T. Baker

Grade. . . . . Baker Analyzed Reagent

Lot Number 38742

Analysis . . . . . .

Material	%
Assay (as MoO_3)	99.9
Cl	0.001
NO_3	< 0.003
Arsenate, Phosphate, and Silicate (as SiO_2)	0.0002
SO_4	0.005
NH_4	0.001
Heavy Metals (as Pb)	0.001

6. Nitric Acid: HNO_3

Manufacturer . . . . J. T. Baker

Grade. . . . . Baker Analyzed Reagent

Lot Number 36400

Analysis . . . . . .

Material	%
Assay (HNO_3)	70.4
Cl	0.000008

Material	%
PO_4	0.00001
SO_4	0.00003
As	0.0000001
Cr	0.000005
Cu	0.000005
Heavy Metals (as Pb)	0.000005
Fe	0.000008
Ni	0.000005

7. Zinc Acetate, Dihydrate: $(CH_3COO)_2Zn \cdot 2H_2O$

Form . . . . Crystal

Manufacturer . . . . J. T. Baker

Grade... . . . . . . Baker Analyzed Reagent

Lot Number 35121

Analysis . . . . . .

Material	%
Assay $((CH_3COO)_2Zn \cdot 2H_2O)$	99.8
Insolubles	0.003
Cl	0.0002
SO_4	0.001
As	0.00001
Pb	0.0008
Fe	0.0002

XII.   APPENDIX B: WASSON'S METHOD OF PEAK AREA DETERMINATION

Baedecker studied the precision attainable by several digital methods of integrating peaks in gamma-ray spectra [1].   These included the "total peak area" method, the methods proposed by Covell [13], Sterlinski [57, 58], and Quittner, and some modifications of these methods.   Baedecker concluded that a method suggested by Wasson which modified the total peak area method was the most advantageous because of its simplicity and high precision.

The total peak area method and the modification by Wasson are illustrated in Fig. B-1.
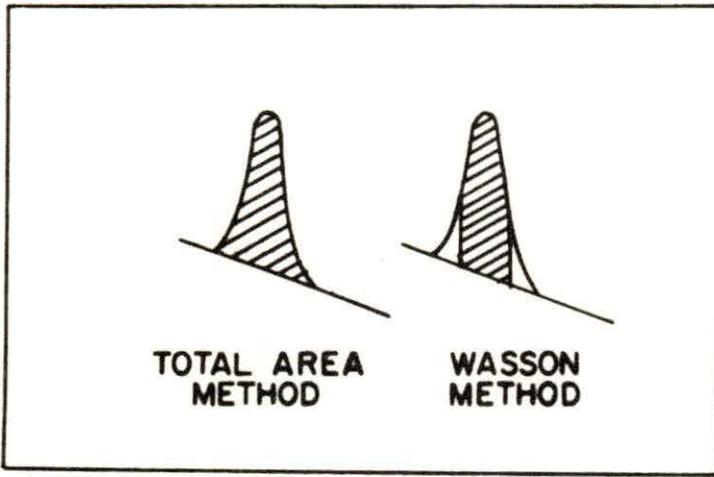

TOTAL AREA METHOD   **WASSON METHOD**

Fig. B-1.   Two methods of peak integration.

The calculation of the area by the Wasson modification is given by the following:

$$A = \sum_{i=-n}^{i=+n} a_i - (n + \frac{1}{2})(b_n + b_{-n})$$

where a_i = number of counts accumulated in channel i,

n = the number of channels on the left and right from

channel zero (the centermost channel), and

b_n = the background in channel n as determined from a

straight line drawn between channels 1 and r (the left

and right hand limits of the peak).

The Wasson method modifies the total area method to account for the

fact that the wings of the total peak contribute considerably to the

error of the peak integration but add little to the net number of

counts.

The variance of the area by Wasson's method, calculated from

propagation of errors theory [2, 47], is as follows:

$$Var = \sum_{i=-n}^{i=+n} a_i + (n + \frac{1}{2})^2 (b_n + b_{-n})$$

This derivation is based on the assumption that the number of counts

in any two adjacent channels are independent, which is a valid as-

sumption at counting rates which are used in this work. The deriva-

tion also assumes that the counting statistics follow a Poisson

distribution; therefore, the variance of the number of counts in any

channel (or group of channels) equals the number of counts in that

channel (or group of channels).

One uncertainty which is not accounted for in this calculation

is that associated with choosing the best base line. In Baedecker's

comparison study of the various methods [1], he established the

straight line background base line through channel 1 (the channel at

the left hand limit of the peak) and channel r (the channel at the

right hand limit of the peak). These peak limit channels were

established by a computer program which determined the first derivative at each channel and used the first derivatives to locate peaks and determine the peak limits as described by Yule [62, 64]. Then the number of counts in the background channels l and r were taken as the average of the counts accumulated in the three channels centered on l and r. Also in his study, Baedecker smoothed the spectra before processing it by the various methods studied. Additionally, Baedecker set n = 3 in the above two equations for the number of channels on each side of the centermost channel for peaks in Ge(Li) detector spectra.

Wasson's method was used in this work with one major change to that of Baedecker's application. The peak limits were not determined by computer but were determined visually from the oscilloscope display. A 3-channel group which appeared to represent the average background was chosen for each side of the peak. The counts accumulated in each group were averaged for the value of the background at channel l and channel r, the center channels of the 3-channel groups. From the straight line constructed between these two points, the values of the two channels b_n and b_{-n} were computed by program MASS. Then program MASS used the input values of n and the a_i to calculate the area and variance of the modified peak by the above equations.

Another change in this work was that n was not always given a value of 3. Some of the peaks evaluated were so narrow that n was set at 2 or 1. For comparison of a peak in an unknown spectrum to one of the same energy in a standard spectrum, the value of n was always the same for both peaks. However, the centermost channels

or the groups of channels used for estimating the background were not necessarily the same for the unknown and standard peaks.

XIII. APPENDIX C: PROGRAM "ICPEAX"

"ICPEAX"[a] is a FORTRAN IV program written for the IBM 360/65 computer. Its purpose is to detect peaks in gamma-ray spectra accumulated by Ge(Li) semiconductor detectors. Available user options include production of semi-log plots of selected spectra, listing of selected spectra, and calculation of linear and least square energy calibration curves. The main utility of the program is to perform an energy qualitative analysis of a spectrum and to calculate peak areas and standard deviations with which one can perform a quantitative analysis.

The program detects peaks by analyzing the smoothed second derivative of a spectrum. An initial search is performed between specified channels (first and last 20 channels are ignored if a region is not specified) for up to 100 peaks. All negative minima in the smoothed second derivative are considered peak locations if both of the following criteria are met:

1) The number of channels between the points of inflection is between 3 and 15.

2) The magnitude of the minimum is at least 0.35 times its standard deviation.

If a peak width exceeds 15 channels, a test is made for the presence of other local minima. If there are any, the peak is assumed to be

---

[a]Unpublished program documentation provided by Mr. Jim Wright, 115 Research Building, Iowa State University.

a multiplet. Output from this preliminary search includes channel location, peak width, and both linear and quadratic energies for all detected peaks.

The program next corrects the counts within the predetermined peak limits for underlying Compton and background events. This is done by fitting a least square straight line through 5 channels to the left and right of the peak and then subtracting this background from the peak region. The first point of each 5-channel group on either side of the peak is a minimum of 1.5 times the peak width, measured from the center of the peak. Before the equation of the straight line is calculated, a test is made to determine if there are other peaks in the region of the 5 channels. If so, a common correction line is computed for both peaks by shifting the 5-channel group to the right (or left) of this second peak. Consequently, a number of peaks can share the same background line, and the accuracy of this background line decreases as the number of peaks increases.

The peaks sharing a common background line are tested to determine if there is a contribution from one in the region of the other in which a Gaussian fit will be attempted later. If there is a contribution, the peaks are considered to form a multiplet, and they are fitted simultaneously. Otherwise, they are fitted separately.

After the background correction is made, a Gaussian fitting is attempted for each of the detected peaks. This subroutine is based on the one described by Heath [33]. The subroutine evaluates 3 parameters for the top 75% of the peak, a region which has been found empirically to yield consistently the best results by minimizing errors

for such sources as poor background corrections, non-Gaussian peaks, etc. The variables evaluated are the location, height, and width from which the peak area is calculated. If fitting convergence is not obtained in 10 iterations, the peak is considered to be non-Gaussian. The remaining, Gaussian peaks are considered to be "real" peaks. The program lists the following results of the Gaussian fitting for all peaks which were initially detected:

1) Channel location to three decimal places and its standard deviation.

2) Width and height.

3) Area and its standard deviation.

4) Line slope, intercept, and fit.

5) Energies computed from linear and quadratic calibration curves.

Energy recalibration, an optional feature, is then performed based on Gaussian fitting of the calibration peaks in the spectrum. The above parameters of the real peaks are then recalculated and listed.

The raw spectrum data from the 1024 channels can be input by punch cards or magnetic tape, as indicated in Fig. 1. For this investigation, the raw spectra data were converted from paper tape to magnetic tape by use of a paper tape converter. The object deck of the ICPEAX program was obtained from Roberts [50].

XIV. APPENDIX D: EQUIPMENT LISTING

Item	Manufacturer	Model	Serial number
High Voltage Power Supply	(Local)	—	AEC 17322
Power Supply	General Electric	TDM 110	—
Detector-Cryostat System (Coaxial, Lithium-Drifted Germanium)	ORTEC, Inc.	8101-0629	B465
Preamplifier	ORTEC, Inc.	120	331
Spectroscopy Amplifier	ORTEC, Inc.	451	42
Series 2200 System Analyzer	Nuclear Data		
Analog to Digital Converter	Nuclear Data	74-0090	67-232
Master Control	Nuclear Data	74-0093	67-168
Memory	Nuclear Data	74-0101	67-141
Magnetic Tape Transport	Nuclear Data	880135	67-14
Magnetic Tape Data Reduce	Nuclear Data	740136	67-4
Digital Readout-Teletype Drive	Nuclear Data	740096	67-33
Read-In/Out Display	Nuclear Data	—	—
Bin and Power Supply	Nuclear Data	510	—
Oscilloscope	Hewlett-Packard	H77-120B	601-11140
Teletype	Teletype Corporation	33TC	—

XV.   APPENDIX E: CORRECTIONS FOR ELEMENTS IN THE WATER OF

THE STANDARDS AND IN THE IRRADIATION VIALS

This appendix is devoted to the derivation of an expression for
the estimated corrected mass of the unknown element by considering cor-
rections for the mass of the unknown element contained in the water and
vial of the standard and in the material of the irradiation vial containing
the unknown matrix. This technique applies when the same vial is used
for irradiating and counting the unknown matrix.

The mass of the unknown element before the correction, computed
from Eq. (27), is given by $m_u^o = M_{std}K'$ where K' is the proportionality
constant. Then K' is given by Eq. (E-1) where M_{std} is the mass of the
standard placed in the standard vial. This is a change in notation
from the previously used m_s in order to maintain consistency throughout
this derivation.

$$K' = \frac{m_u^o}{M_{std}} \qquad (E-1)$$

The mass of the unknown element in the water and vial of the
standard is estimated by irradiating, along with the standard, a "blank"
vial containing an equal volume of water from the same source (without
the standard element added). Then the balance equation of the unknown
element is given by Eq. (E-2) where M is the mass of the unknown
element:

$$(M_{vial} + M_{H_2O} + M_{std})K = M_{H_2O} + M_{vial} \qquad (E-2)$$

Let w equal the mass of the unknown element determined by NAA to be in the "blank" (water and vial). Assume K is approximately represented by

$$K = \frac{\text{mass of unknown element in the "blank"}}{\text{mass of standard element placed in standard vial}} = \frac{w}{M_{std}}$$

which is the analytical method of obtaining K from the results of calculations using Eq. (27). K represents the ratio of the saturated activities of the "blank" to standard, Eq. (12).

Let $\alpha = M_{vial} + M_{H_2O}$ where α = mass of unknown element in the "blank" (water and vial). Then $(\alpha + M_{std})K = \alpha$, from Eq. (E-2). Substitution for K in this expression results in

$$\alpha = \frac{w M_{std}}{M_{std} - w} \tag{E-3}$$

Similarly, the mass of the unknown element in the empty vial, determined in the same irradiation and by comparison to the same standard, is given by the following:

$$(M_{vial} + M_{H_2O} + M_{std})K'' = M_{vial} \tag{E-4}$$

where $\quad K'' = \dfrac{\text{mass of unknown element in empty vial}}{\text{mass of standard element placed in the standard vial}}$

Thus, K" is the ratio of saturated activities of the unknown element in the empty vial to the unknown element placed in the standard.

Let V = mass of unknown element determined by NAA to be in the empty vial; then

$$K'' = \frac{V}{M_{std}}$$

Substitution of α and V into Eq. (E-4) results in the following:

$$M_{vial} = (\alpha + M_{std}) \frac{V}{M_{std}} \tag{E-5}$$

The mass of the unknown element in the material being analyzed, M_u, is given by Eq. (E-6):

$$(M_{vial} + M_{H_2O} + M_{std})K' = M_u + M_{vial} \tag{E-6}$$

where K' is given by Eq. (E-1). Substitution of α and for K' and M_{vial} in Eq. (E-6) results in Eq. (E-7):

$$(\alpha + M_{std}) \frac{m_u^o}{M_{std}} = M_u + (\alpha + M_{std}) \frac{V}{M_{std}} \tag{E-7}$$

Therefore, the corrected mass of the unknown is given by Eq. (E-8):

$$M_{u \; corr} = (\alpha + M_{std}) \left[\frac{m_u^o}{M_{std}} - \frac{V}{M_{std}} \right] \tag{E-8}$$

which is the same as

$$M_{u \; corr} = (\alpha + M_{std})(K' - K'')$$

Substitution of Eq. (E-3) for α results in

$$M_{u \; corr} = \left[\frac{wM_{std}}{M_{std} - w} + M_{std} \right] \left[\frac{m_u^o - V}{M_{std}} \right]$$

which reduces to Eq. (E-9):

$$M_{u \; corr} = \left[\frac{M_{std}}{M_{std} - w} \right] (m_u^o - V) \tag{E-9}$$

From propagation of errors theory [2, 47], the uncertainty in this expression can be derived, and it is given by Eq. (E-10):

$$\sigma_{M_u \, corr} = \frac{M_{std}}{M_{std} - w} (m_u^o - V) \times$$

$$\sqrt{\frac{w^2 \sigma_{M_{std}}^2 + M_{std}^2 \sigma_w^2}{(M_{std} - w)^2 M_{std}^2} + \frac{\sigma_{m_u^o}^2 + \sigma_V^2}{(m_u^o - V)^2}} \qquad \text{(E-10)}$$

From the notation used in Section III, the corrected mass and its standard deviation are given by the following:

$$m_u \, corr \pm \sigma_{m_u \, corr} = \left[\frac{m_s}{m_s - w}\right] (m_u^o - V) \times$$

$$\left[1 \pm \sqrt{\frac{w^2 \sigma_{m_s}^2 + m_s^2 \sigma_w^2}{(m_s - w)^2 m_s^2} + \frac{\sigma_{m_u^o}^2 + \sigma_V^2}{(m_u^o - V)^2}}\right] \qquad \text{(E-11)}$$

where $m_u^o \pm \sigma_{m_u^o}$ is given by Eq. (27) for the unknown element in the matrix material being analyzed.

XVI. APPENDIX F: PROGRAM "ACTY"

Program ACTY was written to calculate the expected activity re-
sulting from the irradiation of one gram of plant material at a thermal
neutron flux of 10^{10} n/cm^2-sec for variable irradiation and decay times.
This program can be used to estimate the activity resulting from the
irradiation of any material for any combination of irradiation and
decay times if the user can estimate the concentrations of the elemental
constituents in the material.

Program ACTY uses solutions to differential equations representing
various activation and decay schemes for the nuclides being activated.
There are eight different subprograms in ACTY, designated as CALC1,
CALC2, etc., which perform calculations for each different "type" of
activation and decay scheme utilizing the solution equations and the
input times of irradiation and decay. Other input data include
nuclear and abundance data for the target and product nuclides and the
estimated concentration or mass of each elemental constituent in one
gram of material.

The eight types of activation and decay schemes are listed below
with the applicable differential equations, the solution equations, and
the elements (nuclides) contained in plant material in concentrations
of about 1 ppm or greater. The notation follows that of Section III.

1)   Type 1:

Scheme: $N_1 \xrightarrow{\sigma_1} N_2 \xrightarrow{\lambda_2}$ Stable
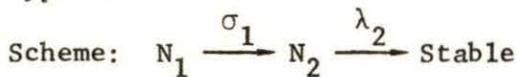
Differential Equation: $\dfrac{dN_2}{dt} = N_1 \sigma_1 \phi - N_2 \lambda_2$

Solution: with $R = N_1^o \sigma_1 \phi$

$$A_2 = R(1 - e^{-\lambda_2 t_e}) e^{-\lambda_2 t_d}$$

Applies to the following target nuclides in this matrix:

^{11}B	^{44}Ca	^{112}Sn
^{13}C	^{55}Mn	^{116}Sn
^{23}Na	^{54}Fe	^{118}Sn
^{27}Al	^{58}Fe	^{120}Sn
^{30}Si	^{63}Cu	^{122}Sn
^{31}P	^{64}Zn	^{132}Ba
^{34}S	^{68}Zn	^{134}Ba
^{36}S	^{70}Zn	^{136}Ba
^{41}K	^{92}Mo	

2) Type 2:

Scheme: $N_1 \xrightarrow{\sigma_1} N_2 \xrightarrow{\lambda_2} N_3 \xrightarrow{\lambda_3}$ Stable
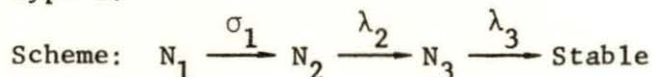
Differential Equations: Same as 1) above plus

$$\frac{dN_3}{dt} = N_2 \lambda_2 - N_3 \lambda_3$$

Solutions: A_2 from 1) above plus

$$A_3 = R\left[(1 - e^{-\lambda_3 t_e}) + \frac{\lambda_3}{\lambda_3 - \lambda_2} (e^{-\lambda_3 t_e} - e^{-\lambda_2 t_e}) \right]$$

$$\times e^{-\lambda_3 t_d} + \frac{R\lambda_3}{\lambda_3 - \lambda_2} (1 - e^{-\lambda_2 t_e})(e^{-\lambda_2 t_d} - e^{-\lambda_3 t_d}).$$

$$A_{total} = A_2 + A_3$$

Applies to the following target nuclides in this matrix:

^{46}Ca ^{98}Mo ^{124}Sn

^{48}Ca ^{100}Mo ^{130}Ba

^{68}Zn ^{112}Sn ^{132}Ba

^{92}Mo

3)   Type 3:

      Scheme: $^{65}Cu \xrightarrow{\sigma_1} {}^{66}Cu \xrightarrow{\lambda_2}$ Stable

              (N_1) (N_2)

                        $\downarrow \sigma_2$

                     $^{67}Cu \xrightarrow{\lambda_3}$ Stable

                     (N_3)
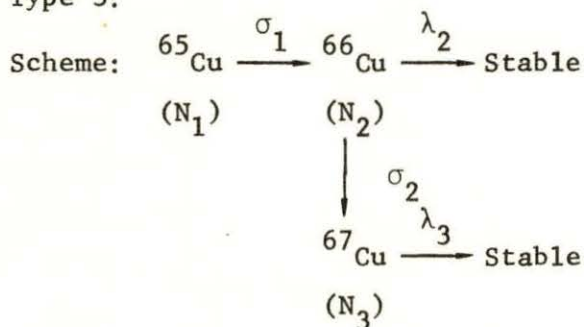
Differential Equations: $\dfrac{dN_2}{dt} = N_1 \sigma_1 \phi - (\lambda_2 + \sigma_2 \phi) N_2$

$$\frac{dN_3}{dt} = N_2 \sigma_2 \phi - N_3 \lambda_3$$

Solutions: $A_2 \cong A_2$ from 1) above plus

$$A_3 \cong \frac{R \sigma_2 \phi}{\lambda_2} \left[(1 - e^{-\lambda_3 t_e}) + \frac{\lambda_3}{\lambda_3 - \lambda_2} (e^{-\lambda_3 t_e} - e^{-\lambda_2 t_e}) \right] e^{-\lambda_3 t_d} .$$

$$A_{total} = A_2 + A_3$$

Applies only to ^{65}Cu in this matrix.

4)   Type 4:

      Scheme: $^{26}Mg \xrightarrow{\sigma_1} {}^{27}Mg \xrightarrow{\sigma_2} {}^{28}Mg$

              (N_1) (N_2) (N_3)

                     $\downarrow \lambda_2$ $\downarrow \lambda_3$

                  Stable ^{28}Al

                        (N_4)

                        $\downarrow \lambda_4$

                    Stable

128

Differential Equations: Same as 3) above plus

$$\frac{dN_4}{dt} = N_3\lambda_3 - N_4\lambda_4$$

Solutions: $A_2 = A_2$ from 3) above.

$A_3 = A_3$ from 3) above.

$$A_4 = \frac{A_3\lambda_4}{\lambda_4 - \lambda_3}(1 - e^{-(\lambda_4-\lambda_3)t_d})$$
$$+ [\frac{R\sigma_2\phi}{\lambda_2}(1 - e^{-\lambda_4 t_e}) + \frac{R\lambda_4\sigma_2\phi}{(\lambda_3 - \lambda_2)(\lambda_4 - \lambda_3)} \times$$
$$(e^{-\lambda_3 t_e} - e^{-\lambda_4 t_e}) + \frac{R\lambda_4\lambda_3\sigma_2\phi}{\lambda_2(\lambda_3 - \lambda_2)(\lambda_4 - \lambda_2)} \times$$
$$(e^{-\lambda_4 t_e} - e^{-\lambda_2 t_e})]e^{-\lambda_4 t_d} .$$

$$A_{total} = A_2 + A_3 + A_4 .$$

Applies only to ^{26}Mg in this matrix.

5)   Type 5:

Scheme:
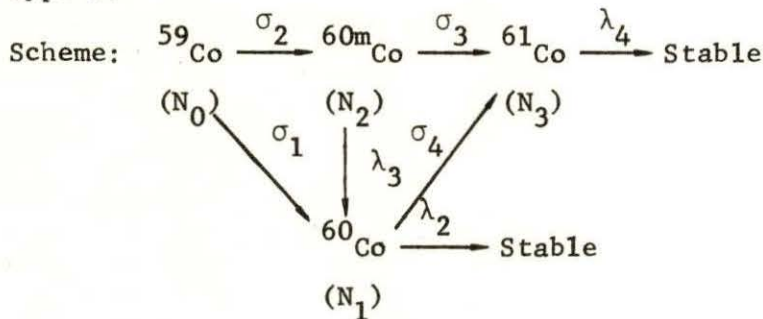
Differential Equations:
$$\frac{dN_2}{dt} = N_0\sigma_2\phi - N_2\sigma_3\phi - N_2\lambda_3$$
$$\frac{dN_1}{dt} = N_0\sigma_1\phi + N_2\lambda_2 - N_1\sigma_4\phi - N_1\lambda_2$$
$$\frac{dN_3}{dt} = N_2\sigma_3\phi + N_1\sigma_4\phi - N_3\lambda_4$$

Solutions: with $R = N_0^o\sigma_2\phi$

$$A_2 = R(1 - e^{-\lambda_3 t_e})e^{-\lambda_3 t_d}$$

$$A_1 = \frac{\lambda_2 A_2}{\lambda_2 - \lambda_3} + \frac{N_0^o \phi [\sigma_1 (\lambda_2 - \lambda_3) - \sigma_2 \lambda_3]}{\lambda_2 - \lambda_3}$$

$$\times (1 - e^{-\lambda_2 t_e}) e^{-\lambda_2 t_d} .$$

$$A_3 = (K_1 + K_2 + K_3)(1 - e^{-\lambda_4 t_e}) e^{-\lambda_4 t_d}$$

$$+ \frac{\lambda_4}{\lambda_4 - \lambda_3} (K_1 + K_2)(e^{-\lambda_4 t_e} - e^{-\lambda_3 t_e}) e^{-\lambda_4 t_d}$$

$$+ \frac{\lambda_4 K_3}{\lambda_4 - \lambda_2} (e^{-\lambda_4 t_e} - e^{-\lambda_2 t_e}) e^{-\lambda_4 t_d} .$$

where $\quad K_1 = R\sigma_3 \phi / \lambda_3$

$$K_2 = R\sigma_4 \phi / (\lambda_2 - \lambda_3)$$

$$K_3 = N_0^o \sigma_4 \phi^2 [\sigma_1 (\lambda_2 - \lambda_3) - \sigma_2 \lambda_3] / \lambda_2 (\lambda_2 - \lambda_3)$$

$$A_{total} = A_1 + A_2 + A_3$$

Applies only to ^{59}Co in this matrix.

6)   Type 6:

Scheme: ^{138}Ba $\xrightarrow{\sigma_1}$ ^{139}Ba $\xrightarrow{\sigma_2}$ ^{140}Ba $\xrightarrow{\sigma_3}$ ^{141}Ba

$\quad\quad\quad$ (N_1) $\quad\quad$ (N_2) $\quad\quad\quad$ (N_3) $\quad\quad\quad$ (N_5)

$\quad\quad\quad\quad\quad\quad\quad\quad\quad$ $\Big\downarrow \lambda_2$ $\quad\quad\quad$ $\Big\downarrow \lambda_3$ $\quad\quad\quad$ $\Big\downarrow \lambda_5$

$\quad\quad\quad\quad\quad\quad\quad\quad$ Stable $\quad\quad$ ^{140}La $\quad\quad$ ^{141}La

$\quad\quad\quad\quad\quad\quad\quad\quad\quad\quad\quad\quad\quad$ (N_4) $\quad\quad\quad\quad$ (N_6)

$\quad\quad\quad\quad\quad\quad\quad\quad\quad\quad\quad\quad\quad$ $\Big\downarrow \lambda_4$ $\quad\quad\quad$ $\Big\downarrow \lambda_6$

$\quad\quad\quad\quad\quad\quad\quad\quad\quad\quad\quad\quad\quad\quad\quad\quad\quad\quad\quad$ Disregarded

$\quad\quad\quad\quad\quad\quad\quad\quad\quad\quad\quad\quad\quad$ Stable
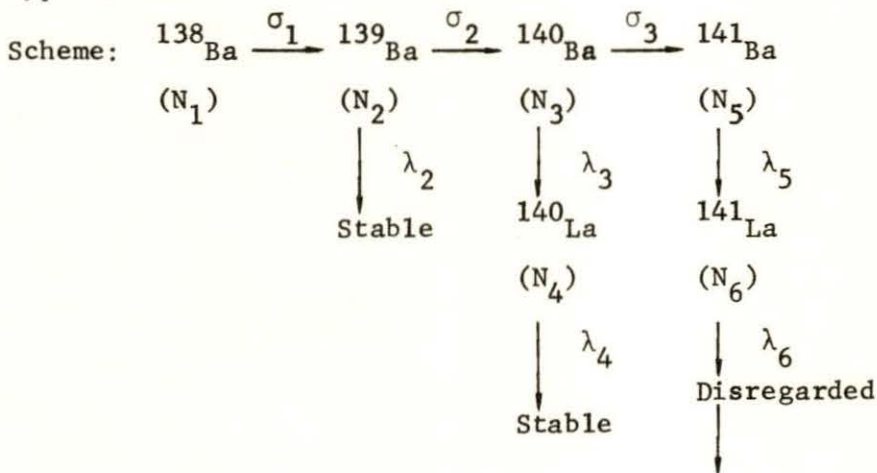
Differential Equations: $\dfrac{dN_2}{dt} = N_1 \sigma_1 \phi - (\lambda_2 + \sigma_2 \phi) N_2$
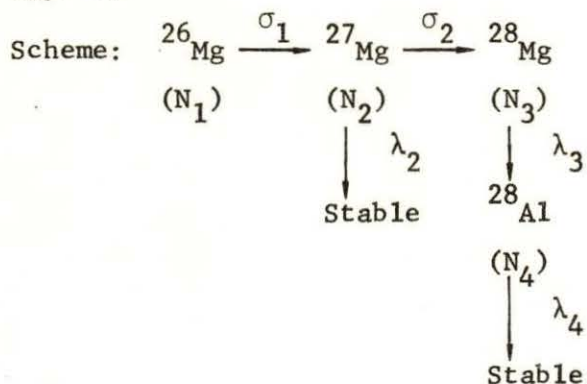
$$\dfrac{dN_3}{dt} = N_2 \sigma_2 \phi - (\lambda_3 + \sigma_3 \phi) N_3$$

$$\frac{dN_4}{dt} = N_3\lambda_3 - N_4\lambda_4$$

$$\frac{dN_5}{dt} = N_3\sigma_3\phi - N_5\lambda_5$$

Solutions: with $R = N_1^o\sigma_1\phi$,

$A_2 = A_2$ from 3) above.

$A_3 = A_3$ from 3) above.

$$A_4 = R\sigma_2\phi e^{-\lambda_4 t_d}[\frac{1 - e^{-\lambda_4 t_e}}{\lambda_2} - \frac{\lambda_4(e^{-\lambda_3 t_e} - e^{-\lambda_4 t_e})}{(\lambda_3 - \lambda_2)(\lambda_4 - \lambda_3)}$$

$$+ \frac{\lambda_4\lambda_3}{\lambda_2(\lambda_3 - \lambda_2)(\lambda_4 - \lambda_2)} \times (e^{-\lambda_4 t_e} - e^{-\lambda_2 t_e})]$$

$$+ \frac{\lambda_4 A_3}{\lambda_4 - \lambda_3}(1 - e^{-(\lambda_4 - \lambda_3)t_d}).$$

$$A_5 = [\lambda_5 K_4(1 - e^{-\lambda_5 t_e}) + \lambda_5(K_5 - K_6) \times$$

$$(e^{-\lambda_5 t_e} - e^{-\lambda_3 t_e}) + \lambda_5 K_7(e^{-\lambda_5 t_e} - e^{-\lambda_2 t_e})]e^{-\lambda_5 t_d}.$$

where

$$K_4 = K_8/\lambda_2\lambda_3\lambda_5$$

$$K_5 = K_8/\lambda_2\lambda_3(\lambda_5 - \lambda_3)$$

$$K_6 = K_8/\lambda_2(\lambda_3 - \lambda_2)(\lambda_5 - \lambda_3)$$

$$K_7 = K_8/\lambda_2(\lambda_3 - \lambda_2)(\lambda_5 - \lambda_2)$$

$$K_8 = R\sigma_2\sigma_3\phi^2$$

$$A_{total} = A_2 + A_3 + A_4 + A_5$$

Applies only to ^{138}Ba in this matrix.

7) Type 7:

   Scheme: $N_1 \xrightarrow{\sigma_1} N_2 \xrightarrow{\lambda_2}$
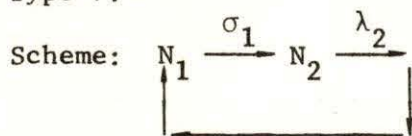
   which applies to (n, p) reactions followed by β^- decay.

   Differential Equations: $\dfrac{dN_1}{dt} = N_2\lambda_2 - N_1\sigma_1\phi$

   $\dfrac{dN_2}{dt} = N_1\sigma_1\phi - N_2\lambda_2$

   Solution: $A_2 = N_1^o\sigma_1\phi(1 - \dfrac{\sigma_1\phi}{\Lambda})(1 - e^{-\Lambda t_e})e^{-\lambda_2 t_d}$

   where $\Lambda = \sigma_1\phi + \lambda_2$

Applies to ^{14}N and ^{33}S in this matrix.

8) Type 8:

   Scheme: ^{37}Cl $\xrightarrow{\sigma_2}$ ^{38m}Cl

   $(N_1) \xrightarrow{\sigma_1}$ (N_3)

   $\Big\downarrow \lambda_3$

   ^{38}Cl $\xrightarrow{\lambda_2}$ Stable

   (N_2)
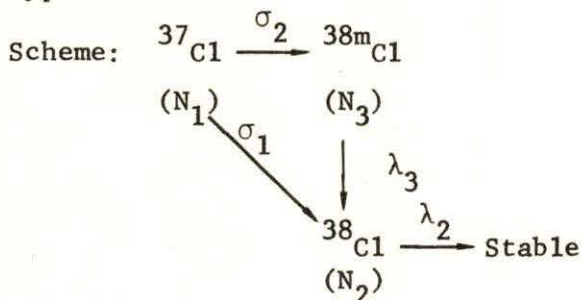
   Differential Equations: $\dfrac{dN_2}{dt} = N_1\sigma_1\phi + N_3\lambda_3 - N_2\lambda_2$

   $\dfrac{dN_3}{dt} = N_1\sigma_2\phi - N_3\lambda_3$

   Solutions: with $R = N_1^o\sigma_2\phi$,

   $A_3 = R(1 - e^{-\lambda_3 t_e})e^{-\lambda_3 t_d}$

   $A_2 = \dfrac{\lambda_2 A_3}{\lambda_2 - \lambda_3} + \dfrac{[N_1^o\sigma_1\phi(\lambda_2 - \lambda_3) - R\lambda_3]}{\lambda_2 - \lambda_3} \times$

   $(1 - e^{-\lambda_2 t_e})e^{-\lambda_2 t_d}$.

$$A_{total} = A_2 + A_3$$

Applies only to ^{37}Cl in this matrix.

The data cards for input to this program are as follows:

1) Card 1: Variable name NS, Format I5. This indicates the number of cards which follow with data for the nuclides being calculated in this program run.

2) Cards 2 through NS + 1: Data cards with the following format:

Item	Description	Format	Columns
1	Mass of element in grams	F8.0	1-8
2	Atomic weight of element in grams	F4.0	9-12
3	Relative abundance of target nuclide in relation to all other stable nuclides of the same element	F7.0	13-19
4	Reaction cross section in barns, σ_1	F4.0	20-23
5	Reaction cross section in barns, σ_2	F4.0	24-27
6	Reaction cross section in barns, σ_3	F4.0	28-31
7	Half-life of product nuclide corresponding to λ_2	F5.0	32-36
8	Time unit code for item 7 (Y, D, H, M, or S)	A1	37
9	Half-life of product nuclide corresponding to λ_3	F4.0	38-41
10	Time unit code for item 9	A1	42
11	Half-life of product nuclide corresponding to λ_4	F5.0	43-47
12	Time unit code for item 11	A1	48

Item	Description	Format	Columns
13	Half-life of product nuclide corresponding to λ_5	F3.0	49-51
14	Time unit code for item 13	A1	52
15	Activation and decay scheme "type" code (1. through 8.)	F2.0	61-62
16	Alphanumeric designation of the target nuclide, e.g., ^{55}Mn as 55 MN		63-70
			(Right justified)

3) Cards NS + 2 to the end of the data: time variables with the following format:

Item	Description	Format	Columns
1	Time of irradiation in seconds	F10.0	1-10
2	Time of decay in seconds	F10.0	11-20

The program prints headings for each set of time variables, calculates the activity resulting from the activation and decay scheme, prints this activity for each target nuclide scheme, and prints the total activity for all the target nuclides used. The individual nuclide activities are listed in disintegrations per second (dps) and the total activities are listed in dps and in microcuries.

The program listing is on the following pages.

```
C
C
C
C PROGRAM ACTY IS A FORTRAN IV COMPUTER PROGRAM FOR CALCULATION OF THE
C EXPECTED ACTIVITIES RESULTING FROM IRRADIATING ONE GRAM OF MATERIAL
C AT A THERMAL FLUX OF 10 TO THE 10TH NEUTRONS PER CM SQUARED PER SECOND
C FOR VARIABLE IRRADIATION AND DECAY TIMES.
C
      REAL      SS/'S    '/,MM/'M    '/,HH/'H    '/,DD/'D    '/,YY/'Y    '/
      DIMENSION S(60,30),E(2)
      REAL CALC1,CALC2,CALC3,CALC4,CALC5,CALC6,CALC7,CALC8
      DIMENSION ID(60),IDI(60)
C
C READ IN NUMBER OF NUCLIDES, NS
C
      READ (5,1) NS
    1 FORMAT (I5)
C
C  READ IN DATA CARDS FOR NS NUCLIDES
C
      DO 100 I=1,NS
      READ (5,8) (S(I,J),J=1,15),ID(I),IDI(I)
    8 FORMAT (F8.0,F4.0,F7.0,3F4.0,F5.0,A1,F4.0,A1,F5.0,A1,F3.0,A1,F10.0
     X,2A4)
C
C CONVERT ALL HALF-LIVES TO SECONDS
C
      DO 200 K=8,14,2
      L=K-1
      M=K+12
      IF (S(I,K).EQ.SS) S(I,M)=S(I,L)
      IF (S(I,K).EQ.MM) S(I,M)=S(I,L)*60
      IF (S(I,K).EQ.HH) S(I,M)=S(I,L)*60*60
      IF (S(I,K).EQ.DD) S(I,M)=S(I,L)*24*3600
      IF (S(I,K).EQ.YY) S(I,M)=S(I,L)*365*24*3600
  200 CONTINUE
  100 CONTINUE
```

```
C
C READ IN TIME VARIBLES
C
   50 READ (5,7,END=60) E(1), E(2)
    7 FORMAT (2F10.0)
C
C PRINT OUTPUT HEADINGS
C
      WRITE (6,25)
   25 FORMAT (1H1)
      WRITE (6,9)  NS,E(1),E(2)
    9 FORMAT (///' ',10X,'NUMBER OF CALCULATIONS = ',I2,', EXPOSURE TIME
     X = ',E11.5,1X,'SEC, DECAY TIME = ',E13.7,1X,'SEC, FLUX = 1.0E 10:'
     X)
      WRITE (6,12)
   12 FORMAT ('0',10X,'NO',3X,'TARGET ISOTOPE',3X,'ACTIVITY OF PRODUCTS
     XIN DPS PER GRAM OF PLANT TISSUE:')
C
C CALCULATE ACTIVITIES BASED ON "TYPE" ACTIVATION AND DECAY SCHEME
C
      ACTY=0.0
      DO 300 I=1,NS
      XNO=S(I,1)*.6023E24*S(I,3)/S(I,2)
      IF(S(I,15).EQ.1.)X=CALC1(XNO,S,I,E)
      IF(S(I,15).EQ.2.)X=CALC2(XNO,S,I,E)
      IF(S(I,15).EQ.3.)X=CALC3(XNO,S,I,E)
      IF(S(I,15).EQ.4.)X=CALC4(XNO,S,I,E)
      IF(S(I,15).EQ.5.)X=CALC5(XNO,S,I,E)
      IF(S(I,15).EQ.6.)X=CALC6(XNO,S,I,E)
      IF(S(I,15).EQ.7.)X=CALC7(XNO,S,I,E)
      IF(S(I,15).EQ.8.)X=CALC8(XNO,S,I,E)
C
C PRINT ACTIVITIES
C
      WRITE (6,13) I,ID(I),IDI(I),X
   13 FORMAT (' ',10X,I2,3X,2A4,7X,E15.7)
      ACTY=ACTY+X
```

```
    300 CONTINUE
        WRITE (6,3) ACTY
      3 FORMAT (' ',10X,'TOTAL ACTIVITY IN DPS PER GRAM OF TISSUE:',2X,E13
       X.7)
        XMICCI=ACTY/3.7E4
        WRITE (6,15) XMICCI
     15 FORMAT (' ',10X,'TOTAL ACTIVITY IN MICROCURIES PER GRAM OF TISSUE:
       X',2X,E13.7)
C
C READ IN TIME VARIABLES FOR NEXT CALCULATIONS AND REPEAT UNTIL
C REMAINING DATA CARDS ARE EXPENDED
C
        GO TO 50
     60 CONTINUE
C
C PRINT DATA WHICH WERE INPUT FOR ALL NUCLIDES
C
        WRITE (6,25)
        WRITE (6,4)
      4 FORMAT (////' ',10X,'SAMPLE DATA FOLLOW:')
        WRITE (6,14)
     14 FORMAT ('0',10X,'NO',4X,'TARGET',4X,'MASS,3',3X,'A.W.',3X,'REL AB'
       X,3X,'SIG 1',4X,'SIG 2',3X,'SIG 3',4X,'HLFLF2',4X,'HLFLF3',2X,'HLFL
       XF4',2X,'HLFLF5',2X,'EQN TYPE')
        WRITE (6,6) (I,ID(I),IDI(I),(S(I,J),J=1,15),I=1,NS)
      6 FORMAT ((' ',10X,I2,2X,2A4,2X,F9.7,F7.2,F9.6,F8.4,2F8.2,2X,F8.3,A1
       X,2X,F6.2,A1,2(2X,F5.2,A1),6X,F2.0))
        STOP
        END
C
C
        REAL FUNCTION CALC1(YNO,SAM,J,T)
        REAL SAM (60,30),T(2)
        XLAMTW=.693/SAM(J,20)
        CALC1=YNO*SAM(J,4)*.1E-13*(1-EXP(-XLAMTW*T(1)))*EXP(-XLAMTW*T(2))
        RETURN
        END
```

```
C
C
      REAL FUNCTION CALC2(YNO,SAM,J,T)
      REAL SAM (60,30),T(2)
      XLAMTW=.693/SAM(J,20)
      XLAMTH=.693/SAM(J,22)
      ACCUM=0.0+YNO*SAM(J,4)*.1E-13*(1-EXP(-XLAMTW*T(1)))*EXP(-XLAMTW*T(
     X2))
      CALC2=ACCUM+YNO*SAM(J,4)*.1E-13*((1-EXP(-XLAMTH*T(1)))+XLAMTH/(XLA
     XMTH-XLAMTW)*(EXP(-XLAMTH*T(1))-EXP(-XLAMTW*T(1))))*EXP(-XLAMTH*T(2
     X))
      CALC2=CALC2+XLAMTH*YNO*SAM(J,4)*.1E-13*(1-EXP(-XLAMTW*T(1)))/(XLAM
     XTH-XLAMTW)*(EXP(-XLAMTW*T(2))-EXP(-XLAMTH*T(2)))
      RETURN
      END
C
C
      REAL FUNCTION CALC3(YNO,SAM,J,T)
      REAL SAM (60,30),T(2)
      XLAMTW=.693/SAM(J,20)
      XLAMTH=.693/SAM(J,22)
      ACCUM=0.0+YNO*SAM(J,4)*.1E-13*(1-EXP(-XLAMTW*T(1)))*EXP(-XLAMTW*T(
     X2))
      CALC3=ACCUM+YNO*SAM(J,4)*SAM(J,5)*.1E-27/XLAMTW*((1-EXP(-XLAMTH*T(
     X1)))+XLAMTH/(XLAMTH-XLAMTW)*(EXP(-XLAMTH*T(1))-EXP(-XLAMTW*T(1))))
     X*EXP(-XLAMTH*T(2))
      RETURN
      END
C
C
      REAL FUNCTION CALC4(YNO,SAM,J,T)
      REAL SAM (60,30),T(2)
      XLAMTW=.693/SAM(J,20)
      XLAMTH=.693/SAM(J,22)
      XLAMFO=.693/SAM(J,24)
      ACCUM=0.0+YNO*SAM(J,4)*.1E-13*(1-EXP(-XLAMTW*T(1)))*EXP(-XLAMTW*T(
     X2))
```

```
      ACCUM=ACCUM+YNO*SAM(J,4)*SAM(J,5)*.1E-27/X_AMTW*((1-EXP(-XLAMTH*T(
     X1)))+XLAMTH/(XLAMTH-XLAMTW)*(EXP(-XLAMTH*T(1))-EXP(-XLAMTW*T(1))))
     X*EXP(-XLAMTH*T(2))
       CALC4=ACCUM+YNO*SAM(J,4)*SAM(J,5)*.1E-27*((1-EXP(-XLAMFO*T(1)))/XL
     XAMTW+XLAMFO/((XLAMTH-XLAMTW)*(XLAMFO-XLAMTH))*(EXP(-XLAMTH*T(1))-E
     XXP(-XLAMFO*T(1)))+XLAMTH*XLAMFO/(XLAMTW*(XLAMTH-XLAMTW)*(XLAMFO-XL
     XAMTW))*(EXP(-XLAMFO*T(1))-EXP(-XLAMTW*T(1))))*EXP(-XLAMFO*T(2))
       CALC4=CALC4+YNO*SAM(J,4)*SAM(J,5)*.1E-27/XLAMTW*((1-EXP(-XLAMTH*T(
     X1)))+XLAMTH/(XLAMTH-XLAMTW)*(EXP(-XLAMTH*T(1))-EXP(-XLAMTW*T(1))))
     X*XLAMFO/(XLAMFO-XLAMTH)*(EXP(-XLAMTH*T(2))-EXP(-XLAMFO*T(2)))
      RETURN
      END
C
C

      REAL FUNCTION CALC5(YNO,SAM,J,T)
      REAL SAM (60,30),T(2)
      HL2=.693/SAM(J,20)
      HL3=.693/SAM(J,22)
      HL4=.693/SAM(J,24)
      PR=YNO*SAM(J,4)*.1E-13
      A2=PR*(1-EXP(-HL3*T(1)))*EXP(-HL3*T(2))
      A1=HL2/(HL2-HL3)*A2+(YNO*SAM(J,5)*.1E-13*(HL2-HL3)-PR*HL3)/(HL2-HL
     X3)*(1-EXP(-HL2*T(1)))*EXP(-HL2*T(2))
       B1=PR*SAM(J,6)*.1E-13/HL3
       B2=PR*6.*.1E-13/(HL2-HL3)
       B3=(YNO*6.*SAM(J,5)*.1E-27*(HL2-HL3)-PR*6.*.1E-13*HL3)/(HL2*(HL2-H
     XL3))
       A3=(B1+B2+B3)*(1-EXP(-HL4*T(1)))*EXP(-HL4*T(2))+HL4/(HL4-HL3)*(B1+
     XB2)*(EXP(-HL4*T(1))-EXP(-HL3*T(1)))*EXP(-HL4*T(2))+HL4/(HL4-HL2)*B
     X3*(EXP(-HL4*T(1))-EXP(-HL2*T(1)))*EXP(-HL4*T(2))
       CALC5=A1+A2+A3
      RETURN
      END
C
C

      REAL FUNCTION CALC6(YNO,SAM,J,T)
      REAL SAM (60,30),T(2)
```

```
      HL2=.693/SAM(J,20)
      HL3=.693/SAM(J,22)
      HL4=.693/SAM(J,24)
      HL5=.693/SAM(J,26)
      A2=YNO*SAM(J,4)*.1E-13*(1-EXP(-HL2*T(1)))*EXP(-HL2*T(2))
      A=YNO*SAM(J,4)*SAM(J,5)*.1E-27
      C1=A/HL2
      B=C1*SAM(J,6)*.1E-13
      B1=HL3-HL2
      B2=HL4-HL3
      B3=HL4-HL2
      B4=HL5-HL3
      B5=HL5-HL2
      A3=C1*((1-EXP(-HL3*T(1)))+HL3/B1*(EXP(-HL3*T(1))-EXP(-HL2*T(1))))*
     XEXP(-HL3*T(2))
      A4=A*((1-EXP(-HL4*T(1)))/HL2-HL4*(EXP(-HL3*T(1))-EXP(-HL4*T(1)))/(
     XB1*B2)+HL3*HL4/(HL2*B1*B3)*(EXP(-HL4*T(1))-EXP(-HL2*T(1))))*EXP(-H
     XL4*T(2))
      A4A=HL4*A3/B2*(1-EXP(-B2*T(2)))
      C2=B/(HL3*HL5)
      C3=B/(HL3*B4)
      C4=B/(B1*B4)
      C5=B/(B1*B5)
      C9=HL5*C2
      A5=C9*(1-EXP(-HL5*T(1)))+HL5*(C3-C4)*(EXP(-HL5*T(1))-EXP(-HL3*T(1)
     X))+HL5*C5*(EXP(-HL5*T(1))-EXP(-HL2*T(1)))*EXP(-HL5*T(2))
      CALC6=A2+A3+A4+A4A+A5
      RETURN
      END
C
C

      REAL FUNCTION CALC7(YNO,SAM,J,T)
      REAL SAM (60,30),T(2),LAM
      LAM=.693/SAM(J,20)
      CAPL=SAM(J,4)*.1E-13+LAM
      CALC7=SAM(J,4)*.1E-13*YNO*(1-SAM(J,4)*.1E-13/CAPL)*(1-EXP(-CAPL*T(
     X1)))*EXP(-LAM*T(2))
```

```
      RETURN
      END
C
C

      REAL FUNCTION CALC8(YNO,SAM,J,T)
      REAL SAM (60,30),T(2)
      HL2=.693/SAM(J,20)
      HL3=.693/SAM(J,22)
      PR=YNO*SAM(J,4)*.1E-13
      A2=PR*(1-EXP(-HL3*T(1)))*EXP(-HL3*T(2))
      A1=HL2/(HL2-HL3)*A2+(YNO*SAM(J,5)*.1E-13*(HL2-HL3)-PR*HL3)/(HL2-HL
     X3)*(1-EXP(-HL2*T(1)))*EXP(-HL2*T(2))
      CALC8=A1+A2
      RETURN
      END
```

NUMBER OF CALCULATICNS = 48, EXPOSURE TIME = 0.36000E 04 SEC, DECAY TIME = 0.4320000E 05 SEC, FLUX = 1.0E 10:

NO	TARGET ISOTOPE	ACTIVITY OF PRODUCTS IN DPS PER GRAM OF PLANT TISSUE:
1	11B	0.0000000E 00
2	13C	0.1491639E-03
3	14N	0.1380316E 01
4	23NA	0.0000000E 00
5	23NA	0.6443015E 03
6	26MG	0.1681781E-10
7	27AL	0.0000000E 00
8	30SIG2	0.1755315E 02
9	31P	0.2107793E 03
10	33S	0.8117344E-02
11	34S	0.1746830E 01
12	36S	0.1669707E-41
13	37CL	0.1751927E-03
14	41K	0.7756855E 04
15	44CA	0.1928978E 01
16	46CA	0.4927476E-01
17	48CA	0.1614119E 00
18	55MN	0.1091051E 04
19	54FE	0.6289405E-01
20	58FE	0.2613104E-01
21	59CC	0.1711367E-01
22	63CU	0.2264631E 03
23	65CU	0.6940915E-08
24	64ZN	0.5120638E-01
25	68ZN	0.2934599E-01
26	68ZN	0.1995559E 01
27	70ZN	0.0000000E 00
28	70ZN	0.2385303E-02
29	92MC	0.2493572E-05
30	92MC	0.1711181E-02
31	98MC	0.3662174E-01
32	100MC	0.3258312E-13
33	112SN	0.4755151E-02
34	112SN	0.5416022E-10
35	116SN	0.1912296E-02
36	118SN	0.3083984E-03
37	120SN	0.9571499E 00
38	120SN	0.3938713E-06
39	122SN	0.1208284E-04
40	122SN	0.2593185E-04
41	124SN	0.7876602E-03
42	124SN	0.1952022E-03
43	130BA	0.9461805E-02
44	132BA	0.3291211E-04
45	132BA	0.1216299E-02
46	134BA	0.3039533E-01
47	136BA	0.0000000E 00
48	138BA	0.1209056E 00

TOTAL ACTIVITY IN DPS PER GRAM OF TISSUE: 0.9955586E 04
TOTAL ACTIVITY IN MICROCURIES PER GRAM OF TISSUE: 0.2690699E 00

SAMPLE CATA FOLLOW:

NO	TARGET	MASS,G	A.W.	REL AB	SIG 1	SIG 2	SIG 3	HLFLF2	HLFLF3	HLFLF4	HLFLF5	EQN TYPE
1	11B	0.0000320	10.80	0.803000	0.0050	0.00	0.00	0.020S	0.00	0.00	0.00	1.
2	13C	0.4500000	12.00	0.011080	0.0010	0.00	0.00	5730.000Y	0.00	0.00	0.00	1.
3	14N	0.0300000	14.00	0.996000	1.8100	0.00	0.00	5730.000Y	0.00	0.00	0.00	7.
4	23NA	0.0001790	23.00	1.000000	0.4000	0.00	0.00	0.020S	0.00	0.00	0.00	1.
5	23NA	0.0001790	23.00	1.000000	0.5300	0.00	0.00	15.000H	0.00	0.00	0.00	1.
6	26MG	0.0027000	24.30	0.111703	0.0270	0.03	0.00	9.500M	21.20H	2.31M	0.00	4.
7	27AL	0.0000100	27.00	1.000000	0.2350	0.00	0.00	2.310M	0.00	0.00	0.00	1.
8	30SIO2	0.0053000	60.10	0.030900	0.1100	0.00	0.00	2.620H	0.00	0.00	0.00	1.
9	31P	0.0029000	31.00	1.000000	0.1900	0.00	0.00	14.3000	0.00	0.00	0.00	1.
10	33S	0.0025000	32.10	0.007600	0.0020	0.00	0.00	25.0000	0.00	0.00	0.00	7.
11	34S	0.0025000	32.10	0.042200	0.2700	0.00	0.00	88.0000	0.00	0.00	0.00	1.
12	36S	0.0025000	32.10	0.000140	0.1400	0.00	0.00	5.070M	0.00	0.00	0.00	1.
13	37CL	0.0000100	35.50	0.244700	0.0050	0.40	0.00	37.300M	0.74S	0.00	0.00	8.
14	41K	0.0223000	39.10	0.067700	1.2000	0.00	0.00	12.400H	0.00	0.00	0.00	1.
15	44CA	0.0051000	40.10	0.020600	0.7000	0.00	0.00	165.0000	0.00	0.00	0.00	1.
16	46CA	0.0051000	40.10	0.000033	0.3000	0.00	0.00	4.5300	3.430	0.00	0.00	2.
17	48CA	0.0051000	40.10	0.001850	1.1000	0.00	0.00	8.800H	57.50M	0.00	0.00	2.
18	55MN	0.0000800	54.90	1.000000	13.3000	0.00	0.00	2.576H	0.00	0.00	0.00	1.
19	54FE	0.0001130	55.80	0.058400	2.9000	0.00	0.00	2.600Y	0.00	0.00	0.00	1.
20	58FE	0.0001130	55.80	0.003100	1.1000	0.00	0.00	45.6000	0.00	0.00	0.00	1.
21	59CO	0.0000003	58.90	1.000000	18.0000	19.00	100.00	5.260Y	10.50M	99.00M	0.00	5.
22	63CU	0.0000279	63.50	0.691000	4.5300	0.00	0.00	12.800H	0.00	0.00	0.00	1.
23	65CU	0.0000200	63.50	0.309000	2.3000	130.00	0.00	5.100H	58.50H	0.00	0.00	3.
24	64ZN	0.0000210	65.40	0.488900	0.4600	0.00	0.00	245.0000	0.00	0.00	0.00	1.
25	68ZN	0.0000210	65.40	0.185600	1.0000	0.00	0.00	57.000M	0.00	0.00	0.00	1.
26	68ZN	0.0000210	65.40	0.185600	0.1000	0.00	0.00	13.800H	57.00M	0.00	0.00	2.
27	70ZN	0.0000210	65.40	0.006200	0.1000	0.00	0.00	2.400H	0.00	0.00	0.00	1.
28	70ZN	0.0000210	65.40	0.006200	0.0100	0.00	0.00	4.000H	0.00	0.00	0.00	1.
29	92MO	0.0000010	95.90	0.158600	0.3000	0.00	0.00	100.000Y	0.00	0.00	0.00	1.
30	92MO	0.0000010	95.90	0.158600	0.0060	0.00	0.00	6.900H	100.00Y	0.00	0.00	2.
31	98MO	0.0000010	95.90	0.237500	0.1500	0.00	0.00	67.000H	6.044	0.00	0.00	2.
32	100MO	0.0000010	95.90	0.096200	0.2000	0.00	0.00	14.600H	14.00M	0.00	0.00	2.
33	112SN	0.0000220	119.00	0.009500	0.9000	0.00	0.00	115.0000	100.00M	0.00	0.00	2.
34	112SN	0.0000220	119.00	0.009500	0.4000	0.00	0.00	20.000M	0.00	0.00	0.00	1.
35	116SN	0.0000220	119.00	0.142400	0.0060	0.00	0.00	14.0000	0.00	0.00	0.00	1.
36	118SN	0.0000220	119.00	0.240100	0.0100	0.00	0.00	250.0000	0.00	0.00	0.00	1.
37	120SN	0.0000220	119.00	0.329700	0.1400	0.00	0.00	27.000H	0.00	0.00	0.00	1.
38	120SN	0.0000220	119.00	0.329700	0.0010	0.00	0.00	76.000Y	0.00	0.00	0.00	1.
39	122SN	0.0000220	119.00	0.047100	0.0010	0.00	0.00	125.0000	0.00	0.00	0.00	1.
40	122SN	0.0000220	119.00	0.047100	0.2000	0.00	0.00	40.000M	0.00	0.00	0.00	1.
41	124SN	0.0000220	119.00	0.059800	0.0040	0.00	0.00	9.4000	2.70Y	0.00	0.00	2.
42	124SN	0.0000220	119.00	0.059800	0.1300	0.00	0.00	9.700M	2.70Y	0.00	0.00	2.
43	130BA	0.0000100	137.00	0.001010	8.8000	0.00	0.00	12.0000	9.70D	0.00	0.00	2.
44	132BA	0.0000100	137.00	0.000970	7.0000	0.00	0.00	7.200Y	0.00	0.00	0.00	1.
45	132BA	0.0000100	137.00	0.000970	0.2000	0.00	0.00	38.900H	7.20Y	0.00	0.00	2.
46	134BA	0.0000100	137.00	0.024200	0.1600	0.00	0.00	28.700H	0.00	0.00	0.00	1.
47	136BA	0.0000100	137.00	0.078100	0.0100	0.00	0.00	2.550M	0.00	0.00	0.00	1.
48	138BA	0.0000100	137.00	0.716600	0.4000	4.00	20.00	82.900M	12.80D	40.22H	18.00M	6.

CORE USAGE   OBJECT CODE= 14360 BYTES   ARRAY AREA= 7748 BYTES   TOTAL AREA AVAILABLE= 38912 BYTES

DIAGNOSTICS   NUMBER OF ERRORS= 0,   NUMBER OF WARNINGS= 0,   NUMBER OF EXTENSIONS= 0